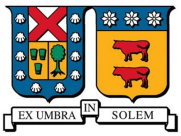

UNIVERSIDAD TECNICA
FEDERICO SANTA MARIA

PONTIFICIA
UNIVERSIDAD
CATÓLICA DE
VALPARAÍSO

Holographic Strongly-Coupled Materials with Dislocations

by:

Francisca Gabriela Ramírez Carrasco

Directors of the thesis:

Dr. Vladimir Juričić &
Dr. Olivera Mišković

Thesis submitted to the Pontificia Universidad Católica de Valparaíso and Universidad Técnica Federico Santa María in partial fulfillment of the requirements to qualify for the degree of PhD in Physical Sciences

Valparaíso, Chile, November 2025

CONSTANCIA DE VALIDACIÓN Y CONFIDENCIALIDAD DE MONOGRAFÍA A REPOSITORIO ACADÉMICO

1.- IDENTIFICACIÓN DEL TRABAJO ACADÉMICO

Tipo de monografía (marcar una opción): ☐ Memoria o trabajo de título **x** Tesis de Postgrado

Título del trabajo: Holographic Strongly-Coupled Materials with Dislocations

Nombre del candidato(a): Francisca Gabriela Ramírez Carrasco

Carrera / Grado: Doctorado en Ciencias Físicas

Campus: Casa Central **Departamento:** Física

2.- VALIDACIÓN DEL PROFESOR GUÍA/DIRECTOR DE TESIS

Yo, Vladimir Juricic, en mi calidad de profesor(a) guía/director(a) del trabajo académico mencionado anteriormente **DEJO CONSTANCIA** que:

- He revisado esta versión del documento y corresponde a la versión final aprobada del trabajo.
- El trabajo cumple con los requisitos académicos y de formato establecidos por la institución.

3.- EVALUACIÓN DE CONFIDENCIALIDAD POR PROPIEDAD INDUSTRIAL (marcar una opción)

x El trabajo **NO contiene** información que amerite confidencialidad y puede ser publicado de inmediato en repositorio con acceso abierto.

☐ El trabajo **CONTIENE** información con potenciales implicancias de propiedad industrial o intelectual y requiere un periodo de confidencialidad (**embargo**) por **(marcar una opción)**:

☐ 6 meses ☐ 12 meses ☐ 2 años ☐ 3 años ☐ 5 años ☐ 10 años

Fundamentación de la necesidad de confidencialidad (obligatorio si se solicita embargo):

4.- FIRMAS

Profesor(a) guía o director(a) de memoria o tesis: Vladimir Juricic

Fecha: 28-11-2025 **Firma:** 

Estudiante o Candidato(a):

Fecha: 28-11-2025 **Firma:** 

Este formulario debe ser insertado como página 2 de la memoria o tesis, completado y firmado por estudiante y profesor(a) antes de la entrega en portal PRISMA de Biblioteca USM.

Thesis Evaluation Committee

The examination committee for this thesis included the following members. The committee's decision was reached by a majority vote.

Advisers: Dr. Vladimir Juričić
Associate Professor,
Universidad Técnica Federico Santa María
Dr. Olivera Mišković
Full Professor,
Pontificia Universidad Católica de Valparaíso

Internal Referees: Dr. Radouane Gannouji
Full Professor,
Instituto de Física, Pontificia Universidad Católica de Valparaíso.
Dr. Ayan Mukhopadhyay
Associate Professor,
Pontificia Universidad Católica de Valparaíso.

External Referees: Dr. Rodrigo Soto
Associate Professor,
Pontificia Universidad Católica de Chile.

Abstract

Weyl semimetals (WSMs) are three-dimensional topological states with no energy gap, characterized by monopole-antimonopole pairs of Abelian Berry curvature at band contact points in momentum space. These materials exhibit chiral anomalies, manifested through crystalline dislocation defects associated with the discrete translational symmetry of the lattice. This thesis, based primarily on the work presented in [1] and some still unpublished results, lays the foundations for constructing a holographic model of WSMs with dislocations, using a $(4+1)$-dimensional Chern-Simons gravitational theory in an anti-de Sitter space, without resorting to external sources of matter. This theoretical framework incorporates torsion, offering a holographic representation of dislocation defects in the crystal lattice and possibly captures the chiral anomaly. By solving the gravitational equations of motion with an asymptotic expansion near the boundary, it is shown that this theory admits axially symmetric solutions in the bulk and on the boundary of $(3+1)$-dimensional spacetime. These solutions can be interpreted as holographic field theories with dislocation defects at finite temperature, encoded by a black hole in the bulk gravitational theory. Two types of black hole horizons are examined: the planar case and the hyperbolic case. Notably, these solutions reveal an odd parity Abelian current exhibiting an anomaly proportional to the Nieh-Yan invariant, which can be interpreted as a holographic chiral anomaly. Therefore, the obtained field theory is a candidate for a holographic WSM. These findings open new perspectives for exploring holographic topological phases using bulk gravitational Chern-Simons theories and establish torsion as a holographic analogue of crystalline dislocation defects.

Resumen

Los semimetales de Weyl (WSMs, por sus siglas en inglés) son estados topológicos tridimensionales sin brecha energética, caracterizados por pares monopolo-antimonopolo de la curvatura de Berry abeliana en puntos de contacto de bandas en el espacio de momentos. Estos materiales exhiben anomalías quirales, manifestadas a través de defectos de dislocación cristalina asociados con la simetría de traslación discreta de la red. Esta tesis, basada principalmente en el trabajo presentado en [1] y algunos resultados aún no publicados, sienta las bases para la construcción de un modelo holográfico de WSM con dislocaciones, utilizando una teoría gravitacional de Chern-Simons $(4+1)$-dimensional en un espacio anti-de Sitter, sin recurrir a fuentes externas de materia. Este marco teórico incorpora torsión, ofreciendo una representación holográfica de los defectos de dislocación en la red cristalina y posiblemente captura la anomalía quiral. Al resolver las ecuaciones gravitacionales de movimiento con una expansión asintótica cerca del borde, se muestra que esta teoría admite soluciones axialmente simétricas en el borde del espaciotiempo $(3+1)$-dimensional. Estas soluciones pueden interpretarse como teorías de campo holográficas con defectos de dislocación a temperatura finita, codificadas por un agujero negro en la teoría gravitacional interior. Se examinan dos tipos de horizontes de agujero negro: el caso planar y el caso hiperbólico. En particular, estas soluciones revelan una corriente Abeliana de paridad impar que exhibe una anomalía proporcional al invariante de Nieh-Yan, que puede interpretarse como una anomalía quiral holográfica. Por lo tanto, la teoría de campo obtenida es candidata para un WSM holográfico. Estos hallazgos abren nuevas perspectivas para explorar las fases topológicas holográficas utilizando teorías gravitacionales de Chern-Simons en le intrior y establecen la torsión como un análogo holográfico de los defectos de dislocación cristalina.

Acknowledgements

First of all, I would like to thank my life partner Francisco and my son Víctor. In the hardest moments, they have been the lighthouse that shines through the darkness. Thank you so much for your patience, love, and companionship, for cheering me up and making me laugh every day. Without you, none of this would make any sense.

Secondly, I want to thank my family, especially my parents Ximena and Lilo, who have always believed in me, accompanied me, and comforted me in sad times—but above all, because they made it possible for me to embark on this crazy adventure of physics. I am infinitely grateful to my siblings Javiera, Lilo, Varinia, and Ignacio, to my aunt Carla, and to my grandmother Ximena, always attentive to my moods, with so much love and joy. I have felt you in every step of my academic path—thank you for believing in me.

I cannot fail to thank my other families, those that are not bound by blood but chosen for life—my beloved friends, almost siblings, Lia, Juan, Lorena, Paloma, Antonieta, Leonardo, Karla, Jeremy, Guillermo and Laura. My heart holds nothing but gratitude for you, for sharing your lives with me and for always supporting me.

I would also like to take this opportunity to thank my thesis advisors, Vladimir and Olivera. When I first met Olivera, I knew I wanted to work with her and that she would be my supervisor. After a few semesters, she accepted me, and my path became beautiful alongside her. Thank you so much for sharing with me all your wisdom and knowledge, for your kindness and warmth, for your dedication and care—I will always carry my affection for her throughout my life. But I was not only lucky to meet Olivera; my reward was double with Vladimir—a very dedicated, empathetic, kind, and generous professor. Thank you for embarking on this project with me, for sharing all your knowledge, and for your patience with someone who is not from the condensed matter area. It has been a beautiful journey with both of you—these have been some of the best years, whose memories I will always treasure.

I would also like to thank all the professors who have been part of my education, who with great care and perseverance have shared their knowledge and wisdom. I especially wish to acknowledge professors Radouane, Ayan, and Rodrigo, who kindly agreed to be

part of the committee for this thesis. I would also like to highlight professors Jorge, Alfonso, Oscar, Patricio, Claudio, Antonio, Gorazd, Fuster, Marat, and Carlos, as well as professors Viktor and Iván, who are no longer with us but have left a lasting mark on me.

Finally, I am grateful to the state scholarships (ANID) and to Universidad Técnica Federico Santa María for funding my studies during these years of doctoral research.

"Cuando vas en barco y miras hacia la orilla, puedes cometer el error de creer que es la orilla del río la que se mueve. Pero si posas la mirada atentamente sobre tu propia embarcación, comprenderás que en realidad es el barco el que se mueve. De la misma manera, si examinas la multitud de fenómenos a través de tu percepción confusa, cometerás el error de pensar que tu propia mente es permanente. Pero si practicas íntimamente y retornas a lo que eres, comprenderás que nada posee naturaleza propia."

Eihei Dōgen, Shōbōgenzō

Contents

Chapter 1

Introduction

Between the topological phases of matter, three-dimensional Weyl semimetals (WSMs) hold a prominent position as they correspond to pairs of nodal points in momentum space, which act as monopoles (sources) and antimonopoles (sinks) of the Abelian Berry curvature [2, 3]. At these nodal points, the valence and conduction bands touch, giving rise to massless (gapless) pseudo-relativistic Weyl quasiparticles in their vicinity [4]. These systems are further characterized by zero-energy Fermi arc surface states that connect the nodal points.

A defining feature of WSMs is the manifestation of the chiral anomaly [5], which results in anomalous magnetotransport responses [6, 7, 8, 9]. This universal signature can be traced back to the axion, or θ-term, in the effective action governing the electrodynamics of $(3+1)$-dimensional WSMs [6, 7], as summarized in recent reviews [10]. Fundamentally, this phenomenon can be viewed as a consequence of the underlying Chern-Simons (CS) theory in one higher dimension [11].

The connection between anomalies and CS gravity has been extensively explored within the framework of holography. For instance, in the absence of torsion, the holographic Weyl anomaly has been studied in Refs.[12, 13], while gravitational and Lorentz anomalies have been addressed in Refs.[14, 15, 16, 17]. Moreover, it is known that the holographic dual of $(4+1)$-dimensional anti-de Sitter (AdS) gravity, as introduced in Refs. [18, 19], exhibits chiral currents [20]. These connections inspire the first guiding principle of this work: the use of a $(4+1)$-dimensional CS gravitational theory in the bulk to construct a holographic

field theories on a $(3+1)$-dimensional boundary that might allow interpretation in terms of a WSM.

The concept of WSMs with isolated band-touching points in momentum space can be extended to gapless states where band touching occurs along lines or surfaces, leading to nodal-line [21, 22, 23, 24] and nodal-surface [25, 26, 27] semimetals, respectively. These systems also exhibit anomalous transport properties, as observed particularly in nodal-line semimetals [28, 29, 30].

Dislocations, which are crystal-lattice defects associated with discrete translational symmetry, play a critical role in WSMs. These defects can realize the chiral anomaly [31, 32, 33, 34, 35, 36, 37] and serve as probes for monopole charges [38]. Within continuum elastic theory, dislocations correspond to torsion fields, with their topological charge, the Burgers vector, representing a point-like source of torsion [39]. A single dislocation can thus be conceptualized as a "torsional vortex", where the torsion flux determines the Burgers vector. This relationship between dislocations and anomalies motivates the second guiding principle of this work: the representation of dislocations in the bulk gravitational theory via torsion fields.

Guided by these physically motivated principles, we construct a topological defect solution in a $(3+1)$-dimensional spacetime, arising from the bulk $(4+1)$-dimensional Chern–Simons gravitational theory in asymptotically AdS spacetime, with the black hole geometry encoding the temperature and torsion representing the dislocation defects [1]. The bulk theory incorporates a black hole to encode temperature and torsion to represent dislocation defects. Specifically, two types of black hole horizons are explored: one with a planar three-dimensional spatial section and another with negative curvature. By employing an asymptotic (Fefferman-Graham [40]) expansion near the boundary, explicit solutions to the bulk equations of motion are obtained.

The analysis reveals that, for the planar case, only a family of axially symmetric solutions exists at a finite-radius (purely spatial) ring, as described by Eq. (6.74). These solutions describe holographic disclocations and possess an odd parity Abelian anomalies. As such, they therefore represent candidates for WSMs. The relationship between temperature, radius, and the dislocation parameter characterizing the torsion field is presented in

Figs. 6.4, 6.6, and 6.7. Furthermore, it is demonstrated that these solutions exhibit a non-trivial Abelian anomaly of odd parity, that may be interpreted as chiral anomaly, as shown in Eq. (6.92) and Fig. 6.8, further reinforcing their interpretation as $(3+1)$-dimensional WSMs with dislocation-induced chiral anomalies. Finally, this anomaly is shown to scale with the Nieh-Yan invariant [41], as expressed in Eq. (6.97).

Recently, there has been significant interest in crystalline systems with hyperbolic geometry, which exhibit unique topological and physical properties that distinguish them from their Euclidean counterparts [42, 43]. Hyperbolic lattices, characterized by negative curvature, provide a natural framework for exploring novel phases of matter and new geometric perspectives in condensed matter systems. These structures, have been realized experimentally using circuit quantum electrodynamics [44], opening pathways for studying hyperbolic band theory and associated topological phenomena. Unlike planar lattices, hyperbolic systems accommodate richer connectivity and higher-dimensional symmetry groups, enabling new types of topological and transport phenomena [45, 46, 47, 48, 49, 50, 51]. These developments have profound implications, bridging condensed matter, high-energy physics, and quantum information science, and suggest that crystalline systems with hyperbolic geometry could unveil uncharted physical phenomena and novel states of matter. This class of systems is implemented in this work through a black hole solution with a hyperbolic 3-dimensional horizon. Due to the complexity of the equations of motion (7.41)–(7.44), the analysis is restricted to a space of solutions in which the torsion fields depend only on the radial coordinate (7.76)–(7.78). It is found that a consistent solution exists only for a finite set of points in the parameter space, such that both the axial and diagonal torsion fields (7.92), as well as the Abelian anomaly (7.99), exist at discrete values of the radial coordinate, as shown in Fig. 7.2 and Fig. 7.3.

This thesis is organized as follows. The first two chapters, 2 and 3, present the state of the art on the two main topics of this research: Weyl semimetals and the holographic principle applied to condensed matter physics. Chapter 2 covers the fundamental aspects necessary to characterize Weyl semimetals and dislocations in crystalline systems, while chapter 3 introduces the key properties of gauge/gravity duality, specifically its application to low-energy systems, that its, condensed matter theory. In chapter 4, we discuss Einstein-Gauss-Bonnet gravity in $4+1$ spacetime dimensions, from which the gravita-

tional Chern-Simons theory emerges, and that will be the bulk gravitational theory for the holography application. The holographic model is introduced in chapter 5, where temperature is encoded through a black hole and dislocations are represented by torsion fields, outlining the general setup for constructing the holographic strongly-coupled metal with dislocations. Chapter 6 explicitly derives the solutions for the planar case, representing the holographic strongly-coupled system with dislocations and computing the corresponding Abelian anomaly. In chapter 7, the explicit calculations for the hyperbolic case are presented. Concluding remarks are provided in chapter 8, with additional calculations included in the Appendices.

Chapter 2

Weyl semimetals

Weyl semimetals (WSMs) represent an exciting class of topological quantum materials characterized by the presence of Weyl fermions as low-energy quasiparticles. These materials are defined by their unique electronic structure, where Weyl nodes of band crossings in momentum space act as monopoles of Berry curvature. This topological property gives rise to fascinating physical phenomena, such as the chiral anomaly and surface states known as Fermi arcs.

In this chapter, an overview of Weyl semimetals is provided, focusing on the chiral anomaly associated with Weyl nodes and the role of crystal dislocations as probes of this anomaly. These interesting features serve as a guiding star in the quest of trying to construct a holographic model for WSMs with dislocations.

2.1 Introduction to Weyl Semimetals

The concept of Weyl semimetals (WSMs) has its origins in 1937, when Conyers Herring first identified the electronic band structure describing these systems in the article Accidental Degeneracy in the Energy Bands of Crystals [52]. Decades later, between 1980 and 1983, Nielsen and Ninomiya published a series of seminal articles [2, 53, 3, 5], where they explored lattice models as a framework for simulating the Standard Model of particle physics. Their

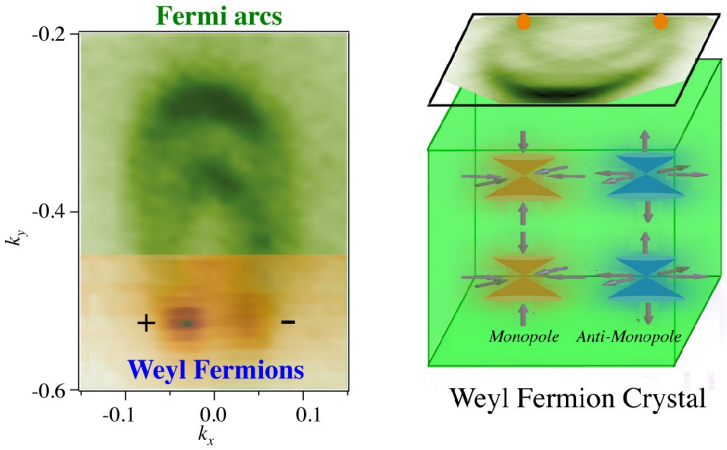

Figure 2.1: The first experimental observation of a WSM was in a TaAs crystal [54].

work demonstrated the existence of chiral particles from a high-energy physics perspective, laying the groundwork for understanding WSMs.

Weyl semimetals (WSMs) highlight a unifying thread across fundamental physics, linking the concept of Weyl fermions arising from high-energy physics with their condensed-matter realization. Proposed in particle physics as solutions to the Weyl equation yet not observed as elementary particles, Weyl fermions emerge in WSMs as quasiparticles. This emergence enables controlled laboratory studies of quantum anomalies and gauge-field responses.

It was not until 2015, however, that WSMs were experimentally discovered. A group of researchers successfully identified these systems in the compound tantalum arsenide (TaAs) [54]. Figure 2.1 illustrates this breakthrough, showing the characteristic Fermi arc that serves as a hallmark of WSMs.

Weyl semimetals are crystal in three-spatial dimension where the low-energy excitations are described by the four dimensional Weyl equation:

$$i\partial_t \Psi_\pm = \mp v_F \, \vec{p} \cdot \vec{\sigma} \Psi_\pm, \tag{2.1}$$

with $\vec{\sigma} = (\sigma_x, \sigma_y, \sigma_z)$ a vector which component are the Pauli matrices, v_F as the Fermi velocity of the Weyl quasiparticles which is typically of a few percent of the speed of light,

and $\Psi_\pm$ the two-component Weyl spinors. These can be embedded into four-component Dirac spinors $\Phi_\pm$ in the chiral basis as

$$\Phi_+ = \begin{pmatrix} 0 \\ \Psi_+ \end{pmatrix}, \quad \Phi_- = \begin{pmatrix} \Psi_- \\ 0 \end{pmatrix}, \tag{2.2}$$

such that they become eigenstates of the chirality operator:

$$\gamma_5 \Phi_\pm = \pm \Phi_\pm \,. \tag{2.3}$$

In other words, this is a (pseudo-)relativistic equation for massless fermions. Assuming plane-wave solutions $\Psi_\pm(\mathbf{r}, t) = e^{\imath(\vec{p}\cdot\mathbf{r} - Et)}\psi_\pm$, the time-dependent equation reduces to the eigenvalue problem

$$H\psi_\pm = E\psi_\pm \,, \tag{2.4}$$

with $H = \mp v_F \, \vec{p}\cdot\vec{\sigma}$. The matrix $\vec{p}\cdot\vec{\sigma}$ has eigenvalues $\pm|\vec{p}|$, so the energy eigenvalues are

$$E = \pm v_F |\vec{p}| \,, \tag{2.5}$$

yielding the characteristic linear dispersion relation of Weyl semimetals, where v_F plays the role of the speed of light. The chirality of massless Weyl fermions, coincides with the helicity defined as the projection of the pseudo-spin onto the direction of momentum, representing the direction of the motion, that is, if the particle move parallel or anti-parallel to the direction of its pseudo-spin. In the following, we set $v_F = 1$, unless otherwise stated.

From band theory, it is evident that Weyl semimetals exhibit a structure where the valence and conduction bands touch each other at two points in the Brillouin zone. These points have opposite chirality and are known as Weyl nodes, which always appear in pairs [5]. They act as sources and sinks of Berry curvature and carry opposite chiral charges. For a pictorial representation, refer to Fig. 2.2. The separation of Weyl nodes in momentum space or energy is a hallmark of these materials, arising due to broken time-reversal symmetry (TRS) or inversion symmetry (IS).

Based on the linear energy dispersion relation, three types of Weyl semimetals can be identified. In Fig.2.3, the left side illustrates a standard Weyl semimetal, while the right side shows a nodal line Weyl semimetal (NLWSM)[21, 22, 23, 24]. In the latter (NLWSM),

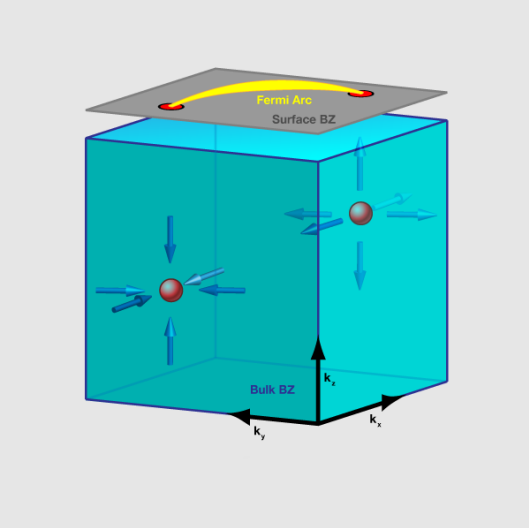

Figure 2.2: A representation of the Brillouin zone in a WSM [55], where one of the Weyl nodes acts as source and the other one acts as sink of the Berry curvature. When this nodes are projected in the upper or in the lower surfaces of the Brillouin zone, a Fermi arc emerge as a surface states.

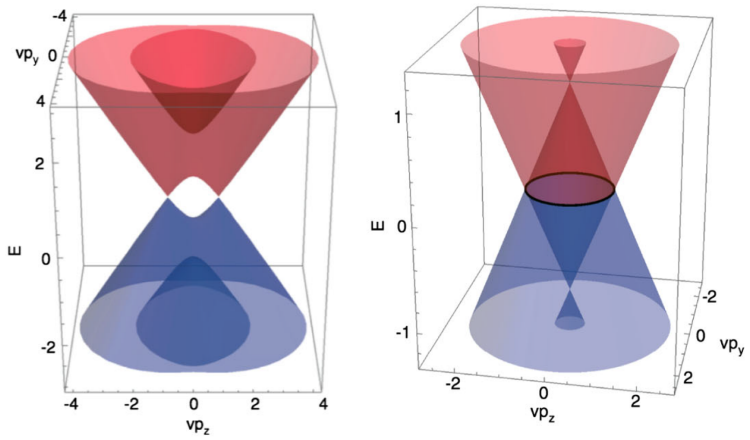

Figure 2.3: Dispersion relation of energy for two types of Weyl semimetals: on the left, a typical WSM with a single pair of Weyl nodes, and on the right side, a nodal line WSM, with a circle of Weyl nodes [4].

an infinite number of Weyl node pairs form a closed loop or circle. Additionally, there is a third type, characterized by a nodal surface in the Weyl semimetal [25, 26, 27].

The existence of Weyl nodes is guaranteed by topology. Specifically, each node is associated with a topological charge defined by the Chern number, which quantifies the flux of Berry curvature through a surface enclosing the node. Considering that the electronic states in a WSM are described in terms of Bloch wave functions $|u_n(\vec{k})\rangle$, with band index n and momentum $\vec{k}$, the Berry connection and its corresponding Berry curvature can be defined as:

$$A_n(\vec{k}) = i\langle u_n(\vec{k})|\nabla_{\vec{k}}|u_n(\vec{k})\rangle, \quad F_n^{ab}(\vec{k}) = \partial_{k_a} A_n^b - \partial_{k_b} A_n^a \,, \tag{2.6}$$

where $F_n^{ab} = F_n$ when the bands are considered isolated. In this case, the Berry flux can be defined as a topological number

$$\int \frac{d^2\vec{k}}{2\pi} F_n(\vec{k}) = N_n \quad \in \mathbb{Z} \,, \tag{2.7}$$

with the surface integral enclosing the Weyl node. This topological protection ensures that the nodes cannot be eliminated unless they merge and annihilate with nodes of opposite chirality. In three-spatial dimensional crystals, the Berry flux behaves like a dual magnetic field with magnetic monopoles. This is visualized in the Fig. 2.4.

One of the most striking manifestations of the topology of WSMs is the presence of Fermi arc surface states. Unlike conventional surface states, which form closed loops in momentum space, Fermi arcs connect the projections of Weyl nodes with opposite chirality on the surface Brillouin zone. Furthermore, from the point of view of electron transport, when an electric field is applied, this translates into a flow of electrons from one Weyl node to the other, as can be seen in the Fig. 2.5, being connected by the Fermi arcs. These arcs are a direct consequence of the bulk-boundary correspondence and provide a unique signature of Weyl semimetals in experiments.

Overall, Weyl semimetals exemplify the profound interplay between topology and condensed matter physics, with their unique properties arising from the topological nature of their electronic structure.

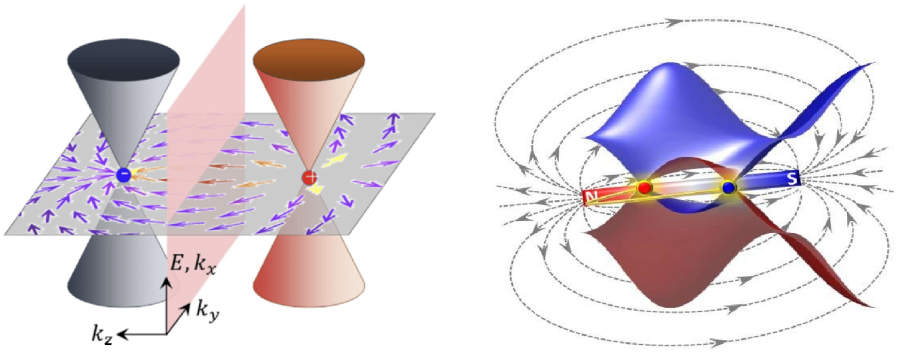

Figure 2.4: On the left, a representation of a transverse section of the Berry flux is shown [56], while on the right, a representation of the dual magnetic field generated by the Weyl nodes as monopoles is depicted (https://phys.org/news/2018-08-marriage-topology-magnetism-weyl.html).

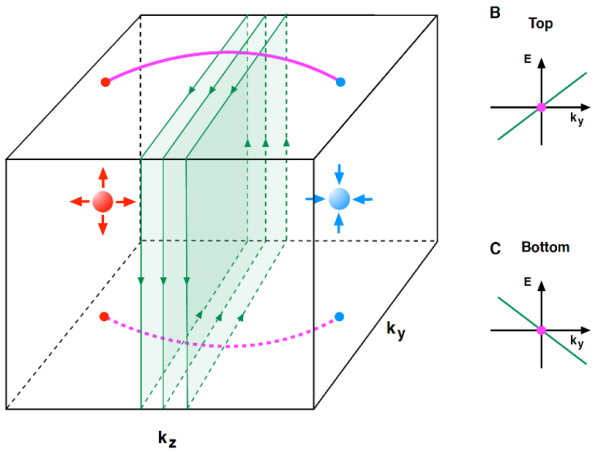

Figure 2.5: Representations of Fermi arcs emerging as surface states formed by the edge fermionic states with zero energy (Fermi energy). These surface states connect the projections of the Weyl nodes on the upper and lower faces of the first Brillouin zone [57].

2.2 The Chiral Anomaly in Weyl Semimetals

The chiral anomaly arises due to the non-conservation of chiral charge in the presence of electromagnetic fields. In WSMs, this phenomenon can be interpreted as the transfer of

electronic states between Weyl nodes with opposite chirality [5].

Weyl nodes can also be understood through the magnetic chiral effect [6, 7, 8, 9], where an external magnetic field $\vec{B}$ generates a current:

$$\vec{j}_{\pm} = C_{\pm}\frac{e^2}{4\pi^2}\vec{B}\,, \tag{2.8}$$

where the chiral current $\vec{j}_{\pm}$ and $C_{\pm} = \pm 1$ represents the respective Chern number of each node. As expected, the sum of the two chiral currents cancels out:

$$\vec{j}_5 = \frac{e^2}{4\pi^2}\vec{B}\sum_{\pm} C_{\pm} = 0\,. \tag{2.9}$$

When an external electric field $\vec{E}$ is applied along the k direction, the equilibrium is broken, causing the occupied states to shift toward the node aligned with $\vec{E}$. As a result, a measurable chiral current emerges. An anomaly, in this context, is proportional to the divergence of the associated current. Specifically,

$$\partial_t \rho_5 + \nabla \cdot \vec{j}_5 = \frac{e^2}{2\pi^2}\vec{E}\cdot\vec{B}, \tag{2.10}$$

where ρ_5 and $\vec{j}_5$ are the chiral charge density and current, respectively. A representation of this chiral anomaly, can be seen in the Fig. 2.6

This consequence of the chiral anomaly translates to the appearance of negative longitudinal magnetoresistance [59]. Specifically, when an electric field $\vec{E}$ is applied parallel to a magnetic field $\vec{B}$, charge carriers with opposite chirality are pumped between Weyl nodes, resulting in an enhancement of conductivity. This phenomenon has been experimentally observed [60] and serves as a hallmark of the chiral anomaly in these materials.

2.3 Crystal Dislocations

A dislocation is a one-dimensional (line) crystallographic defect in a three-dimensional periodic solid, along which the lattice translation symmetry is obstructed. If one traverses

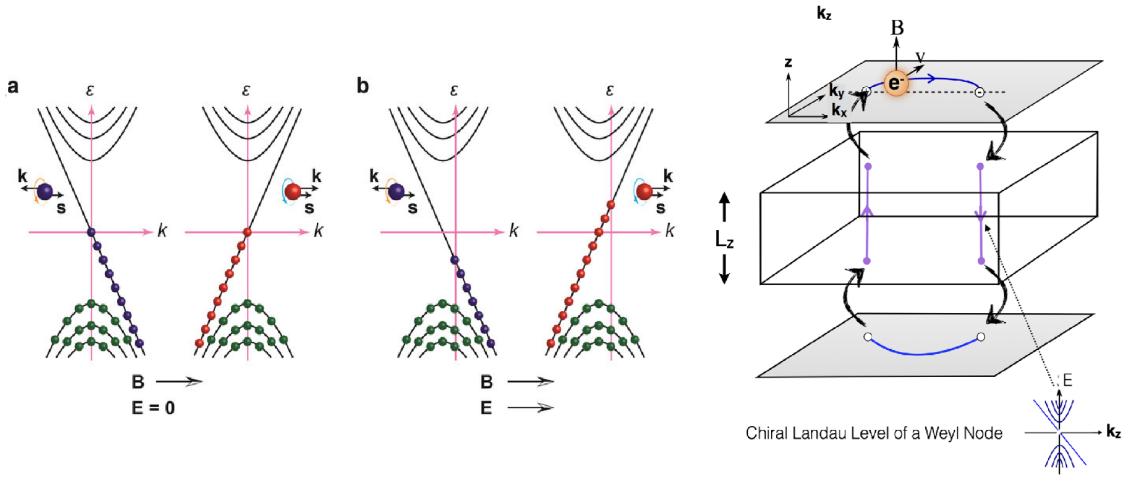

Figure 2.6: On the left, a WSM is depicted under the influence of (a) an external magnetic field and (b) combined external magnetic and electric fields [58]. On the right, a representation of electric transport is shown, where electrons travel along the surface Fermi arcs and are absorbed by the chiral bulk Landau level, which connecting the opposite surfaces. [4].

a closed circuit C around the line, the displacement field $\vec{u}$ fails to close by the **Burgers vector** $\vec{b}$ [61]:

$$\oint_C d\vec{u} = \vec{b}\,. \tag{2.11}$$

The vector $\vec{b}$, a lattice translation, sets the magnitude and direction of the net shear associated with the defect. Together with the local line direction $\vec{L}$, it classifies the dislocation as edge ($\vec{b} \perp \vec{L}$), screw ($\vec{b} \parallel \vec{L}$), or mixed (a general angle between $\vec{b}$ and $\vec{L}$). The Burgers vector [39] is defined as the flux of the torsion tensor over a spatial surface, whose components are

$$b^i = \int T^i\,, \tag{2.12}$$

with T^i as the torsion tensor characterizing the distortion of the crystal, so that dislocations can be regarded as topological defects. In Fig. 2.7, two different types of dislocations are shown: screw dislocations and edge dislocations. These types are chosen because they are of particular interest in this investigation. Specifically, the latter serves as a guide for

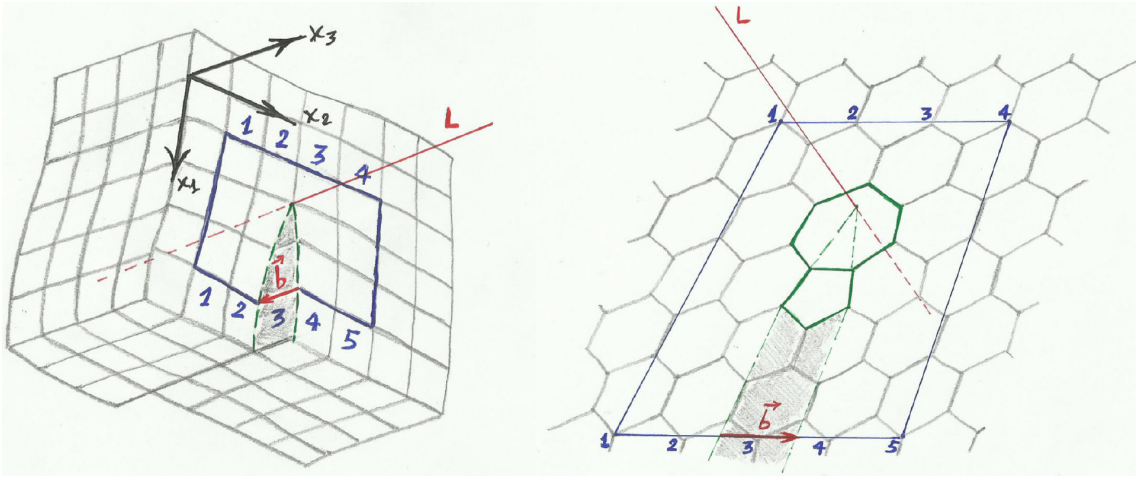

Figure 2.7: On the left side, a *screw dislocation* is shown in a cubic lattice, where the Burgers vector $\vec{b}$ and the dislocation line L are parallel. On the right side, an *edge dislocation* is depicted in a hexagonal two-dimensional lattice, with the Burgers vector lying within the plane and the dislocation line L oriented perpendicular to it, thus always orthogonal to $\vec{b}$ [62].

establishing an ansatz for the antisymmetric part of the spin connection on the gravitational side.

In WSMs, dislocations play a unique role due to their ability to host topologically protected states, effectively acting as "bulk probes" of the topological properties of the systems. Specifically, in WSMs they can realize chiral anomaly [31, 32, 33, 34, 35, 36, 37]. Furthermore, these studies highlight how dislocations affect electronic transport by inducing axial currents and altering the local density of states.

Experimentally, dislocations provide a direct way to probe the chiral anomaly in WSMs. Techniques such as scanning tunneling microscopy (STM) and transport measurements have been used to investigate the effects of dislocations on the electronic structure and conductivity of these materials. These experiments confirm the theoretical predictions and underscore the importance of dislocations as tools for exploring the topological properties of WSMs.

These characteristics, especially the connection between the dislocation and the chiral

anomaly, inspire the second guiding principle of this framework: representing a dislocation in the bulk gravitational theory through the torsional field.

To conclude this chapter, it is evident that Weyl semimetals stand at the crossroads of topology, quantum field theory, and condensed matter physics, offering a rich platform to explore phenomena such as the chiral anomaly and the role of crystal dislocations as topological probes. These insights not only deepen our understanding of these materials but also pave the way for innovative theoretical approaches.

The framework presented in this thesis seeks to harness the principles of gauge/gravity duality to model holographic field theories with dislocations, which might be interpreted in terms of WSMs. Finally, by embedding dislocations into the bulk geometry as torsional fields, this holographic perspective aspires to shed new light on the interplay between topology, anomalies, and transport phenomena, offering a unique lens to study the rich physics of these remarkable quantum systems.

Chapter 3

CMT Gauge/Gravity Duality

The interplay between gauge/gravity duality and condensed matter theory (CMT) represents a profound leap in our understanding of strongly correlated systems. Traditional approaches to quantum many-body systems often face limitations when dealing with phenomena such as unconventional superconductivity, non-Fermi liquids, and quantum criticality, which emerge under strong coupling regimes. The holographic principle, originating from string theory and formalized through the AdS/CFT correspondence, provides a powerful framework to explore these challenges by geometrizing complex quantum interactions.

This duality offers a unique perspective: it maps the dynamics of a strongly coupled quantum field theory (QFT) in d-dimensions to a classical gravitational theory in $d+1$-dimensional anti-de Sitter (AdS) spacetime. Within this framework, thermodynamic and transport properties of condensed matter systems at finite temperature can be described in terms of black hole physics. Moreover, the introduction of additional bulk fields allows us to capture the behavior of quantum phases of matter, such as superconductors and topological phases, while the emergence of holographic renormalization provides insight into the universality of quantum phase transitions.

By leveraging gauge/gravity duality, condensed matter physicists gain access to computational tools and conceptual frameworks capable of tackling some of the most enigmatic problems in the field, such as the understanding of Weyl semimetals systems with strong interacions. This chapter aims to bridge these domains by presenting the foundational

ideas of holography, the technical framework of AdS/CFT correspondence, and its groundbreaking applications to condensed matter theory.

3.1 Foundational Idea: The Holographic Principle

The holographic principle represents a form of duality, arising when two distinct theories—characterized by different parameters and variables—describe identical dynamics. This implies that the two theories share the same number of degrees of freedom, Hilbert space, and symmetries. In other words, through an appropriate transformation of coordinates and fields, the two theories can be mapped onto each other. This duality is encapsulated in the following relation between their coupling constants:

$$g_{strong}, g_{weak} \sim 1\,, \tag{3.1}$$

where one system exhibits a strong coupling constant, while the other features a weak coupling constant.

The holographic principle, originally introduced within the framework of black hole thermodynamics, suggests that the informational content of a physical system confined within a volume V_{d+1} can be entirely encoded on its boundary, A_d [63, 64]. Known as the Bekenstein-Hawking entropy, this principle establishes that the maximum entropy that can be accommodated within a given volume is determined by its boundary area

$$S = \frac{A_d}{4\,G_N}\,, \tag{3.2}$$

where G_N is the Newton constant. This principle is formalized in string theory through the $\mathrm{AdS}_5/\mathrm{CFT}_4$ correspondence [65], which establishes a duality between type IIB superstring theory on $\mathrm{AdS}_5\times\mathrm{S}^5$ and $\mathcal{N}=4$ super Yang-Mills (YM) theory in $(3+1)$ dimensions with gauge group $SU(N)$. The latter is a conformal field theory (CFT) defined on the boundary of the AdS_5 space. At a deeper, more fundamental level, this duality originates from the open-closed string duality, as illustrated in Fig. 3.1. Additionally, as part of the duality, a dictionary between the coupling constants of the two theories is established

$$g^2_{YM} = 2\pi g_s\,, \quad 2\,g^2_{YM}\,N = \frac{L^4}{l_s^4}\,, \tag{3.3}$$

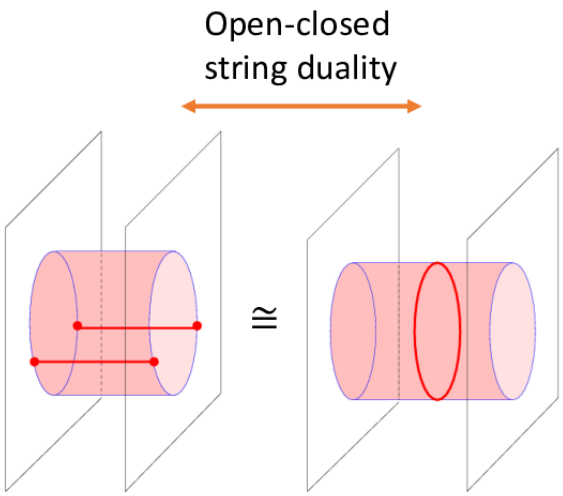

Figure 3.1: A representation of the duality between open and closed string [66].

here, g_{YM} and g_s denote the coupling constants of the super Yang-Mills (YM) theory and the superstring theory, respectively, N represents the rank of the gauge group $SU(N)$, and L and l_s correspond to the AdS radius and the string length, respectively. Within this duality, the dynamics of a supergravity theory in a $(d+1)$-dimensional AdS space are mapped to the dynamics of a d-dimensional CFT on its boundary. This connection arises naturally from string theory, where D-branes and their low-energy limits provide a concrete framework for realizing such dualities.

3.2 AdS/CFT Correspondence

3.2.1 Anti-de Sitter Space and Conformal Field Theories

The AdS/CFT correspondence relies on the properties of Anti-de Sitter spaces and conformal field theories. An AdS_{d+1} space is a maximally symmetric spacetime with constant negative curvature -1, described by the metric

$$ds^2 = \frac{L^2}{r^2}dr^2 + \frac{r^2}{L^2}\eta_{\mu\nu}dx^\mu dx^\nu\,, \tag{3.4}$$

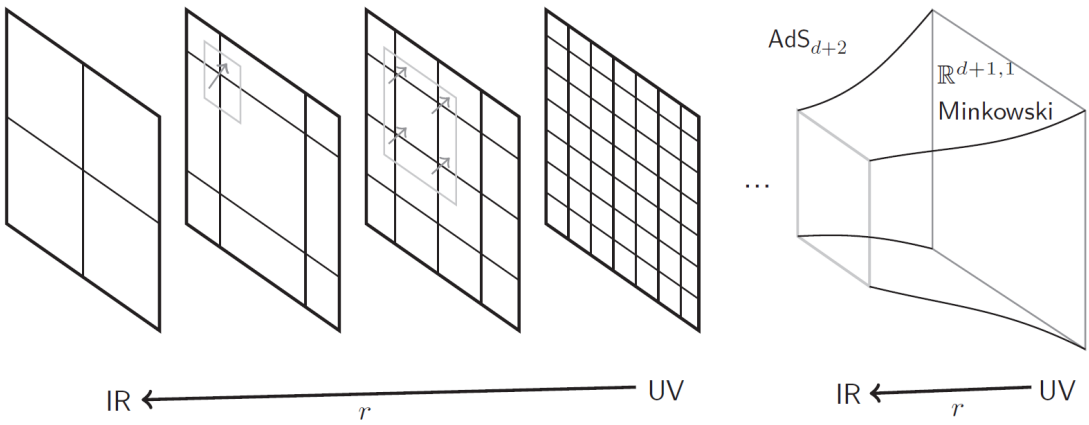

Figure 3.2: A representation of the geometrization of the renormalization group flow direction as an extra dimension [67].

here, L denotes the AdS radius, r is the radial coordinate, with $r \to \infty$ representing the boundary (UV limit) and $r \to 0$ corresponding to the interior region (IR limit), and $\eta_{\mu\nu}$ represents the metric of the flat d-dimensional space [67, 68]. Under a change of coordinates, specifically $z = \frac{L}{r}$, the metric transforms into a conformal form

$$ds^2 = \frac{L^2}{z^2}\left(\eta_{\mu\nu}dx^\mu dx^\nu + dz^2\right) , \tag{3.5}$$

with the conformal factor $\Omega(z) = \frac{L^2}{z^2}$, the metric becomes conformally invariant. Consequently, the isometry group of AdS$_{d+1}$, $SO(d,2)$, is isomorphic to the conformal group in d dimensions, emphasizing the dual relationship between AdS spaces and CFTs. Conformal field theories exhibit scale invariance and universality near quantum critical points, at zero temperature, making them ideal frameworks for describing second-order quantum phase transitions [69, 70]. Moreover, the holographic duality provides a geometrization of the renormalization group flow, where the radial coordinate r in the AdS space corresponds to the energy scale of the CFT, as illustrated in Fig. 3.2 [65].

3.2.2 Partition Functions and Correlation Functions

The holographic dictionary establishes an equivalence between classical gravity in AdS space and a strongly coupled quantum field theory (QFT) on the boundary, which exists in one fewer dimension [71, 65, 72]. This duality is expressed through the equality of the quantum partition functions of the two theories. Specifically, on the gravity side, the Chern-Simons (CS) partition function in the classical approximation is given by

$$Z_{\mathrm{CS}}[A_{(0)}] \simeq \mathrm{e}^{\mathrm{i}I^{\mathrm{ren}}_{\mathrm{CS}}[A]}\big|_{A(0)} \,, \tag{3.6}$$

where A represents a bulk field, $A_{(0)}$ is its boundary value, and $I^{\mathrm{ren}}_{\mathrm{CS}} = I_{\mathrm{CS}} + I_{\mathrm{B}}$ is the renormalized CS action. The latter includes a surface term, I_{B}, that ensures the action principle is satisfied under appropriate boundary conditions, $A \to A_{(0)}$. It also contains counterterms that make $I^{\mathrm{ren}}_{\mathrm{CS}}$ finite in the asymptotic region. As is well known, AdS space introduces divergences at large distances due to the boundary metric having a pole of order two [73].

On the other hand, the holographically dual conformal field theory (CFT)—a QFT—has its partition function expressed as

$$Z_{\mathrm{QFT}}[A_{(0)}] = \mathrm{e}^{\mathrm{i}W[A_{(0)}]} \,, \tag{3.7}$$

where $W[A_{(0)}]$ is the non-local quantum effective action obtained after integrating out all boundary fields coupled to the external source $A_{(0)}$. The AdS/CFT correspondence equates the renormalized classical AdS gravity action in five dimensions with the quantum effective action in four dimensions:

$$I^{\mathrm{ren}}_{\mathrm{CS}}[A_{(0)}] \simeq W[A_{(0)}] \,. \tag{3.8}$$

To apply this prescription to gravitational and quantum theories, the initial step involves determining the boundary terms, I_{B}, as well as the boundary conditions for $A_{(0)}$. This procedure is thoroughly detailed in [20], where the results are summarized and subsequently utilized in applications aimed at understanding Weyl semimetal systems.

In the context of correlation functions of operators $\mathcal{O}$ in the CFT, the holographic principle is employed to compute these operators by varying the bulk action with respect

to $A_{(0)}$, as follows:

$$\langle \mathcal{O}_1(x_1) \cdots \mathcal{O}_n(x_n) \rangle_{CFT} = \left. \frac{\delta^n W}{\delta A^1_{(0)}(x_1) \cdots \delta A^n_{(0)}(x_n)} \right|_{A^i_{(0)}=0}. \tag{3.9}$$

For instance, the energy-momentum tensor and spin current, which correspond to the Poincaré symmetry, are holographic currents represented as one-point correlation functions. This correspondence illustrates how holography translates classical gravitational dynamics in the bulk into quantum field-theoretic observables on the boundary [67, 68].

3.3 AdS/CMT

The application of holographic duality to condensed matter theories (AdS/CMT) has established a powerful framework for studying strongly correlated systems, such as high-temperature superconductors and quantum critical phases in general [68, 70, 74]. A notable example involves the quantum phase transition in a superfluid-insulator system, as illustrated in Fig. 3.3. In such systems, a phase transition occurs at $T = 0$, where the correlation length diverges, indicating that the system becomes fully correlated. However, traditional condensed matter approaches struggle to describe the dynamics of these systems at $T > 0$, a regime known as the quantum critical region. In this context, the AdS/CMT duality provides a novel perspective through the introduction of a black hole solution in the AdS bulk. This black hole generates an energy scale (temperature) in the boundary theory, breaking conformal invariance and enabling the analysis of finite-temperature systems [75]

3.3.1 Hawking Temperature

In the AdS/CMT duality, the Hawking temperature (temperature of the black hole) $T_H \sim r_H$, with r_H the horizon radius of the black hole, corresponds to the temperature of the boundary QFT, as can be appreciated in the Fig. 3.4, establishing a direct connection between gravitational dynamics and thermal physics. Where typical planar Schwarzschild AdS black hole metric is typically expressed as

$$ds^2 = -f(r)dt^2 + \frac{dr^2}{f(r)} r^2 d\Omega^2, \tag{3.10}$$

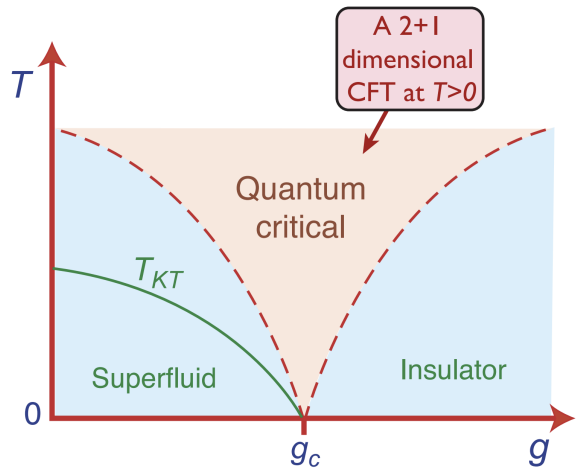

Figure 3.3: A phase diagram of the superfluid-insulator transition in two spatial dimensions ($D = 3$). The quantum critical point is at $g = gc$, $T = 0$, where a CFT domain can be appreciate (the quantum critical region) [76].

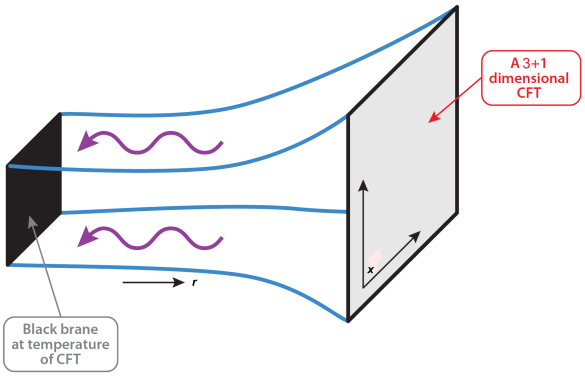

Figure 3.4: A representation of the energy scale introduced by a black hole metric, along with its corresponding Hawking temperature, serves as a dual description of the temperature in the conformal field theory (CFT) [76]. The gravity theory is defined on the bulk 4-dimensional spacetime. The CFT resides on the boundary at $r \to \infty$.

where $d\Omega^2$ correspond to the planar transversal section, and $f(r) = \frac{r^2}{L^2} - \frac{M}{r}$ encodes the black hole horizon with M the mass of the black hole, and its asymptotic behavior determines the thermodynamic properties of the boundary theory [77, 68, 75].

To conclude this chapter, it is important to highlight the transformative impact of the gauge/gravity duality. This duality has revolutionized our understanding of strongly correlated systems by offering a geometric framework for the study of quantum field theories. Through its applications in condensed matter physics, particularly within the AdS/CMT correspondence, it continues to reveal universal features of critical phenomena and transport properties. Moreover, the holographic principle offers a promising avenue for exploring the intricate topological and transport properties of Weyl semimetals, providing a deeper understanding of the connection between the chiral anomaly and dislocations.

Chapter 4

Einstein-Gauss-Bonnet AdS_5 Gravity at the Chern-Simons Point

In this chapter, it is presented the gravitational theory that have all the properties and characteristic necessary to construct the holographic dual theory. Recalling that we are looking for dislocation in a topological state of matter, the gravitational theory must belong to a five dimensional space with asymptotic anti-de Sitter symmetry and a non-trivial topology. Under these conditions, the perfect candidate is AdS_5 gravity at the Chern-Simons point.

In the follow, it is presented the principal properties concerning to the gravitational theory that, after being taken to the boundary, provides the appropriate structure to build a holographic field theory with dislocations.

4.1 Einstein-Gauss-Bonnet AdS_5 Gravity

The Einstein-Gauss-Bonnet (EGB) gravity in five-dimension [78], its the most general higher-curvature correction of the General Relativity in 4+1 dimensions that still possessing second-order gravitational equations. Considering a negative cosmological constant $\Lambda < 0$ in order to have an anti-de Sitter space, the action functional of the Einstein-Gauss-Bonnet

AdS_5 is given by

$$I_{\rm EGB}[\hat{g}] = \frac{1}{16\pi G}\int \mathrm{d}^5x\,\sqrt{-\hat{g}}\left(\hat{R} - 2\Lambda + \alpha\,\mathfrak{R}^2\right)\,, \tag{4.1}$$

where G is the gravitational constant with dimension $G \sim (\text{length})^3$ in the natural units, $\hat{g}_{\Lambda\Sigma}(x)$, $\Lambda, \Sigma = 0, \ldots, 4$, is the space-time metric with the mostly positive signature, and $\mathfrak{R}^2$ denotes the Gauss-Bonnet term quadratic in the Riemann tensor, with the associated coupling constant $\alpha \sim (\text{length})^2$. The Ricci scalar is define as

$$\hat{R} = \hat{g}^{\Lambda\Sigma}\hat{R}_{\Lambda\Sigma}\,, \tag{4.2}$$

with $\hat{R}_{\Lambda\Sigma}$ the Ricci tensor define has the contraction of the Riemann tensor

$$\hat{R}_{\Lambda\Sigma} = \hat{R}^{\Gamma}{}_{\Lambda\Gamma\Sigma}\,. \tag{4.3}$$

And the Gauss-Bonnet term has the form

$$\mathfrak{R}^2 = \hat{R}^{\Lambda\Sigma\Gamma\Pi}\hat{R}_{\Lambda\Sigma\Gamma\Pi} - 4\hat{R}^{\Lambda\Sigma}\hat{R}_{\Lambda\Sigma} + \hat{R}^2\,. \tag{4.4}$$

In this investigation it is needed a gravitational theory that has torsional degrees of freedom, since it is sought that the dual theory contains dislocation defects. Under this premise, it is established a dictionary between the torsion field of the gravitational theory and the torsion field in the limit of the continuous elastic theory represented by its topological charge, the Burgers vector [39].

Because of this, it is better to work in the first order formalism where the introduction of the torsion field is natural, i.e. in terms of the vielbein 1-form $\hat{e}^A = \hat{e}^A_\Lambda(x)\,\mathrm{d}x^\Lambda$ and the spin connection 1-form $\hat{\omega}^{AB} = \hat{\omega}^{AB}_\Lambda(x)\,\mathrm{d}x^\Lambda$ being the fundamental fields. In this formalism differential forms are used in the local coordinate basis $\mathrm{d}x^\Lambda$, with $A = 0, \ldots, 4$ being Lorentz indices in the tangent space. As is well known, the vielbeins and their inverses are projectors that transform vectors in curved space into vectors in flat tangent space and *vice versa* (bulk tensors to tangent tensors). The flat tangent space is endowed with the Minkowski metric $\eta_{AB} = \mathrm{diag}\,(-,+,+,+,+)$, and the relation between the metric and the vielbein is given by the usual expression

$$\hat{g}_{\Lambda\Sigma} = \eta_{AB}\,\hat{e}^A_\Lambda\hat{e}^B_\Sigma\,. \tag{4.5}$$

So in the Riemann-Cartan space, where the torsion field is non trivial, the vielbein 1-form are the fields that encodes all the metric information, i.e. everything related to measurements of length, angles, areas or volumes. But the spin connection 1-form, that is independent gauge field of the vielbein, encodes all the information regarding affinity, that is, everything that remains invariant under translations or affine transformations such as parallel transport. In this form we can define the associated Lorentz field-strength 2-form:

$$\hat{R}^{AB} = \mathrm{d}\hat{\omega}^{AB} + \hat{\omega}^{A}{}_{C} \wedge \hat{\omega}^{CB} \,, \tag{4.6}$$

with the Riemann tensor obtained from $\hat{R}^{AB} = \frac{1}{2}\,\hat{R}^{AB}_{\Lambda\Sigma}\,\mathrm{d}x^{\Lambda} \wedge \mathrm{d}x^{\Sigma}$ by projecting the Lorentz indices of the Lorentz field-strength to the spacetime indices as $\hat{R}^{\Gamma\Pi}_{\Lambda\Sigma} = \hat{R}^{AB}_{\Lambda\Sigma}\,\hat{e}^{\Gamma}_{A}\hat{e}^{\Pi}_{B}$, using the inverse vielbein $\hat{e}^{\Lambda}_{A}$.

Using the first-order formulation, the Einstein-Gauss-Bonnet AdS action (4.1) acquires the form

$$I_{\mathrm{EGB}}[\hat{e},\hat{\omega}] = \kappa \int \epsilon_{ABCDE} \left(\frac{4\alpha}{\ell^3}\,\hat{R}^{AB}\hat{R}^{CD} + \frac{2}{3\ell^3}\,\hat{R}^{AB}\hat{e}^{C}\hat{e}^{D} + \frac{1}{5\ell^5}\,\hat{e}^{A}\hat{e}^{B}\hat{e}^{C}\hat{e}^{D} \right) \hat{e}^{E} \,, \tag{4.7}$$

where the wedge product $\wedge$ between the form have been omitted for the sake of simplicity, and the dimensionless gravitational constant is redefined as $\kappa = \frac{\ell^3}{64\pi G}$ with $\ell^2 = -\frac{3}{\Lambda}$ the AdS radius.

The next step, is to bring up this theory to the Chern-Simons point, where the gravity becomes a gauge theory, but more importantly where there exists chiral current with anomaly [20], which is essential to obtain a dual theory with Weyl semimetal structure.

4.2 AdS Gravity at the Chern-Simons Point

Motivated by the fact that the holographic Weyl semimetal requires a chiral anomaly generated by a chiral current, a search is conducted for a spacetime that asymptotically aproach to AdS space: $\hat{R}^{AB} \to -\frac{1}{\ell^2}\hat{e}^{A} \wedge \hat{e}^{B}$. This means that it is needed a theory with global AdS solution, but due to the quadratic term in $\hat{R}^{AB}$ in the action (4.7), the vacua structure of the AdS gravity have two global different solution for generic values [78] of

$\alpha > \alpha_{\rm CS}$, with $\alpha_{\rm CS} = \frac{\ell^2}{4}$ the so-called Chern-Simons point, where the vacua structure becomes unique. Outside the Chern-Simons point, there are two effective radii [79]:

$$\ell_{\mathit{eff}}^{(\pm)2} = \frac{2\alpha\,(D-3)\,(D-4)}{1 \pm \sqrt{1 - \frac{4\alpha}{\ell^2}\,(D-3)\,(D-4)}}\,, \tag{4.8}$$

that in the limit $\alpha \ll \frac{\ell^2}{4(D-3)(D-4)}$ lead to two branches:

i) **Einstein branch**: $\ell_{\mathit{eff}}^{(-)2} \to \ell^2 + \mathcal{O}(\alpha^2)$

ii) **Stringy branch**: $\ell_{\mathit{eff}}^{(+)2} \to \mathcal{O}(\alpha) \to 0$.

First, it is noted that the AdS radius in CS gravity it is not the same that the AdS radius in Einstein-Hilbert (EH) gravity: $\alpha = 0$, $\Lambda_{EH} = -\frac{6}{\ell^2}$. And second, how the two theories drastically changes, the limit $\alpha \to \alpha_{\rm CS}$ is discontinuous. Not only the vacua structure will change, otherwise the CS gravity with negative cosmological constant becomes a gauge theory for the AdS group: $SO(4,2)$. So, the Einstein-Gauss-Bonnet AdS gravity action in five dimensions in the CS point is

$$I_{\rm CS}[\hat{e},\hat{\omega}] = \kappa \int \epsilon_{ABCDE} \left(\frac{1}{\ell}\,\hat{R}^{AB}\hat{R}^{CD} + \frac{2}{3\ell^3}\,\hat{R}^{AB}\hat{e}^C\hat{e}^D + \frac{1}{5\ell^5}\,\hat{e}^A\hat{e}^B\hat{e}^C\hat{e}^D \right) \hat{e}^E. \tag{4.9}$$

Being the CS AdS gravity a gauge theory, the action can be described in terms of a dynamical Lie-algebra valued gauge field 1-form $A = A_\Lambda(x)\,\mathrm{d}x^\Lambda$ that is the connection on a fiber bundle define as

$$A = \frac{1}{\ell}\,\hat{e}^A P_A + \frac{1}{2}\,\hat{\omega}^{AB} J_{AB}\,, \tag{4.10}$$

where $\{J_{AB} = -J_{BA}, P_A\}$ are the generators of $SO(4,2)$, locally isomorphic with AdS_5 group. For completeness, a summary of the algebra of AdS space is presented in the following.

AdS Algebra

Starting with the convention that the flat metric of the tangent space is mostly positive, $\eta_{AB} = \text{diag}(-,+,+,+,+)$, the common Lorentz isometries are extended to anti-de Sitter (AdS) isometries in Chern-Simons AdS gravity. Due to the isomorphism between the five-dimensional AdS algebra and $\mathfrak{so}(2,4)$, it can be written in the basis of the Lorentz rotations $J_{AB} = -J_{BA}$ and the AdS translations P_A as

$$\begin{aligned} [J_{AB}, J_{CD}] &= \eta_{AD}J_{BC} - \eta_{BD}J_{AC} - \eta_{AC}J_{BD} + \eta_{BC}J_{AD}, \\ [J_{AB}, P_C] &= -\eta_{AC}P_B + \eta_{BC}P_A\,, \qquad [P_A, P_B] = J_{AB}\,. \end{aligned} \tag{4.11}$$

Using the decomposition of Lorentz indices $A = (a, 4)$ and the fact that $\eta_{44} = 1$ and $\eta_{ab} = \text{diag}(-,+,+,+)$, the above algebra can be rewritten in the basis $\{J_{ab}, J_a^{\pm}\}$, where $J_a^{\pm} \equiv P_a \pm J_{a4}$, as

$$\begin{aligned} [J_{ab}, J_{cd}] &= \eta_{ad}J_{bc} - \eta_{bd}J_{ac} - \eta_{ac}J_{bd} + \eta_{bc}J_{ad}\,, \\ \left[J_{ab}, J_c^{\pm}\right] &= -\eta_{ac}J_b^{\pm} + \eta_{bc}J_a^{\pm}\,, \\ \left[J_a^{+}, J_b^{-}\right] &= 2J_{ab} - 2\eta_{ab}P_4\,, \qquad \left[J_a^{\pm}, P_4\right] = \pm J_a^{\pm}\,, \end{aligned} \tag{4.12}$$

where all other commutators are zero.

As in every Lie algebra with a well-defined gauge connection, there exists an associated Lie-algebra valued field strength 2-form: $F = \frac{1}{2}\,F_{\Lambda\Sigma}(x)\,\mathrm{d}x^{\Lambda} \wedge \mathrm{d}x^{\Sigma} = \mathrm{d}A + A \wedge A$, with the following components

$$F = \frac{1}{\ell}\,\hat{T}^A P_A + \frac{1}{2}\left(\hat{R}^{AB} + \frac{1}{\ell^2}\,\hat{e}^A \wedge \hat{e}^B\right) J_{AB}\,. \tag{4.13}$$

Accordingly, it follows that $F^{AB} = \hat{R}^{AB} + \frac{1}{\ell^2}\,\hat{e}^A \wedge \hat{e}^B$ is the AdS curvature of the spacetime, with the AdS vacuum that is the pure gauge ($F^{AB} = 0$) of the theory.

Of course, it is possible to write the (4.9) action as a gauge theory for the AdS_5 group explicitly in terms of the gauge connection and its associated field strength

$$I_{\text{CS}}[A] = \frac{\kappa}{3}\int \text{Tr}\left(AF^2 - \frac{1}{2}\,A^3F + \frac{1}{10}\,A^5\right)\,, \tag{4.14}$$

where κ is the level of the CS action and the trace is defined as a symmetric invariant tensor of the AdS group, with the only non-vanishing components

$$\frac{1}{4}\,\mathrm{Tr}\,(J_{AB}J_{CD}P_E) = \epsilon_{ABCDE}\,, \tag{4.15}$$

where it is neglected all the boundary terms. The action principle problem and the counterterms that render the action (4.14) finite have been analyzed in [20]. See for example, Ref. [80], a comprehensive review on CS (super)gravities.

Finally, varying the action functional (4.14) and asking it to be stationary, it is arrived at the equations of motion

$$\begin{aligned} \delta\hat{e}^E \quad &: \quad 0 = \epsilon_{ABCDE}\,F^{AB}\wedge F^{CD}\,, \\ \delta\hat{\omega}^{DE} \quad &: \quad 0 = \epsilon_{ABCDE}\,F^{AB}\wedge \hat{T}^C\,. \end{aligned} \tag{4.16}$$

Where the first equation is the generalized EGB field equation that includes torsional degrees of freedom, whereas that the second equation is a characteristic of the $\hat{T}^A \neq 0$ sector, and as already mentioned above, it is interested in a non-trivial torsion field as it is a source for fermions and may be for chiral anomaly in a holographically dual theory.

In the next chapter, will focus on taking CS theory in AdS_5 space to the boundary, where the asymptotic limit will be taken; being the starting point for constructing the holographic theory, the action (4.9) and the equations of motion (4.16) describing the bulk dynamics of the gravitational fields $\hat{e}^A_\Lambda(x)$ and $\hat{\omega}^{AB}_\Lambda(x)$.

In the literature, solutions of five-dimensional CS (super)gravity with non-vanishing torsion have been previously considered. A stable global AdS_5 geometry containing Abelian matter with nontrivial winding was discussed in [81], while degenerate AdS_5 black holes were investigated in [82]. More aligned with this research, CS AdS_5 black holes with axial torsion were analyzed in [83] and with the addition of Abelian and non-Abelian solitons in [84]. Other black hole solutions in CS AdS_5 gravity were discussed in [85]. And when the cosmological constant is slightly modified, CS gravity becomes effectively EGB gravity, which was studied [86].

Chapter 5

Construction of the model

5.1 The model at the boundary and holographic gauge-fixing

In order to analyze the boundary theory arising from the asymptotic limit of CS gravity, it is necessary to solve the first-order differential equations (4.16) in the radial coordinate. These equations, subject to specific boundary conditions, determine the radial evolution of the fields. This is done in [20], in the follow the results are summarize. But first, it is necessary to introduce the notation and some conventions that is used in this investigation.

Notation: local coordinates

It is considered the five-dimensional spacetime that locally has the form of the cylinder $\mathcal{M} = \mathbb{R} \times \Sigma$, such that $\mathbb{R}$ corresponds to the time coordinate and Σ is the spatial manifold at constant time. Notation for the local coordinates, in both the manifold and tangent

spaces, are summarized in the following table:

5D Lorentz indices:	**4D Lorentz indices:**	**3D Lorentz indices:**
$A = (a, 4)$	$a = (0, m)$	$m = 1, 2, 3$
$A = 0, 1, 2, 3, 4$	$a = 0, 1, 2, 3$	
5D spacetime:	**4D boundary:** $\sigma = \text{const.}$	**3D space:** $t, \sigma = \text{const.}$
$\mathcal{M} = \mathbb{R} \times \Sigma$	$\partial\mathcal{M} = \mathbb{R} \times \partial\Sigma_\infty$	$\partial\Sigma$
$x^\Lambda = (x^\mu, \sigma)$	$x^\mu = (t, x^i)$	$x^i\,, i = 1, 2, 3$
5D black hole:	**4D black-hole boundary:**	**3D flat space:**
$x^\Lambda = (t, y^i, \sigma)$	$x^\mu = (t, y^i)$	$y^i = (\rho, \varphi, z)$
$t \in \mathbb{R}$, $\sigma \geq 0$		$\rho \geq 0$, $\varphi \in [0, 2\pi]$, $z \in \mathbb{R}$
		3D hyperbolic space:
		$y^i = (\chi, \theta, \varphi)$
		$\chi \geq 0$, $\theta \in [0, \pi]$, $\varphi \in [0, 2\pi]$

For three-dimensional indices, we use the Latin letters

$$\begin{array}{ll} \text{flat indices:} & m, n, s, p, q, \dots\,, \\ \text{curved indices:} & i, j, k, l, \dots\,. \end{array} \tag{5.1}$$

Convention: Levi-Civita symbol

It is defined the five- and four-dimensional volume elements as

$$\begin{aligned} \mathrm{d}x^\Lambda \wedge \mathrm{d}x^\Sigma \wedge \mathrm{d}x^\Pi \wedge \mathrm{d}x^\Delta \wedge \mathrm{d}x^\Gamma &= -\mathrm{d}^5x\, \epsilon^{\Lambda\Sigma\Pi\Delta\Gamma}\,, \\ \mathrm{d}x^\mu \wedge \mathrm{d}x^\nu \wedge \mathrm{d}x^\alpha \wedge \mathrm{d}x^\beta &= -\mathrm{d}^4x\, \epsilon^{\mu\nu\alpha\beta}\,, \\ \mathrm{d}t \wedge \mathrm{d}y^i \wedge \mathrm{d}y^j \wedge \mathrm{d}y^k &= -\mathrm{d}^4x\, \epsilon^{ijk}\,, \end{aligned} \tag{5.2}$$

and the following notation for the constant Levi-Civita symbol:

$$\begin{aligned} \epsilon_{abcd4} &= \epsilon_{abcd}, \qquad \epsilon_{tijk} \equiv \epsilon_{ijk} \\ \epsilon^{tijk} &= -\epsilon^{ijk}\,. \end{aligned} \tag{5.3}$$

Explicitly, in cylindrical coordinates, we use the conventions $\epsilon_{t\rho\varphi z} = 1$ and $\epsilon_{\rho\varphi z} = 1$ for the planar horizon case, and $\epsilon_{t\chi\theta z} = 1$ and $\epsilon_{\chi\theta z} = 1$ for the hyperbolic horizon case.

Returning to the process of bringing the model to the boundary, consider local coordinates on the 5D spacetime manifold $\mathcal{M} = \mathbb{R} \times \Sigma$, where the spatial section Σ is parameterized as $x^\Lambda = (x^\mu, \sigma)$. Here, $\sigma \geq 0$ represents the radial coordinate, while x^μ, with $\mu = 0, 1, 2, 3$, parameterizes the 4D asymptotic boundary $\partial\mathcal{M} = \mathbb{R} \times \partial\Sigma_\infty$, located at $\sigma = \sigma_{\rm B} = \text{const}$. For convenience, set $\sigma_{\rm B} = 0$ since the focus is on a near-boundary analysis. And the group indices are decomposed accordingly as $A = (a, 4)$.

From this section onward, will set the AdS radius to unity, $\ell = 1$, for simplicity. This choice does not entail any loss of generality, as the holographic prescription employed here is valid exclusively in AdS spaces. Moreover, the flat-space limit $\ell \to \infty$ is ill-defined. For example, the counter-terms used to regularize CS AdS gravity are proportional to ℓ [87].

The following 15 holographic gauge-fixing conditions are imposed on the 15-dimensional $\mathrm{SO}(4,2)$ gauge symmetry [20],

$$A_\sigma = -\frac{1}{2\sigma} P_4 \quad \Leftrightarrow \quad \hat{e}^4_\sigma = -\frac{1}{2\sigma}\,, \quad \hat{e}^a_\sigma = 0\,, \quad \hat{\omega}^{AB}_\sigma = 0\,. \tag{5.4}$$

The component $\hat{e}^4_\sigma$ is selected in such a way that the vielbein remains invertible, with σ becoming the dimensionless Fefferman-Graham (FG) radial coordinate [40]. And an additional condition, which ensures the boundary is orthogonal to the radial coordinate, is also applied

$$\hat{e}^4_\mu = 0\,. \tag{5.5}$$

It can be demonstrated that the above condition is always permissible, as it fixes the residual gauge symmetry. In this way, A_σ is determined by the gauge choice, while A_μ is dynamically obtained as the exact solution of the subset of equations (4.16) that involve radial derivatives,

$$A_\mu(x,\sigma) = \sigma^{\frac{1}{2}P_4}\, A_\mu(x,0)\, \sigma^{-\frac{1}{2}P_4}. \tag{5.6}$$

The boundary value of the gauge field $A_{(0)}(x)$, is the boundary 1-form $A(x,0) = A_\mu(x,0)\,\mathrm{d}x^\mu$, that can be expanded in the AdS basis $J^\pm_a = P_a \pm J_{a4}$ (using the decomposition (4.12)), as

$$\partial\mathcal{M}: \quad A(x,0) = A_\mu(x,0)\,\mathrm{d}x^\mu = e^a(x) J^+_a + k^a_\mu(x) J^-_a + \frac{1}{2}\,\omega^{ab}(x) J_{ab}\,. \tag{5.7}$$

Combining (5.6) and (5.7) and using a the following algebraic identities:

$$\sigma^{\frac{1}{2}P_4}\, J_a^{\pm}\, \sigma^{-\frac{1}{2}P_4} = \sigma^{\mp\frac{1}{2}}\, J_a^{\pm}\,, \tag{5.8}$$

and

$$\sigma^{\frac{1}{2}P_4}\, J_{ab}\, \sigma^{-\frac{1}{2}P_4} = J_{ab}\,, \tag{5.9}$$

the radial evolution of the gauge field takes the form

$$A(x,\sigma) = \frac{1}{\sqrt{\sigma}}\, e^a(x)\, J_a^+ + \sqrt{\sigma} k^a(x)\, J_a^- + \frac{1}{2}\,\omega^{ab}(x)\, J_{ab}\,. \tag{5.10}$$

It means that the bulk vielbein and the spin connection have radial dependence given by

$$\begin{aligned} \hat{e}^a &= \frac{1}{\sqrt{\sigma}}\, e^a + \sqrt{\sigma}\, k^a\,, \\ \hat{\omega}^{ab} &= \omega^{ab}\,, \\ \hat{\omega}^{a4} &= \frac{1}{\sqrt{\sigma}}\, e^a - \sqrt{\sigma} k^a\,. \end{aligned} \tag{5.11}$$

Then, inserting the radial expansion of $\hat{e}^A$ into the five-dimensional line element $d\hat{s}^2 = \eta_{AB}\hat{e}^A\hat{e}^B$ results in the standard FG form [40]

$$\mathrm{d}s^2 = \frac{\mathrm{d}\sigma^2}{4\sigma^2} + \frac{1}{\sigma}\,\left[g_{\mu\nu} + \sigma\,(k_{\mu\nu} + k_{\nu\mu}) + \sigma^2\, k_{a\mu}\, k^b{}_{\nu}\right]\, \mathrm{d}x^\mu \mathrm{d}x^\nu, \tag{5.12}$$

with the induced metric on the surface $\sigma =$ const. expands in a manner consistent with asymptotically AdS spaces, specifically as $\frac{1}{\sigma}\times$ (regular part) when $\sigma \to 0$.

The boundary metric source is denoted by $g_{\mu\nu}(x) = \eta_{ab} e^a_\mu e^b_\nu$, which corresponds to the leading order in the expansion of the induced metric. Similarly, the holographic sources in the first-order formulation can be identified as the leading terms in the near-boundary expansion (5.11). Specifically, as $\sigma \to 0$, and up to a conformal factor, the boundary conditions of the fields are $\hat{e}^a \to e^a$ and $\hat{\omega}^{ab} \to \omega^{ab}$. Therefore, e^a and ω^{ab} represent the boundary sources.

As a consequence of the radial expansion (5.11), the AdS field strength expands as

$$\begin{aligned} F^{ab} &= R^{ab} + 2\left(e^a \wedge k^b - e^b \wedge k^a\right) , \\ F^{a4} &= \frac{1}{\sqrt{\sigma}}\, T^a - \sqrt{\sigma}\, \mathrm{D}k^a , \\ \hat{T}^a &= \frac{1}{\sqrt{\sigma}}\, T^a + \sqrt{\sigma}\mathrm{D}k^a , \\ \hat{T}^4 &= -2\, e^a \wedge k_a , \end{aligned} \tag{5.13}$$

where $\mathrm{D} = \mathrm{d}x^\mu \mathrm{D}_\mu$ is the Lorentz-covariant derivative with respect to the connection ω^{ab} on the boundary and $T^a = \mathrm{D}e^a$. In addition, $R^{ab} = \mathrm{d}\omega^{ab} + \omega^{ac} \wedge \omega_c{}^b$ is the curvature 2-form on the boundary, where it is used the notation(5.3): $\epsilon_{abcd4} = \epsilon_{abcd}$, defined in the convention of the Levi-Civita symbol writing before.

Finally in this section, the equations of motion (4.16) that do not involve radial derivatives must be used to express all the boundary fields in terms of the sources. These constraints are crucial as they define the dynamics of the boundary, and are given by

$$\begin{aligned} C &= \epsilon_{abcd}\, F^{ab} \wedge F^{cd} = 0 , \\ C_a &= \epsilon_{abcd}\, F^{bc} \wedge T^d = 0 , \\ \bar{C}_a &= \epsilon_{abcd}\, F^{bc} \wedge \mathrm{D}k^d = 0 , \\ C_{ab} &= \epsilon_{abcd}\, \left(F^{cd} \wedge e^e \wedge k_e + 2T^c \wedge \mathrm{D}k^d\right) = 0 . \end{aligned} \tag{5.14}$$

Note that they do not depend on the radial coordinate σ, so they are truly holographic equations on the boundary. They govern the dynamics of the boundary fields $e^a(x)$, $\omega^{ab}(x)$ and $k^a(x)$.

5.2 Introduction of temperature

In orden to identify the holographic field theory as a thermal system, the next step is to place the model at a constant temperature T. Thus, the only option is for the gravitational dual to be a black hole, which naturally has the Hawking temperature T.

It is known that CS AdS gravity admits a static, spherically symmetric black hole solution. In Schwarzschild-like coordinates (t, y^i, r), where r is the radial coordinate with the asymptotic boundary located at $r \to \infty$, the solution takes the following form: [88]

$$\mathrm{d}s^2 = -f^2(r)\mathrm{d}t^2 + \frac{\mathrm{d}r^2}{f^2(r)} + r^2\mathrm{d}\Omega^2\,, \tag{5.15}$$

where $f(r) = \sqrt{r^2 - M}$ is the metric function and M is an integration constant. Because this metric is the five-dimensional continuation of the three-dimensional BTZ black hole geometry [89], the above solution is also called *dimensionally continued black hole*.

In Eq. (5.15), $\mathrm{d}\Omega$ represents the line element of the three-dimensional transverse submanifold $t, r = \text{const}$, which is the maximally symmetric space of unit radius. Denoting the "angles" in this space by y^i and the metric by $\gamma_{ij}(y)$, we have $\mathrm{d}\Omega^2 = \gamma_{ij}(y)\mathrm{d}y^i\mathrm{d}y^j$. In AdS space, the transverse space can have curvature $\varkappa = 0, 1$, or -1, corresponding to flat, spherical, and hyperbolic horizon topologies, respectively. Considering this, the condition $M = \mu - \varkappa \geq 0$ must be satisfied, where M is a non-negative parameter ensuring the existence of the horizon, and μ is the dimensionless mass parameter of the black hole.

The black hole (5.15) has the horizon

$$f^2(r_\mathrm{H}) = 0 \quad \Rightarrow \quad r_\mathrm{H} = \sqrt{M}\,, \quad M = \mu - \varkappa \geq 0\,, \tag{5.16}$$

with the Hawking temperature

$$T = \left.\frac{(f^2)'}{4\pi}\right|_{r_\mathrm{H}} = \frac{\sqrt{M}}{2\pi} = \frac{r_\mathrm{H}}{2\pi}\,. \tag{5.17}$$

Here the temperature proportional to the horizon radius is typical of dimensionally continued black holes.

It can be noted that a relation between the FG radial coordinate σ, given by (5.12), and the radial coordinate r in the black hole solution (5.15), can be found exactly. In the calculation, the integral $\int \frac{\mathrm{d}x}{\sqrt{x^2-M}} = \ln\left(x + \sqrt{x^2 - M}\right)$ must be used:

$$\frac{\mathrm{d}r^2}{f^2(r)} = \frac{\mathrm{d}\sigma^2}{4\sigma^2} \quad \Rightarrow \quad \frac{\mathrm{d}r}{f} = -\frac{\mathrm{d}\sigma}{2\sigma} \quad \Rightarrow \quad \sigma = \frac{1}{(r+f)^2}\,, \tag{5.18}$$

where the sign in the second step was chosen such that $\sigma \to 0$ as $r \to \infty$. Inverting the relation, it is following:

$$r = \frac{1}{2}\left(M\sqrt{\sigma} + \frac{1}{\sqrt{\sigma}}\right). \tag{5.19}$$

The black hole metric rewritten in terms of the FG coordinates reads

$$\mathrm{d}s^2 = \frac{\mathrm{d}\sigma^2}{4\sigma^2} - \frac{(M\sigma-1)^2}{4\sigma}\,\mathrm{d}t^2 + \frac{(M\sigma+1)^2}{4\sigma}\,\gamma^{ij}(y)\mathrm{d}y^i\mathrm{d}y^j. \tag{5.20}$$

To express the corresponding vielbein, the 5D Lorentz indices are decomposed as $a = (0, i, 4)$, and the three-dimensional vielbein is denoted by $\tilde{e}^m = \tilde{e}^m_i(y)\,\mathrm{d}y^i$, such that $\gamma_{ij} = \delta_{mn}\tilde{e}^m_i\tilde{e}^n_j$. The non-zero components of the five-dimensional vielbein are then given by:

$$\hat{e}^0 = \frac{1-M\sigma}{2\sqrt{\sigma}}\,\mathrm{d}t\,, \qquad \hat{e}^m = \frac{1+M\sigma}{2\sqrt{\sigma}}\,\tilde{e}^m\,, \qquad \hat{e}^4 = -\frac{\mathrm{d}\sigma}{2\sigma}\,. \tag{5.21}$$

The signs are chosen such that $\hat{e}^0$ and $\hat{e}^m$ have positive orientations with respect to the coordinates when $M = 0$, while the negative sign in $\hat{e}^4$ is consistent with the second expression in (5.18).

To identify the four-dimensional vielbein e^a and the quantity k^a, the induced vielbein (5.21) on the surface $\sigma = \text{const.}$ is compared with (5.11) to obtain:

$$\begin{aligned} e^0 &= \frac{1}{2}\,\mathrm{d}t\,, & k^0 &= -\frac{M}{2}\,\mathrm{d}t\,, \\ e^m &= \frac{1}{2}\,\tilde{e}^m\,, & k^m &= \frac{M}{2}\,\tilde{e}^m\,. \end{aligned} \tag{5.22}$$

Finally, it can constructed the 4D metric $g_{\mu\nu} = e^a_\mu e_{a\nu}$ and the tensor $k_{\mu\nu} = e_{a\mu}k^a{}_\nu$ as

$$g_{\mu\nu} = \frac{1}{4}\begin{pmatrix} -1 & 0 \\ 0 & \gamma_{ij}(y) \end{pmatrix}, \quad k_{\mu\nu} = \frac{M}{4}\begin{pmatrix} 1 & 0 \\ 0 & \gamma_{ij}(y) \end{pmatrix}, \quad \sqrt{|g|} = \frac{\sqrt{\gamma}}{16}\,, \tag{5.23}$$

defined in a conformally flat four-dimensional space. Here, $\gamma = \det[\gamma_{ij}]$.

So far, the quantities e^a and k^a have been obtained. However, the spin-connection source ω^{ab} cannot yet be identified, as the solution for the torsion field that satisfies Eqs. (5.14) has not been found. In the following section, the goal is to introduce an ansatz for the spin connection degree of freedom in order to provide all the necessary elements for obtaining the holographically dual model.

5.3 Introduction of dislocation

This section examines a sector of the solution space that is particularly relevant for holography applied to condensed matter. Since the focus is on dislocations in WSMs, the simplest case with physical significance corresponds to an axially symmetric and static solution, where a dislocation breaks spherical symmetry. The static condition arises from the fact that WSMs are crystals in (boundary) three spatial dimensions that remain unchanged over time.

To impose these conditions, it is necessary to develop the mathematical framework related to the spin connection. In the holographic field theory, the spin connection 1-form is given by

$$\omega^{ab} = \mathring{\omega}^{ab}(e) + K^{ab}\,, \qquad \mathring{\mathrm{D}}e^a = 0\,, \tag{5.24}$$

where $\mathring{\omega}^{ab}$ is the torsion-free or Levi-Civita spin connection that is fully determined by the metric, and the metric-independent part, $K^{ab} = -K^{ba} = K^{ab}{}_{\mu}\,\mathrm{d}x^{\mu}$ is the contorsion tensor. It carries the information about the torsional degrees of freedom, with the four-dimensional torsion 2-form field defined by

$$T^a = \frac{1}{2}\,T^a{}_{\mu\nu}\,\mathrm{d}x^{\mu}\wedge\mathrm{d}x^{\nu} = \mathrm{D}e^a\,. \tag{5.25}$$

There is a one-to-one relationship between the torsion and the contorsion,

$$T^a = K^{ab}\wedge e_b\,, \tag{5.26}$$

or in components $T_{\mu\alpha\beta} = e_{a\mu}\,T^a{}_{\alpha\beta}$ and $K_{\mu\nu\alpha} = e_{a\mu}e_{b\nu}\,K^{ab}{}_{\alpha}$, the relation is

$$T_{\mu\alpha\beta} = K_{\mu\beta\alpha} - K_{\mu\alpha\beta}\,, \tag{5.27}$$

or its inverse form

$$K_{\mu\alpha\beta} = \frac{1}{2}\,\left(T_{\alpha\mu\beta} - T_{\mu\alpha\beta} + T_{\beta\mu\alpha}\right)\,. \tag{5.28}$$

Holographic equations in ω^{ab} (and therefore in K^{ab}) that we want to solve, given by (5.14), are complicated because of their non-linearity. To simplify them, we need a physical ansatz on ω^{ab}, consistent with the black hole metric. The holographic equations for ω^{ab}

(and consequently for K^{ab}), given by (5.14), are complex due to their non-linearity. To simplify them, it is necessary to introduce a physical ansatz for ω^{ab} that is consistent with the black hole metric and satisfies the requirements of axial symmetry and staticity.

The following two subsections develop the details necessary to introduce the dislocation ansatz for the planar and hyperbolic cases, respectively. These cases are chosen because they are of interest for holographic purposes.

5.3.1 Planar case

The most interesting black holes for holographic purposes are black branes, with flat horizons ($\varkappa = 0$). To implement the axial symmetry, will write the three-dimensional transversal section of the metric in cylindrical coordinates $y^i = (\rho, \varphi, z)$, as

$$\mathrm{d}\Omega^2 = \mathrm{d}\rho^2 + \rho^2 \mathrm{d}\varphi^2 + \mathrm{d}z^2 \,. \tag{5.29}$$

Planar black holes have isometries given by the six Killing vectors $\xi \in \{p_m, j_m\}$, where p_m are transversal translations and j_m are transversal rotations, whose explicit expressions in cylindrical coordinates are given by

$$\begin{aligned}
p_0 &= \partial_t \,, \\
p_1 &= \cos\varphi\, \partial_\rho - \frac{\sin\varphi}{\rho}\, \partial_\varphi \,, & j_1 &= -z \sin\varphi\, \partial_\rho - \frac{z}{\rho} \cos\varphi\, \partial_\varphi + \rho \sin\varphi\, \partial_z \,, \\
p_2 &= \sin\varphi\, \partial_\rho + \frac{\cos\varphi}{\rho}\, \partial_\varphi \,, & j_2 &= -z \cos\varphi\, \partial_\rho + \frac{z}{\rho} \sin\varphi\, \partial_\varphi + \rho \cos\varphi\, \partial_z \,, \\
p_3 &= \partial_z \,, & j_3 &= \partial_\varphi \,.
\end{aligned} \tag{5.30}$$

They satisfy the Lie-bracket algebra ISO(3) with non-vanishing Lie brackets

$$[j_m, j_n] = -\epsilon_{mnk}\, j_k \,, \qquad [j_m, p_n] = \epsilon_{mnl}\, p_k \,, \qquad [p_m, p_n] = 0 \,. \tag{5.31}$$

In addition, a static system has also the Killing vector $p_0 = \partial_t$ that commutes with all previous isometries.

Introducing a dislocation in the field theory involves breaking the static spherical symmetry of the metric, reducing it to the static axial symmetry, $\{p_0, p_m, j_m\} \to \{p_0, j_3\}$, of

the torsion field. The isometry $j_3 = \partial_\varphi$ represents invariance under rotations around the z-axis.

The contorsion tensor has isometries $\xi \in \{p_0, j_3\}$ if it satisfies

$$\pounds_\xi K^{ab} = \left(\xi^\alpha \partial_\alpha K^{ab}{}_\lambda + \partial_\lambda \xi^\alpha K^{ab}{}_\alpha\right) \mathrm{d}x^\lambda = 0\,, \tag{5.32}$$

yielding the solution

$$K^{ab} = K^{ab}{}_\mu(\rho, z)\, \mathrm{d}x^\mu\,. \tag{5.33}$$

Similarly, for the torsion, the vanishing Lie derivative

$$\pounds_\xi T^a = \left(\xi^\alpha \partial_\alpha T^a{}_{\mu\nu} + \partial_\mu \xi^\alpha T^a{}_{\alpha\nu} + \partial_\nu \xi^\alpha T^a{}_{\mu\alpha}\right) \mathrm{d}x^\mu \wedge \mathrm{d}x^\nu = 0\,, \tag{5.34}$$

implies $T^a = \frac{1}{2}\, T^a_{\mu\nu}(\rho, z)\, \mathrm{d}x^\mu \wedge \mathrm{d}x^\nu$, which is consistent with K^{ab}.

Finally, it is worth noting that a rank-three tensor in four dimensions, with two anti-symmetric indices, can be expressed as a decomposition into its irreducible components

$$T_{\mu\nu\alpha} = -T_{\mu\alpha\nu} = \sqrt{|g|}\, \epsilon_{\mu\nu\alpha\beta}\, A^\beta + B_\alpha g_{\mu\nu} - B_\nu g_{\mu\alpha} + \tau_{\mu[\nu\alpha]}\,, \tag{5.35}$$

where $g = \det[g_{\mu\nu}]$, A^μ is the *axial torsion* vector describing the completely antisymmetric part of the torsion (4 components),

$$A^\mu = \frac{1}{3!\sqrt{|g|}}\, \epsilon^{\mu\nu\alpha\beta} T_{\nu\alpha\beta}\,, \tag{5.36}$$

B_μ is the *diagonal torsion* vector, corresponding to the trace of the torsion (4 components),

$$B_\mu = \frac{1}{3}\, g^{\alpha\beta} T_{\alpha\beta\mu}\,, \tag{5.37}$$

and the *tensorial torsion* $\tau_{\mu[\nu\alpha]} = -\tau_{\mu[\alpha\nu]}$ is a traceless and non-axial tensor (16 independent components),

$$\epsilon^{\alpha\beta\mu\nu} \tau_{\beta[\mu\nu]} = 0\,, \qquad g^{\mu\nu} \tau_{\mu[\nu\alpha]} = 0\,. \tag{5.38}$$

Similarly, this decomposition can be carried out for the contorsion field using (5.28),

$$K_{\mu\nu\alpha} = -K_{\nu\mu\alpha} = -\frac{1}{2}\sqrt{|g|}\, \epsilon_{\mu\nu\alpha\beta}\, A^\beta - B_\mu g_{\nu\alpha} + B_\nu g_{\mu\alpha} + \frac{1}{2}\, \left(\tau_{\nu[\mu\alpha]} - \tau_{\mu[\nu\alpha]} + \tau_{\alpha[\mu\nu]}\right)\,. \tag{5.39}$$

For simplicity, the analysis is restricted to cases where $\tau_{\mu[\nu\alpha]} = 0$. Consequently, the axial torsion A^μ and the diagonal component B_μ are the only nontrivial elements of T^a and K^{ab}:

$$\begin{aligned} T_{\mu\nu\alpha} &= \sqrt{|g|}\,\epsilon_{\mu\nu\alpha\beta}\,A^\beta + B_\alpha g_{\mu\nu} - B_\nu g_{\mu\alpha}\,, \\ K_{\mu\nu\alpha} &= -\frac{1}{2}\sqrt{|g|}\,\epsilon_{\mu\nu\alpha\beta}\,A^\beta - B_\mu g_{\nu\alpha} + B_\nu g_{\mu\alpha}\,, \end{aligned} \tag{5.40}$$

such that the fields A^μ and B_μ carry all the torsional degrees of freedom in the theory.

5.3.2 Hyperbolic case

The other interesting case, is the hyperbolic horizon with negative constant curvature: $\varkappa = -1$, since, as in the planar case, condensed matter systems are modeled as non-compact systems. The three-dimensional transversal metric in cylindrical coordinates $y^i = (\chi, \theta, z)$ have the form:

$$d\Omega^2 = \mathrm{d}\chi^2 + \sinh^2\chi \mathrm{d}\theta^2 + \cosh^2\chi\,\mathrm{d}z^2\,, \tag{5.41}$$

which describes the hyperbolic space $-(X^1)^2+(X^2)^2+(X^3)^2+(X^4)^2 = -1$, parameterized by

$$\begin{aligned} X^1 &= \cosh\chi\cosh z\,, \\ X^2 &= \cosh\chi\sinh z\,, \\ X^3 &= \sinh\chi\cos\theta\,, \\ X^4 &= \sinh\chi\sin\theta\,. \end{aligned} \tag{5.42}$$

Similar that for the planar horizon, the algebra for the generator of the isometries with $\varkappa = -1$ are equal to

$$\begin{aligned} [p_a, p_b] &= -\epsilon_{abc} j_c\,, \\ [j_a, j_b] &= -\epsilon_{abc} j_c\,, \\ [j_a, p_b] &= \epsilon_{abc} p_c\,. \end{aligned} \tag{5.43}$$

Since θ and z appear as cyclic coordinates in the line element, it is clear that $\partial_\theta = j_2$ and $\partial_z = p_3$ are Killing vectors. In addition, since we are interested in having axial symmetry,

only ∂_θ will be preserved, and also $p_0 = \partial_t$ since it is necessary to describe a static system. Therefore, like in the planar case, these isometries give the solution

$$K^{ab} = K^{ab}_\mu(\chi, z)\mathrm{d}x^\mu\,, \tag{5.44}$$

or equivalently for the torsion $T^a = \frac{1}{2}T^a_{\mu\nu}(\chi, z)\mathrm{d}x^\mu\mathrm{d}x^\nu$.

5.4 Odd-parity Abelian anomaly

Before going deeper into the explicit calculation of the odd-parity Abelian anomaly, it is instructive to recall the general framework of conserved currents in quantum field theories, particularly those arising from global symmetries via Noether's theorem. This provides a more intuitive foundation for understanding the chiral current and its associated chiral anomaly, as well as the Abelian current and anomaly, which play a central role in our holographic setup. As an illustrative example, we will derive the chiral current from the massless Dirac Lagrangian in four dimensions, highlighting its conservation at the classical level and the emergence of anomalies quantum mechanically.

In quantum field theories with fermionic degrees of freedom, an important example is the chiral (or axial) symmetry, which arises for massless Dirac fermions. The Lagrangian for a massless Dirac field in four-dimensional general spacetime is

$$\mathcal{L} = -\frac{\imath}{2}\sqrt{-g}\,\bar{\Psi}\gamma^\mu D_\mu\Psi \;+\; c.c.\,, \tag{5.45}$$

where Ψ is a four-component Dirac spinor, $\bar{\psi} = \psi^\dagger\gamma^0$, and γ^μ are the Dirac matrices satisfying the Clifford algebra $\{\gamma^\mu, \gamma^\nu\} = 2\eta^{\mu\nu}$. The covariant derivative over a spinor field is given by

$$D_\mu\Psi = \partial_\mu\Psi + \omega^{ab}_\mu\Sigma_{ab}\Psi \tag{5.46}$$

where $\Sigma_{ab} = \frac{1}{4}[\gamma_a,\, \gamma_b]$ and $\gamma_a = e^\mu_a\gamma_\mu$. This Lagrangian is invariant under the global chiral transformation

$$\psi \to e^{\imath\gamma^*}\psi, \quad \bar{\psi} \to \bar{\psi}e^{\imath\gamma^*} \tag{5.47}$$

where $\gamma^* = \imath\gamma^0\gamma^1\gamma^2\gamma^3$. Applying Noether's theorem with the transformations for the spinors $\delta\psi = \imath\alpha\gamma^*\psi$ and $\delta\bar{\psi} = \imath\bar{\psi}\gamma^*$, the chiral current is

$$J^{\mu}_{ch} = \bar{\psi}\gamma^{\mu}\gamma^*\psi\,. \tag{5.48}$$

On the other hand, this can be reproduced by the spin tensor current S^{μ}_{ab}, which is related to the chiral current as its completely antisymmetric part:

$$J^{\mu}_{ch} = e^{\mu}_{d}\,\epsilon^{abcd}S_{abc}\,, \tag{5.49}$$

with $S_{abc} = e_{\mu\,c}S^{\mu}_{ab}$. The spin tensor current is given by

$$S^{\mu}_{ab} = \frac{2}{\sqrt{-g}}\frac{\delta\mathcal{L}}{\delta\omega^{ab}_{\mu}} = -\imath e^{\mu\,c}\bar{\Psi}\gamma_c\gamma_{ab}\Psi \tag{5.50}$$

where it takes into account the contribution for the c.c. of the Dirac Lagrangian, and $\gamma_{ab} = \frac{1}{2}[\gamma_a,\,\gamma_b] = 2\Sigma_{ab}$. The antisymmetric part of the spin tensor current is defined as

$$S_{abd} = e_{\mu\,d}\,S^{\mu}_{ab} = -\imath\,e_{\mu\,d}e^{\mu\,c}\bar{\Psi}\gamma_c\gamma_{ab}\Psi\,, \tag{5.51}$$

where $\gamma_{[c}\gamma_{ab]} = \gamma_{cab} = \gamma_{abc}$. Using the properties $\gamma_{abc} = -\imath\epsilon_{abcd}\gamma^*\gamma^d$, $\{\gamma^*,\,\gamma^a\} = 0$ and $\epsilon_{abcd}\epsilon^{abde} = -\delta^e_d$, it obtained the chiral current

$$J^{\mu}_{ch} = \bar{\Psi}\gamma^{\mu}\gamma^*\Psi\,. \tag{5.52}$$

By this illustrative example, it is clear how the chiral currents can be constructed from the spin tensor currents, as an alternative to Noether's theorem.

In a holographic quantum field theory, the observable quantities are introduced as n-point functions calculated from the quantum effective action (3.8). For example, two important holographic currents corresponding to the Poincaré symmetry of the theory are the 1-point functions

$$\langle\tau^{\mu}_{\ a}(x)\rangle = \frac{1}{\sqrt{|g|}}\frac{\delta W[e,\omega]}{\delta e^{a}_{\mu}(x)}\,,\qquad \langle\sigma^{\mu}_{\ ab}(x)\rangle = \frac{1}{\sqrt{|g|}}\frac{\delta W[e,\omega]}{\delta\omega^{ab}_{\mu}(x)}\,, \tag{5.53}$$

where $\tau^{\mu}_{\ a}$ is the energy-momentum tensor and $\sigma^{\mu}_{\ ab}$ is the spin current. And they are derived from the variation

$$\delta W = \int\limits_{\partial\mathcal{M}}\left(\delta e^{a}\wedge\tau_a + \frac{1}{2}\,\delta\omega^{ab}\wedge\sigma_{ab}\right)\,, \tag{5.54}$$

where the 3-forms τ_a and σ_{ab} are Hodge duals to the stress tensor and spin current, respectively. Explicitly, its have that $\tau^{\mu}_{\ a} = -\frac{1}{3!\sqrt{|g|}}\,\epsilon^{\mu\nu\alpha\beta}\tau_{a\,\nu\alpha\beta}$ and $\sigma^{\mu}_{\ ab} = -\frac{1}{3!\sqrt{|g|}}\,\epsilon^{\mu\nu\alpha\beta}\sigma_{ab\,\nu\alpha\beta}$. The variation (5.54) is derived from the renormalized CS AdS gravity action evaluated on-shell, as presented in Ref. [20]. Consequently, the conserved currents are expressed in terms of the gravitational quantities as

$$\begin{aligned}\langle\tau_a\rangle &= -8\kappa\,\epsilon_{abcd}\left(R^{bc} + 2\,e^b\wedge k^c\right)\wedge k^d\,,\\ \langle\sigma_{ab}\rangle &= -16\kappa\,\epsilon_{abcd}\,T^c\wedge k^d\,.\end{aligned} \tag{5.55}$$

These quantities satisfy the quantum conservation laws (know as Ward identities) associated with diffeomorphisms and Lorentz transformations. Additionally, the energy-momentum tensor exhibits the Weyl anomaly, which is proportional to the Euler invariant [90, 91, 92, 93]:

$$\langle\tau^{a}_{\ a}\rangle = -\frac{\kappa}{4}\,\epsilon^{\mu\nu\lambda\sigma}\,\epsilon_{\alpha\beta\gamma\delta}\,R^{\alpha\beta}_{\ \ \mu\nu}\,R^{\gamma\delta}_{\ \ \lambda\sigma}\,, \tag{5.56}$$

because the classical conservation law for the Weyl dilatations is $\tau^{a}_{\ a} = e^{a}_{\mu}\tau^{\mu}_{\ a} = 0$.

A key focus of this investigation is the odd-parity Abelian[1] anomaly, $\mathcal{A}_{\rm odd}$, which might correspond to the chiral anomaly that represents a universal feature of WSMs. It is directly connected to the odd-parity Abelian current, derived from the spin current as its fully antisymmetric component [94, 95, 96]:

$$J^{\mu}_{\rm odd} = \frac{1}{3!}\,\epsilon^{abcd}\,e^{\mu}_{a}\sigma_{bcd}\,, \tag{5.57}$$

where $\sigma_{bcd} = e_{b\mu}\sigma^{\mu}_{\ cd}$. If its classical conservation law is $\frac{1}{\sqrt{|g|}}\,\partial_\mu(\sqrt{|g|}J^{\mu}_{\rm odd}) = 0$, then the Ward identity associated with the odd-parity Abelian transformations is

$$\mathcal{A}_{\rm odd} = \frac{1}{\sqrt{|g|}}\,\partial_\mu\left(\sqrt{|g|}\,\langle J^{\mu}_{\rm odd}\rangle\right)\,, \tag{5.58}$$

where the Abelian anomaly is non-vanishing only if this conservation law is broken at the quantum level.

[1] Throughout this thesis, "odd-parity Abelian" and "Abelian" are used interchangeably.

The holographic duality can be employed to express $\mathcal{A}_{\text{odd}}$ in terms of gravitational quantities. By utilizing (5.55) and (5.57), the holographic Abelian anomaly is given by

$$\mathcal{A}_{\text{odd}} = \frac{8\kappa}{3\sqrt{|g|}}\,\epsilon^{\lambda\nu\alpha\beta}\partial_\mu\left(k^\mu{}_\nu T_{\lambda\alpha\beta} - k_{\lambda\nu}T^\mu{}_{\alpha\beta}\right)\,. \tag{5.59}$$

The next step is to explicitly evaluate this anomaly based on the solution of the constraints (5.14). The result is anticipated to be proportional to a topological invariant density. On a Riemannian manifold, a natural candidate is the Pontryagin density for the Lorentz group, $R^{ab}\wedge R_{ab}$. However, in a Riemann-Cartan space, the Pontryagin density for the AdS_4 group emerges as a more suitable candidate, given by $R^{ab}\wedge R_{ab} + 2\left(R^{ab}\wedge e_a\wedge e_b - T^a\wedge T_a\right)$. There is an ongoing discussion in the literature regarding whether the second invariant contributes to the Abelian anomaly or whether their difference results in a trivial contribution [97, 98, 99]. As will be shown later in Subsec. 6.3.5 for the planar case, the difference between the AdS Pontryagin invariant and the Lorentz invariant, namely, the Nieh-Yan invariant [41], which arises purely from torsion, leads to the topological invariant relevant for the Abelian anomaly in holographic field theories.

In the case addressed by this investigation, for the dimensionally continued black holes, $k_{\mu\nu}$ and $g_{\mu\nu}$ are computed as shown in (5.23). Since $k_{\mu\nu}$ is symmetric, the second term in (5.59) vanishes. By substituting the decomposition (5.40) into the first term, it is found that the only torsion component relevant for the Abelian anomaly is the axial torsion A^μ, such that

$$\mathcal{A}_{\text{odd}} \;=\; -\frac{16\kappa}{\sqrt{\gamma}}\,\partial_\mu\left(\sqrt{\gamma}\,k^\mu{}_\nu\,A^\nu\right)\,, \tag{5.60}$$

where the identity $\epsilon^{\lambda\nu\alpha\beta}\epsilon_{\lambda\alpha\beta\gamma} = -3!\,\delta^\nu_\gamma$ is used. Furthermore, since the solution is static, the term involving ∂_t does not contribute, leading to

$$\mathcal{A}_{\text{odd}} = -\frac{16\kappa M}{\sqrt{\gamma}}\,\partial_i\left(\sqrt{\gamma}A^i\right) = -16\kappa M\,\nabla_i A^i\,, \tag{5.61}$$

where $\nabla_i = \nabla_i(\gamma)$ is the covariant derivative in the Riemannian spatial plane. This very important result implies that, in order to describe a WSM, it is crucial to identify the axial torsion tensor with the component $A^i \neq 0$.

Finally, this last result can be explicitly computed for the two three-dimensional transverse sections of the black hole horizon: the planar and hyperbolic cases.

5.4.1 Abelian anomaly for the planar black hole

For the planar black hole with the transverse section (5.29), $\sqrt{\gamma} = \rho$ and $T^a_{\mu\nu}(\rho, z)$, such that the Abelian anomaly becomes

$$\mathcal{A}_{\text{odd}} = -\frac{16\kappa M}{\rho}\,\partial_i\left(\rho A^i\right) = -16\kappa M\,\left(\frac{1}{\rho}\,A^\rho + \partial_\rho A^\rho + \partial_z A^z\right). \tag{5.62}$$

It remains to solve the boundary equations (5.14) and determine $T^a_{\ \mu\nu}$ with nontrivial A^ρ or A^z.

5.4.2 Abelian anomaly for the hyperbolic black hole

The explicit form of the Abelian anomaly in the hyperbolic 3-space [100] is

$$\mathcal{A}_{\text{odd}} = -\frac{16\kappa}{\sqrt{\gamma}}\,M\,\partial_i\left(\sqrt{\gamma}A^i\right)\,, \tag{5.63}$$

using $\sqrt{\gamma} = \sinh\chi\cosh\chi$ we get

$$\mathcal{A}_{\text{odd}} = -16\kappa\,M\left(\left(\coth\chi + \tanh\chi\right)A^\chi + \partial_\chi A^\chi + \partial_z A^z\right) \tag{5.64}$$

with $i = \chi\,, z$, remembering that $A_\theta = 0$ because of the axial symmetry.

Thus far, the holographic quantum field theory (QFT) at finite temperature has been constructed by applying the holographic dictionary to a dimensionally continued black hole. Furthermore, the holographic dictionary has been employed to map an appropriate ansatz for the torsional degree of freedom, which represents structures in the dual theory that are essential for the existence of the Abelian anomalies described in equations (5.62) and (5.64). At this point, it is crucial to highlight key aspects regarding the anomalies observed in both cases.

It should be emphasized that these Abelian chiral anomalies (5.62) and (5.64), manifest as total divergences, raising the non-trivial question of why they do not vanish globally, as one might anticipate from applying Stokes' theorem or similar integral identities in a topologically trivial spacetime. In a simply connected, non-singular spacetime, the integral

of a total divergence over a closed volume would reduce to a surface term that vanishes at infinity. However, this cancellation is obstructed in our model due to the presence of topological defects encoded by the torsion fields. As elaborated in chapters 6 and 7, the torsion fields that satisfy the system of equations emerge as topological defects—manifestations of broken discrete translational symmetry in the crystal lattice, analogous to dislocations. These defects introduce a non-trivial topology, preventing a globally consistent definition of the symmetry transformation. Specifically, the torsion solutions exist only for constant coordinate values (e.g., a fixed radial coordinate). Consequently, the anomalies, which are sourced by these torsion fields and proportional to topological invariants such as the Nieh-Yan term in the planar case, persist and do not integrate to zero globally.

In the following two chapters, the field equations at the boundary will be solved for both the planar and hyperbolic cases.

Chapter 6

Application 1: Planar Case

In this chapter, the equations (5.14) are solved with a focus on solutions featuring a non-vanishing A^μ field. This emphasis arises from equation (5.62), which requires a non-trivial A^μ to generate a non-vanishing Abelian anomaly in certain regions, following the approach developed in [1].

In this case, $k_{\mu\nu}$ is found to be symmetric, resulting in $k^a \wedge e_a = 0$. Consequently, the equations (5.14) simplify to:

$$\begin{aligned} C &= \epsilon_{abcd}\, F^{ab} \wedge F^{cd}\,, & C_a &= \epsilon_{abcd}\, F^{bc} \wedge T^d\,, \\ C_{ab} &= 2\epsilon_{abcd}\, T^c \wedge \mathrm{D}k^d\,, & \bar{C}_a &= \epsilon_{abcd}\, F^{bc} \wedge \mathrm{D}k^d\,, \end{aligned} \tag{6.1}$$

where

$$\begin{aligned} \mathrm{D}k^a &= \mathring{\mathrm{D}}k^a + K^{ab} \wedge k_b\,, \\ F^{ab} &= \mathring{\mathrm{D}}K^{ab} + K^{ac} \wedge K_c{}^b + 2\left(e^a \wedge k^b - e^b \wedge k^a\right)\,. \end{aligned} \tag{6.2}$$

In the above expressions, it is used the boundary metric (5.23), so it can be find the torsion-free spin connection $\mathring{\omega}^{ab}$ that satisfies $\mathring{\mathrm{D}}e^a = \mathrm{d}e^a + \mathring{\omega}^{ab} \wedge e_b = 0$, which has only one non-zero component,

$$\mathring{\omega}^{12} = \mathring{\omega}^{12}\,\delta^{ab}_{12} = -\delta^{ab}_{12}\,\mathrm{d}\varphi = -\mathrm{d}\varphi \quad \Rightarrow \quad \mathring{R}^{ab} = 0\,. \tag{6.3}$$

To proceed with solving equation (6.1), it is necessary to establish appropriate notation and perform some preliminary calculations, including the derivation of relevant identities. This is essential because equation (6.1) is non-linear, originating from a non-linear gravitational theory.

6.1 Notations and general identities: Planar case

Although the notation and conventions were already established in Subsections 5.1 and 5.1, the elements necessary for developing the equations (6.1) are revisited here. As a first step, Eqs. (6.1) are written in tensorial form and are simultaneously decomposed into $x^\mu = (t, y^i)$, where $y^i = (\rho, \varphi, z)$ are the cylindrical coordinates of the flat horizon. The Lorentz indices are decomposed in the tangent space as $a = (0, m)$, with $m = 1, 2, 3$. Since both tangent and spacetime indices use Latin characters, they are assigned as follows: the curved indices are taken from the beginning of the alphabet $(i, j, k, l, \ldots)$, while the flat indices are taken from the middle of the alphabet $(m, n, s, p, q, \ldots)$.

Notice that the 3D flat space is without torsion, namely,

$$\tilde{T}^m = \mathrm{d}\tilde{e}^m + \mathring{\omega}^{mn} \wedge \tilde{e}_n = 0\,. \tag{6.4}$$

As a consequence, we have the identity

$$\mathring{\mathrm{D}}k^a \;=\; \frac{M}{2}\,\delta^a_m \tilde{T}^m = 0\,. \tag{6.5}$$

To reduce the four-dimensional Levi-Civita symbol to three dimensions, the convention $\epsilon_{tijk} \equiv \epsilon_{ijk}$ is used, and the 3D surface element is denoted as $\mathrm{d}\sigma_i = \dfrac{\rho}{2}\,\epsilon_{ijk}\,\mathrm{d}y^j \wedge \mathrm{d}y^k$.

Axial and diagonal torsion. The axial torsion field $A^\mu(x)$ and the diagonal torsion field $B_\mu(x)$ are 4-vectors. However, under the axially symmetric ansatz introduced in Sec. 5.3, where the temporal components vanish identically and the fields are static, $A^i(y)$ and $B_i(y)$ become 3-vectors defined in the transversal section $\partial\Sigma$. In this context, the metric γ_{ij} and its inverse γ^{ij} are used to lower and raise the spatial indices. Additionally,

a tilde is used to indicate that the quantity is treated as three-dimensional, following the notation:

$$\boxed{\begin{array}{lll} \mathrm{d}\sigma_i = \dfrac{\rho}{2}\,\epsilon_{ijk}\,\mathrm{d}y^j\wedge\mathrm{d}y^k\,, & \mathrm{d}\tilde{\sigma}_m = \tilde{e}^i_m\,\mathrm{d}\sigma_i\,, & \\ A_{ij} = \rho\,\epsilon_{ijk}\,A^k, & \tilde{A}^m_j = \tilde{e}^{mi}A_{ij}\,, & A_i = \gamma_{ij}A^j\,, \\ \tilde{A}^{mn} = \tilde{e}^{mi}\tilde{e}^{nj}A_{ij}, & \tilde{A} = \dfrac{1}{2}\,A_{ij}\,\mathrm{d}y^i\wedge\mathrm{d}y^j\,, & \\ \tilde{A}^m = \tilde{A}^m_i\mathrm{d}y^i, & A^m = \tilde{e}^m_i A^i\,, & A^2 = \gamma_{ij}A^iA^j\,, \\ \tilde{B}^m = \tilde{e}^{mi}B_i\,, & \tilde{B} = B_i\mathrm{d}y^i\,, & B^2 = \gamma^{ij}B_iB_j\,, \end{array}}$$

which results in the identities

$$\tilde{A}^m\wedge\tilde{e}_m = -2\tilde{A}\,,\qquad \tilde{A}^{mn}\,\tilde{e}_n = \tilde{A}^m\,,\qquad \tilde{B}^n\tilde{e}_n = \tilde{B}\,. \tag{6.6}$$

General identities. The building blocks of the holographic equations are the following differential forms, expressed in terms of the quantities defined in the preceding paragraph:

- 1-form $K^{ab} = e^{a\mu}e^{b\nu}K_{\mu\nu\lambda}\mathrm{d}x^\lambda$

$$\begin{aligned} K^{0m} &= \frac{1}{\ell}\,\tilde{B}^m\,\mathrm{d}t + \frac{\ell^2}{8}\,\tilde{A}^m + \ell B_t\,\tilde{e}^m\,, \\ K^{mn} &= \frac{\ell}{8}\left(-\tilde{A}^{mn}\mathrm{d}t + A^t\,\epsilon^{mnk}\tilde{e}_k\right) - \tilde{B}^m\tilde{e}^n + \tilde{B}^n\tilde{e}^m\,; \end{aligned} \tag{6.7}$$

- 2-form $\mathrm{D}k^a$

$$\begin{aligned} \mathrm{D}k^0 &= \frac{M}{2}\,\mathrm{d}t\wedge\tilde{B} - \frac{\ell^3 M}{8}\,\tilde{A}\,, \\ \mathrm{D}k^m &= \frac{\ell M}{2}\left(B_t\,\mathrm{d}t\wedge\tilde{e}^m - \frac{\ell}{4}\,A^t\,\mathrm{d}\tilde{\sigma}^m + \tilde{e}^m\wedge\tilde{B}\right); \end{aligned} \tag{6.8}$$

- 2-form $T^a = \frac{1}{2}\,e^{a\mu}T_{\mu\alpha\beta}\,\mathrm{d}x^\alpha\wedge\mathrm{d}x^\beta$

$$\begin{aligned} T^0 &= \frac{1}{2}\,\mathrm{d}t\wedge\tilde{B} - \frac{\ell^3}{8}\,\tilde{A}\,, \\ T^m &= -\mathrm{d}t\wedge\left(\frac{\ell^2}{8}\,\tilde{A}^m + \frac{\ell}{2}\,B_t\,\tilde{e}^m\right) - \frac{\ell^2}{8}\,A^t\,\mathrm{d}\tilde{\sigma}^m - \frac{\ell}{2}\,\tilde{B}\wedge\tilde{e}^m; \end{aligned} \tag{6.9}$$

- 2-form F^{ab} with $A_t = 0$ y $B^t = 0$

$$
\begin{aligned}
F^{0m} &= \frac{1}{\ell}\,\mathrm{d}t \wedge \left(-\mathring{\mathrm{D}}\tilde{B}^m + \tilde{B}^m\tilde{B} - B^2\tilde{e}^m - \frac{\ell^4}{64}\,\tilde{A}^{mn}\tilde{A}_n\right) \\
&\quad + \frac{\ell^2}{8}\,\left(\mathring{\mathrm{D}}\tilde{A}^m - 2\tilde{A}\,\tilde{B}^m - \tilde{B}^n\tilde{A}_n \wedge \tilde{e}^m\right)\,, \\
F^{mn} &= \frac{\ell}{8}\,\mathrm{d}t \wedge \left[\mathring{\mathrm{D}}\tilde{A}^{mn} + 2\tilde{B}^m\tilde{A}^n - 2\tilde{B}^n\tilde{A}^m + \left(\tilde{A}^{ms}\tilde{e}^n - \tilde{A}^{ns}\tilde{e}^m\right)\tilde{B}_s\right] \\
&\quad -\mathring{\mathrm{D}}\tilde{B}^m \wedge \tilde{e}^n + \mathring{\mathrm{D}}\tilde{B}^n \wedge \tilde{e}^m + \left(-\tilde{B}^m\tilde{e}^n + \tilde{B}^n\tilde{e}^m\right) \wedge \tilde{B} \\
&\quad + \frac{\ell^4}{64}\,\tilde{A}^m \wedge \tilde{A}^n + \left(M - B^2\right)\,\tilde{e}^m \wedge \tilde{e}^n\,;
\end{aligned}
\tag{6.10}
$$

6.2 'No-go' solutions for dislocations

The Eqs. (6.1) must be analyzed in different branches of solutions, as not all of them could describe holographic QFT with dislocations.

Since a possible Abelian anomaly depends solely on the axial torsion, it is natural to first consider solving the holographic equations in the branch where the diagonal torsion vector is zero, $B_\mu = 0$. This section focuses on this branch and shows that it does not yield holographic QFTs with dislocation solutions.

6.2.1 Torsion field without diagonal component, $B_\mu = 0$

Although the diagonal torsion, B_μ, does not explicitly appear in the expression for the Abelian anomaly, it will be shown that the holographic QFTs with dislocations cannot exist without its presence. To prove this, assume that $B_\mu = 0$, so that the only non-vanishing component is the axial torsion, $A_\mu \neq 0$.

In this case, the building blocks of the holographic equations (6.1) have simpler form

$$\begin{aligned} K^{0m} &= \frac{\ell^2}{8}\,\tilde{A}^m\,, & K^{mn} &= \frac{\ell}{8}\left(-\tilde{A}^{mn}\mathrm{d}t + A^t\,\epsilon^{mnk}\tilde{e}_k\right)\,, \\ \mathrm{D}k^0 &= -\frac{\ell^3 M}{8}\,\tilde{A}\,, & \mathrm{D}k^m &= -\frac{\ell^2 M}{8}\,A^t\,\mathrm{d}\tilde{\sigma}^m, \\ T^0 &= -\frac{\ell^3}{8}\,\tilde{A}\,, & T^m &= -\frac{\ell^2}{8}\left(\mathrm{d}t\wedge\tilde{A}^m + A^t\,\mathrm{d}\tilde{\sigma}^m\right)\,, \end{aligned} \tag{6.11}$$

and the 2-form F^{ab} has the components,

$$\begin{aligned} F^{0m} &= \frac{\ell^2}{8}\,\mathring{\mathrm{D}}\tilde{A}^m + \frac{\ell^3}{64}\,\left(\tilde{A}^{mn}\tilde{A}_n\wedge\mathrm{d}t - A^t\,\epsilon^{mns}\tilde{A}_n\wedge\tilde{e}_s\right)\,, \\ F^{mn} &= \frac{\ell}{8}\left(-\mathring{\mathrm{D}}\tilde{A}^{mn}\wedge\mathrm{d}t + \mathrm{d}A^t\wedge\epsilon^{mns}\tilde{e}_s\right) + \frac{\ell^4}{64}\,\tilde{A}^m\wedge\tilde{A}^n \\ &\quad + \frac{\ell^2}{64}\left(-\tilde{A}^n{}_p\epsilon^{mps} + \tilde{A}^m{}_p\epsilon^{nps}\right)A^t\,\mathrm{d}t\wedge\tilde{e}_s + \left(M - \frac{\ell^2}{64}\,(A^t)^2\right)\,\tilde{e}^m\wedge\tilde{e}^n\,. \end{aligned} \tag{6.12}$$

Notice that $\mathring{\mathrm{D}}\tilde{A}^m = \mathrm{d}\tilde{A}^m - \mathrm{d}\varphi\,\delta^{mn}_{12}\tilde{A}_n$, and similarly for $\mathring{\mathrm{D}}\tilde{A}^{mn}$.

Now, the equations (6.1) will be solved. First, the equation $C_{ab}=0$ is analyzed. The transversal components

$$C_{mn} = -\frac{\ell^5 M}{32}\,\epsilon_{mns}\,\mathrm{d}t\wedge\tilde{A}^s\wedge\tilde{A} = -\mathrm{d}^4x\,\frac{1}{2}\,\rho^2\tilde{e}^{si}\epsilon_{mns}\epsilon_{ijl}A^jA^l = 0\,, \tag{6.13}$$

vanish identically due to symmetry reasons ($\epsilon_{ijl}A^jA^l\equiv 0$), and only is necessary to solve

$$C_{0m} = \frac{\ell^4 M}{32}\,A^t\epsilon_{mns}\,\mathrm{d}t\wedge\tilde{A}^n\wedge\mathrm{d}\tilde{\sigma}^s \propto A^tA_m = 0 \quad\Rightarrow\quad A^t = 0\,, \tag{6.14}$$

if one wants $A^i\neq 0$.

The next equation to analyze is $\bar{C}_a=0$. While the component $\bar{C}_0=0$ vanishes due to $\mathrm{D}k^m=0$, for other components, it is obtained

$$\bar{C}_m = \frac{\ell^4 M}{64}\,\epsilon_{mns}\,\mathrm{d}t\wedge\tilde{A}\wedge\mathring{\mathrm{D}}\tilde{A}^{ns} = -\mathrm{d}^4x\,\frac{\ell^4 M}{34}\rho\,A^i\mathring{\mathrm{D}}_iA_m\,,$$

which gives three differential equations

$$\begin{aligned} \bar{C}_1 &= 0 \quad\Rightarrow\quad A^i\partial_iA^\rho - \rho(A^\varphi)^2 = 0\,, \\ \bar{C}_2 &= 0 \quad\Rightarrow\quad A^i\partial_i\left(\rho A^\varphi\right) + A^\varphi A^\rho = 0\,, \\ \bar{C}_3 &= 0 \quad\Rightarrow\quad A^i\partial_iA^z = 0\,, \end{aligned} \tag{6.15}$$

where $A^i\partial_i = A^\rho\partial_\rho + A^z\partial_z$. From this equation, the possibilities for horizontal axial torsion, $Az = 0$, and vertical axial torsion, $Az \neq 0$, are distinguished.

Horizontal axial torsion $A_z = 0$

If the axial torsion A_i has only the horizontal components, $A_z = 0$, the equations are reduced to

$$\begin{aligned} 0 &= \frac{1}{2}\,\partial_\rho\,(A^\rho)^2 - \rho(A^\varphi)^2\,, \\ 0 &= A^\rho\left[\partial_\rho\,(\rho A^\varphi) + A^\varphi\right]\,. \end{aligned} \tag{6.16}$$

If $A^\rho = 0$, the first equation implies $A^\varphi = 0$, leading to a trivial solution. Since the Abelian anomaly vanishes in this case, this solution is not of interest. Therefore, $A^\rho \neq 0$ is required, and the equations can be solved as

$$A^\rho = \sqrt{C^2 - \frac{Z^2(z)}{\rho^2}}\,, \qquad A^\varphi(\rho) = \frac{Z(z)}{\rho^2}\,, \qquad A_z = 0\,, \tag{6.17}$$

where $C \neq 0$ is an integration constant and $\zeta(z)$ is an arbitrary, real function that remains to be determined. Note that A^ρ is well-defined only if $|Z(z)| \leq |C|\rho$, so the geometry of the solution must be carefully analyzed. For example, if $\rho = 0$ is allowed, $Z = 0$ is required, and the solution becomes $A^\rho = C$. The other possibility is to impose the existence of a minimum value, $\rho_{\min} \neq 0$, which allows $Z \neq 0$.

Furthermore, the $C_a = 0$ becomes

$$\begin{aligned} C_0 &= -\frac{\ell^2}{8}\,\epsilon_{mns}\,\mathrm{d}t \wedge \left(\frac{\ell^4}{64}\,\tilde{A}^m \wedge \tilde{A}^n + M\,\tilde{e}^m \wedge \tilde{e}^n\right) \wedge \tilde{A}^s = 0\,, \\ C_m &= \frac{\ell^4}{64}\,\epsilon_{mns}\,\mathrm{d}t \wedge \left(2\,\mathring{\mathrm{D}}\tilde{A}^n \wedge \tilde{A}^s + \mathring{\mathrm{D}}\tilde{A}^{ns} \wedge \tilde{A}\right) = 0\,. \end{aligned} \tag{6.18}$$

It can also be written as

$$\begin{aligned} C_0 &\propto \epsilon_{mns}\left(\frac{\ell^4}{64}\,\tilde{A}^m{}_i\tilde{A}^n{}_j + M\,\tilde{e}^m_i\tilde{e}^n_j\right)\tilde{A}^s{}_l\epsilon^{ijl}\,, \\ C_m &\propto \epsilon_{mns}\left(2\,\mathring{\mathrm{D}}_i\tilde{A}^n{}_j\tilde{A}^s{}_l + \frac{1}{2}\,\mathring{\mathrm{D}}_i\tilde{A}^{ns}A_{jl}\right)\epsilon^{ijl}\,. \end{aligned} \tag{6.19}$$

The component C_0 is identically zero due to symmetry. The second equation gives

$$C_m \propto \mathring{\mathrm{D}}_n A^n A_m + 2A^i \mathring{\mathrm{D}}_i A_m = 0\,, \tag{6.20}$$

applying the shorthand notation $\tilde{e}^i_m \mathring{\mathrm{D}}_i = \mathring{\mathrm{D}}_m$. Then, using the definition of the covariant derivative, $\mathring{\mathrm{D}}_i A_m = \partial_i A_m + \mathring{\omega}_{im\tilde{n}}\, A^{\tilde{n}}$, implies that the components have the form

$$\begin{aligned} \mathring{\mathrm{D}}_i A_1 &= \partial_i A^\rho - \delta^\varphi_i \rho A^\varphi\,, \\ \mathring{\mathrm{D}}_i A_2 &= \partial_i \left(\rho A^\varphi\right) + \delta^\varphi_i A^\rho\,, \\ \mathring{\mathrm{D}}_i A_3 &= \partial_i A^z\,, \end{aligned} \tag{6.21}$$

and it also finds

$$\tilde{e}^i_n \mathring{\mathrm{D}}_i A^n = \partial_\rho A^\rho + \partial_z A^z + \frac{1}{\rho}\, A^\rho\,. \tag{6.22}$$

Thus, the equations become

$$\begin{aligned} C_1 &= 0: \quad \left(\partial_\rho A^\rho + \partial_z A^z + \frac{1}{\rho}\, A^\rho\right) A^\rho + 2A^i \partial_i A^\rho - 2\rho (A^\varphi)^2 = 0\,, \\ C_2 &= 0: \quad \left(\partial_\rho A^\rho + \partial_z A^z + \frac{1}{\rho}\, A^\rho\right) \rho A^\varphi + 2A^i \partial_i \left(\rho A^\varphi\right) + 2A^\varphi A^\rho = 0\,, \\ C_3 &= 0: \quad \left(\partial_\rho A^\rho + \partial_z A^z + \frac{1}{\rho}\, A^\rho\right) A^z + 2A^i \partial_i A^z = 0\,. \end{aligned} \tag{6.23}$$

Plugging in the obtained solution (6.17), and knowing that $A^z = 0$ and $\partial_\varphi = 0$, the equation C_3 cancels out and the other two equations yield

$$\begin{aligned} 0 &= \frac{3}{2}\, \partial_\rho (A^\rho)^2 + \frac{1}{\rho}\, (A^\rho)^2 - 2\rho (A^\varphi)^2 = \frac{C^2}{\rho}\,, \\ 0 &= \rho A^\varphi \partial_\rho A^\rho + 5A^\rho A^\varphi + 2\rho A^\rho \partial_\rho A^\varphi = \frac{ZC^2}{\rho^2 \sqrt{C^2 - \frac{Z^2}{\rho^2}}}\,. \end{aligned} \tag{6.24}$$

It can be seen that the equations are satisfied only if the integration constant is $C = 0$, finally giving

$$A^\rho = \sqrt{-\frac{Z^2(z)}{\rho^2}}\,, \qquad A^\varphi = \frac{Z(z)}{\rho^2}\,, \qquad A_z = 0\,, \tag{6.25}$$

and a complex field A^μ. For the last equation, it is found

$$C = \frac{\ell^3}{16}\,\epsilon_{mns}\mathrm{d}t \wedge \left[\mathring{\mathrm{D}}\tilde{A}^m \wedge \mathring{\mathrm{D}}\tilde{A}^{ns} - \tilde{A}^{mq}\tilde{A}_q \wedge \left(\frac{\ell^4}{64}\,\tilde{A}^n \wedge \tilde{A}^s + M\,\tilde{e}^n \wedge \tilde{e}^s\right)\right]. \tag{6.26}$$

It can be analyzed term by term, and the identity can be applied $[\mathring{\mathrm{D}}_i, \mathring{\mathrm{D}}_j]V^m = \mathring{R}^{mn}_{ij}V_n = 0$. It is obtained

$$\begin{aligned}
\epsilon_{mns}\mathrm{d}t \wedge \mathring{\mathrm{D}}\tilde{A}^m \wedge \mathring{\mathrm{D}}\tilde{A}^{ns} &= -2\mathrm{d}^4x\,\partial_i\left[\left(\rho\tilde{e}^{mi}A^j - \rho\tilde{e}^{mj}A^i\right)\mathring{\mathrm{D}}_j A_m\right], \\
-\epsilon_{mns}\mathrm{d}t \wedge \tilde{A}^{mq}\tilde{A}_q \wedge \frac{\ell^4}{64}\,\tilde{A}^n \wedge \tilde{A}^s &= 0\,, \\
-\epsilon_{mns}\mathrm{d}t \wedge \tilde{A}^{mq}\tilde{A}_q M\,\tilde{e}^n \wedge \tilde{e}^s &= -4\mathrm{d}^4x\,M\rho\,A^2\,.
\end{aligned} \tag{6.27}$$

Therefore,

$$C \propto \partial_i\left[\rho\left(\tilde{e}^{mi}A^j - \tilde{e}^{mj}A^i\right)\mathring{\mathrm{D}}_j A_m\right] + 2M\rho\,A^2 = 0\,, \tag{6.28}$$

which is equivalent to

$$\begin{aligned}
0 \;=\; & \partial_\rho\left[\rho\left(A^j\partial_j A^\rho - \rho(A^\varphi)^2\right) - \rho A^\rho\left(\partial_\rho A^\rho + \partial_z A^z + \frac{1}{\rho}\,A^\rho\right)\right] \\
& + \partial_z\left[\rho A^j\partial_j A^z - \rho A^z\left(\partial_\rho A^\rho + \partial_z A^z + \frac{1}{\rho}\,A^\rho\right)\right] \\
& + 2M\rho\,\left(A^\rho\right)^2 + 2M\rho^3\,\left(A^\varphi\right)^2 + 2M\rho\,\left(A^z\right)^2\,.
\end{aligned} \tag{6.29}$$

Finally, replacing the solution (6.17), keeping the constant C for clarity, it is found that all terms cancel out, and it is again obtained that the equation is satisfied only if the integration constant vanishes,

$$0 = C^2\,. \tag{6.30}$$

It is concluded that the final solution is given by Eqs. (6.25). This solution is not satisfactory for two reasons. First, because A^i is a complex vector. Second, the function $Z(z)$ remains undetermined, showing that this branch does not provide a unique solution for the given boundary conditions. So, it is concluded that the holographic QFTs with dislocations do not exist when the only torsion component is the horizontal axial torsion field.

Non-horizontal axial torsion $A_z \neq 0$

Now, the case of vertical axial torsion is considered, that is, $A_z \neq 0$. Linear differential equations need to be solved

$$\begin{aligned}
0 &= \bar{C}_1 \propto A^i \partial_i A^\rho - \rho (A^\varphi)^2 \,, \\
0 &= \bar{C}_2 \propto A^i \partial_i \left(\rho A^\varphi\right) + A^\varphi A^\rho \,, \\
0 &= \bar{C} \propto A^i \partial_i A^z \,, \\
0 &= C_1 \propto \left(\partial_\rho A^\rho + \partial_z A^z + \frac{1}{\rho} A^\rho\right) A^\rho + 2 A^i \partial_i A^\rho - 2\rho (A^\varphi)^2 \,, \\
0 &= C_2 \propto \left(\partial_\rho A^\rho + \partial_z A^z + \frac{1}{\rho} A^\rho\right) \rho A^\varphi + 2 A^i \partial_i \left(\rho A^\varphi\right) + 2 A^\varphi A^\rho \,, \\
0 &= C_3 \propto \left(\partial_\rho A^\rho + \partial_z A^z + \frac{1}{\rho} A^\rho\right) A^z + 2 A^i \partial_i A^z \,,
\end{aligned} \tag{6.31}$$

and also

$$\begin{aligned}
0 = C \propto\ & \partial_\rho \left[\rho \left(A^j \partial_j A^\rho - \rho (A^\varphi)^2\right) - \rho A^\rho \left(\partial_\rho A^\rho + \partial_z A^z + \frac{1}{\rho} A^\rho\right)\right] \\
& + \partial_z \left[\rho A^j \partial_j A^z - \rho A^z \left(\partial_\rho A^\rho + \partial_z A^z + \frac{1}{\rho} A^\rho\right)\right] \\
& + 2\rho \left(A^\rho\right)^2 + 2\rho^3 \left(A^\varphi\right)^2 + 2\rho \left(A^z\right)^2 \,.
\end{aligned} \tag{6.32}$$

Replacing $\bar{C} = 0$ in $C_3 = 0$ and assuming $A^z \neq 0$, it is obtained

$$\partial_\rho A^\rho + \partial_z A^z + \frac{1}{\rho} A^\rho = 0 \,, \tag{6.33}$$

in which case $C_1 = 0$ takes the form

$$A^\rho \partial_\rho A^\rho + A^z \partial_z A^\rho - \rho (A^\varphi)^2 = 0 \,. \tag{6.34}$$

Plugging in all the known quantities in $C = 0$, it is finds

$$0 = \left(A^\rho\right)^2 + \rho \left(A^\varphi\right)^2 + \left(A^z\right)^2 \,. \tag{6.35}$$

The only real solution to the above equation is $A^i = 0$. Even allowing complex values for A^i, the solution has two arbitrary functions, making it undetermined, which is not physical.

It is concluded that the absence of diagonal torsion leads only to non-physical solutions for the torsion field, or those without the Abelian anomaly.

6.3 Holographic field theory with diagonal torsion

As shown in the previous section, a holographic description of dislocations requires a non-trivial diagonal torsion, $B_\mu \neq 0$, even though it does not explicitly enter the Abelian anomaly. This case is the focus of the current section.

To this end taking $\ell = 1$, the equation $C_{ab} = 0$ in (6.1) is considered, with the components

$$\begin{aligned} C_{0m} &= -\frac{M}{2}\,\epsilon_{mns}\,\mathrm{d}t \wedge \left(\frac{1}{4}\,A^t\,\mathrm{d}\tilde{\sigma}^n - \tilde{e}^n \wedge \tilde{B}\right) \wedge \left(\frac{1}{4}\,\tilde{A}^s + 2B_t\,\tilde{e}^s\right)\,, \\ C_{mn} &= -\frac{M}{4}\,\epsilon_{mns}\,B_t\,\mathrm{d}t \wedge \tilde{A} \wedge \tilde{e}^s\,, \end{aligned} \tag{6.36}$$

where $\tilde{B} \wedge \tilde{B} = 0$ and $\tilde{A} \wedge \tilde{A}^s = 0$ for symmetry reasons. The last equation can be solved when $A^i \neq 0$, leading to

$$B_t = 0\,. \tag{6.37}$$

The first equation, in this case, implies

$$\frac{1}{2}\,A^t A_m + \tilde{B}^n \tilde{A}_{nm} = 0\,. \tag{6.38}$$

A consistency relation is found by contracting it with $\tilde{e}_i^m A^i$, yielding

$$A^t = 0\,. \tag{6.39}$$

Then (6.38) implies that

$$\epsilon^{ijk} B_j A_k = 0\,, \tag{6.40}$$

namely, the 3D vectors $A_i = \gamma_{ij} A^j$ and B_i satisfy $\vec{A} \times \vec{B} = 0$, so they are parallel. A particular solution will be chosen where the proportionality factor between the vectors is constant,

$$A_i = 8c\,B_i\,, \qquad c = \text{const.} \neq 0\,. \tag{6.41}$$

The parameter c is referred to as the *dislocation parameter* because it characterizes the strength of the torsion field and its internal structure, i.e., how the diagonal torsion vector is twisted in relation to the axial torsion vector. It is important to note that the equation

(6.41) allows some components of A_i and B_i to vanish, but not all of them, since $\gamma_{ij}A^iA^j \neq 0$.

In that case, the equation $C_0 = 0$ is identically satisfied, while the remaining ones become

$$\begin{aligned}
\bar{C}_0 &\propto \epsilon^{ijk}B_i\partial_j B_k\,,\\
\bar{C}_i &\propto \partial_i B^2 - 2\left[\mathring{\mathrm{D}}_n\tilde{B}^n - M + 3\left(1-c^2\right)B^2\right]B_i - 4c^2\tilde{B}^j\tilde{e}_i^m\mathring{\mathrm{D}}_j\tilde{B}_m\,,\\
C_i &\propto \partial_i B^2 - \left[2\mathring{\mathrm{D}}_n\tilde{B}^n - M + 3\left(1-c^2\right)B^2\right]B_i - 2c^2\tilde{e}_i^m\mathring{\mathrm{D}}_n\left(\tilde{B}_m\tilde{B}^n\right)\,,\\
C &\propto \left(c^2-1\right)\left[\left(\mathring{\mathrm{D}}_m\tilde{B}^m\right)^2 + \mathring{\mathrm{D}}_n\tilde{B}^m\mathring{\mathrm{D}}_m\tilde{B}^n - 2MB^2\right]\\
&\quad + \left(3c^2-1\right)\left(\tilde{B}^i\partial_i B^2 + B^2\mathring{\mathrm{D}}_m\tilde{B}^m\right) + M\mathring{\mathrm{D}}_m\tilde{B}^m\,,
\end{aligned} \tag{6.42}$$

where $B^2 = \gamma^{ij}B_iB_j$ is defined. The form of the above equations simplifies when $c = \pm 1$, so the analysis of these cases will be conducted first.

6.3.1 'No-go' for the dislocation $c^2 = 1$

When $c^2 = 1$, Eqs. (6.42) are simplified to

$$\begin{aligned}
0 &= \partial_i B^2 - 2\left(\mathring{\mathrm{D}}_n\tilde{B}^n - M\right)B_i - 4\tilde{B}^j\tilde{e}_i^m\mathring{\mathrm{D}}_j\tilde{B}_m\,,\\
0 &= \partial_i B^2 - \left(2\mathring{\mathrm{D}}_n\tilde{B}^n - M\right)B_i - 2\tilde{e}_i^m\mathring{\mathrm{D}}_n\left(\tilde{B}_m\tilde{B}^n\right)\,,\\
0 &= 2\tilde{B}^i\partial_i B^2 + 2B^2\mathring{\mathrm{D}}_m\tilde{B}^m + M\mathring{\mathrm{D}}_m\tilde{B}^m\,.
\end{aligned} \tag{6.43}$$

To check their consistency, the first two equations are contracted with $\tilde{B}^i$, yielding

$$\begin{aligned}
0 &= \tilde{B}^i\partial_i B^2 + 2\left(\mathring{\mathrm{D}}_n\tilde{B}^n - M\right)B^2\,,\\
0 &= \left(4\mathring{\mathrm{D}}_n\tilde{B}^n - M\right)B^2\,,\\
0 &= 2\tilde{B}^i\partial_i B^2 + \left(2B^2 + M\right)\mathring{\mathrm{D}}_n\tilde{B}^n\,.
\end{aligned} \tag{6.44}$$

Since $B^2 \neq 0$, the second equation leads to $\mathring{\mathrm{D}}_n\tilde{B}^n = \frac{M}{4}$. As the black hole mass parameter must satisfy the strict inequality $M > 0$ for a QFT at finite temperature, as seen from

(5.17), the other two equations become

$$\tilde{B}^i \partial_i B^2 = \frac{3M}{2} B^2 \,, \qquad B^2 = -\frac{M}{14} \,. \tag{6.45}$$

This result is non-physical because it corresponds to a bulk geometry that is a naked singularity ($M < 0$) at zero temperature. Furthermore, the constant value of B^2 leads to the inconsistent equation $\frac{3M}{2} B^2 = 0$.

Since the goal is to describe a holographic QFTs with dislocation, it will be assumed that $c^2 \neq 1$ for the rest of the chapter.

6.3.2 Holographic field theory with a generic dislocation $c^2 \neq 1$

When the dislocation parameter satisfies $c^2 \neq 0$ and $c^2 \neq 1$, the first two equations of (6.42) can be treated as algebraic equations for $B_i \mathring{\mathrm{D}} n \tilde{B}^n$ and $\tilde{e} i^m \tilde{B}^j \mathring{\mathrm{D}} j \tilde{B} m$, and solved as

$$B_i \mathring{\mathrm{D}}_n \tilde{B}^n = a \partial_i B^2 \,, \qquad \tilde{e}_i^m \tilde{B}^j \mathring{\mathrm{D}}_j \tilde{B}_m = a\, \partial_i B^2 + (m + b B^2)\, B_i \,, \tag{6.46}$$

where the constants are defined as

$$m = \frac{M}{2c^2} > 0 \,, \qquad a = \frac{1}{2\,(1 + 2c^2)} > 0 \,, \qquad b = \frac{3\,(c^2 - 1)}{2c^2} \neq 0 \,. \tag{6.47}$$

By contracting Eqs. (6.46) with $\tilde{B}^i$, useful identities are obtained, mapping the differential expressions into algebraic ones:

$$\mathring{\mathrm{D}}_n \tilde{B}^n = \frac{m + b B^2}{2c^2} \,, \qquad \tilde{B}^i \partial_i B^2 = \frac{(m + b B^2) B^2}{2 a c^2} \,, \tag{6.48}$$

utilizing the identity $1 - 2a = 4ac^2$. As a result,

$$\partial_i B^2 = \frac{m + b B^2}{2 a c^2} B_i \,, \qquad \tilde{e}_i^m \tilde{B}^j \mathring{\mathrm{D}}_j \tilde{B}_m = \frac{m + b B^2}{4 a c^2} B_i \,. \tag{6.49}$$

Observe that (6.49) is merely a consequence of the preceding equations and is not equivalent to them. Therefore, even if (6.49) is satisfied, it remains necessary to verify the first equation in (6.48), as the second equation is automatically fulfilled.

The last equation in (6.42) yields

$$\mathring{\mathrm{D}}_m \tilde{B}^n \mathring{\mathrm{D}}_n \tilde{B}^m = \alpha B^4 + \beta B^2 + \gamma \,, \tag{6.50}$$

with the coefficients

$$\begin{aligned} \alpha &= \frac{3}{4c^4}\left[\frac{3\left(c^2-1\right)^2}{4c^4} - \left(1-3c^2\right)\left(3+4c^2\right)\right] , \\ \beta &= M\left[\frac{3\left(c^2-1\right)}{8c^8} - \frac{\left(1-3c^2\right)\left(3+4c^2\right)}{4c^4\left(c^2-1\right)} + \frac{3}{4c^4} - 2\right] , \\ \gamma &= \frac{M^2}{4c^4}\left(\frac{1}{4c^4} - \frac{1}{1-c^2}\right) . \end{aligned} \tag{6.51}$$

These equations must be solved for the diagonal torsion $B_i(\rho, z)$. In terms of components, the first equation in (6.49) becomes

$$B_\varphi = 0 \,, \qquad \partial_\rho B^2 = \frac{m+bB^2}{2ac^2}\, B_\rho \,, \qquad \partial_z B^2 = \frac{m+bB^2}{2ac^2}\, B_z \,, \tag{6.52}$$

here, $B^2 = B_\rho^2 + B_z^2$. Since $B_\varphi = 0$ and $\partial\varphi = 0$, the equation $\epsilon^{ijk} Bi \partial j Bk = 0$ is automatically satisfied. Meanwhile, the second equation in (6.49) can be expressed in terms of components as follows:

$$\begin{aligned} B_\rho \partial_\rho B_\rho + B_z \partial_z B_\rho &= \frac{m+bB^2}{4ac^2}\, B_\rho \,, \\ B_\rho \partial_\rho B_z + B_z \partial_z B_z &= \frac{m+bB^2}{4ac^2}\, B_z \,. \end{aligned} \tag{6.53}$$

Taking the difference of one (6.52) and two (6.53), a simpler system is obtained:

$$\begin{aligned} B_z\left(\partial_\rho B_z - \partial_z B_\rho\right) &= 0 \,, \\ B_\rho\left(\partial_\rho B_z - \partial_z B_\rho\right) &= 0 \,, \end{aligned} \tag{6.54}$$

where each equation becomes factorized, so the result depends on which factor vanishes.

When one component of B_i vanishes, for instance $B_z = 0$, and $B_\rho = B_\rho(\rho)$, the first differential equation in (6.46) reduces to $(1-2a)B_\rho \frac{\mathrm{d}B_\rho}{\mathrm{d}\rho} = 0$ which is consistent only when $2a = 1$, or equivalently $c = 0$. Since $c \neq 0$, this case is not allowed.

The case with another component vanishing, $B_\rho = 0$, $B_z = B_z(z)$, is equivalent, with the replacement $\rho \to z$, such that there is no solution in this case either.

Therefore, the only allowed possibility corresponds to both components non-vanishing, $B_z B_\rho \neq 0$. Then, it must hold

$$\partial_\rho B_z = \partial_z B_\rho \qquad \Leftrightarrow \qquad \nabla \times \vec{B} = 0\,, \tag{6.55}$$

meaning that the field $\vec{B}$ is irrotational and therefore it is a gradient of some torsion potential,

$$\vec{B} = \nabla\psi \qquad \Leftrightarrow \qquad B_i = \partial_i \psi\,. \tag{6.56}$$

This leaves only two independent equations,

$$\begin{aligned} B_\rho \partial_\rho B_\rho + B_z \partial_z B_\rho &= \frac{m + b\left(B_\rho^2 + B_z^2\right)}{4ac^2} B_\rho\,, \\ B_\rho \partial_z B_\rho + B_z \partial_z B_z &= \frac{m + b\left(B_\rho^2 + B_z^2\right)}{4ac^2} B_z\,. \end{aligned} \tag{6.57}$$

Finally, from (6.52), it becomes evident that there are two solution branches: one corresponding to a constant norm of the diagonal torsion, $B^2 = -\frac{m}{b}$, and another to an arbitrary norm of the diagonal torsion, $B^2 \neq const$. It turns out that only one of these branches leads to a solution with a non-trivial odd-parity Abelian anomaly, describing a holographic field theory with dislocations, as will be shown next.

6.3.3 'No-go' for the constant norm $B^2 = const$

Assuming that the vector B_i has a constant norm, its value is

$$|B| \equiv \sqrt{B_\rho^2 + B_z^2} = \sqrt{-\frac{m}{b}}\,, \qquad 1 - c^2 > 0\,, \tag{6.58}$$

and a general solution for the components reads

$$B_\rho = \sqrt{-\frac{m}{b}}\,\sin\vartheta\,, \qquad B_z = \sqrt{-\frac{m}{b}}\,\cos\vartheta\,, \qquad \vartheta = \vartheta(\rho, z)\,. \tag{6.59}$$

From (6.48), the identities $\mathring{\mathrm{D}}_n\tilde{B}^n = 0$ and $\tilde{B}^i\partial_i B^2 = 0$ can be deduced, allowing the last equation in (6.42) to be written as

$$\mathring{\mathrm{D}}_m\tilde{B}^n\mathring{\mathrm{D}}_n\tilde{B}^m = -2MB^2\,. \tag{6.60}$$

The l.h.s. of the above expression is computed directly from the definition of the covariant derivative,

$$\mathring{\mathrm{D}}_m\tilde{B}^n\mathring{\mathrm{D}}_n\tilde{B}^m = \left(\partial_\rho\tilde{B}^1\right)^2 + \left(\partial_z\tilde{B}^3\right)^2 + 2\partial_\rho\tilde{B}^3\partial_z\tilde{B}^1 + \left(\frac{1}{\rho}\,\tilde{B}^1\right)^2\,. \tag{6.61}$$

Plugging it back into (6.60) and using the solution (6.59), it is obtained

$$\cos^2\vartheta\,(\partial_\rho\vartheta)^2 + \sin^2\vartheta\left((\partial_z\vartheta)^2 + \frac{1}{\rho^2}\right) - 2\sin\vartheta\cos\vartheta\,\partial_\rho\vartheta\partial_z\vartheta = -2M\,. \tag{6.62}$$

Any solution for ϑ, if one exists, satisfies the complete system. However, the identity of the vanishing covariant derivative allows for the determination of

$$\mathring{D}_n\tilde{B}^n = 0 \quad \Rightarrow \quad \partial_\rho\vartheta = \left(\partial_z\vartheta - \frac{1}{\rho}\right)\tan\vartheta\,. \tag{6.63}$$

When $\sin\vartheta \neq 0$, by substituting the expression for $\partial_z\vartheta$ into (6.62), all terms with $\partial_z\vartheta$ cancel out, leading to $\sin^2\vartheta = -2M\rho^2$. This solution is not physical for real ϑ and positive M. Therefore, the only possible scenario is to have $\sin\vartheta = 0$, meaning $\vartheta = n\pi$ ($n \in \mathbb{Z}$), which implies $\tilde{B}^1 = 0$ and $\tilde{B}^3 = const$, and the expression for (6.61) becomes $\mathring{\mathrm{D}}_m\tilde{B}^n\mathring{\mathrm{D}}_n\tilde{B}^m = \left(\partial_z\tilde{B}^3\right)^2$, which leads to an inconsistent result for (6.62), namely $0 = M$.

We therefore conclude that the norm of the vector B_i cannot be constant.

6.3.4 Irrotational holographic dislocation

Finally, consider an irrotational vector $B_i = \partial_i\psi$ whose norm is not constant. The system of equations to solve is given by Eqs. (6.48)–(6.57), with the second equation expressed in components as in (6.57).

The general solution is

$$\psi(\rho,z)=\psi_0-\frac{4ac^2}{b}\,\ln\sin\left(\frac{\sqrt{2mb}}{8ac^2}\,(\rho+z)+\theta\right)\,, \tag{6.64}$$

where ψ_0 and θ are integration constants. The value of θ will be set to 0, as the origin of the coordinate system can always be shifted along the z-axis to satisfy this condition. Additionally, $\psi_0=0$ because the torsional field is the derivative of ψ, thus this constant will not contribute.

Because the root $\sqrt{2mb}$ can become complex for certain values of c, in terms of real functions, the general solution is

$$\psi=\begin{cases}2\zeta\ln\sin\Big(\omega\,(\rho+z)\Big)\,, & c^2-1>0\,,\\ 2\zeta\ln\sinh\Big(\omega\,(\rho+z)\Big)\,, & c^2-1<0\,,\end{cases} \tag{6.65}$$

where the parameters are introduced

$$\zeta=\frac{2c^4}{3\,(1+2c^2)\,(1-c^2)}\,,\qquad \omega=\frac{1+2c^2}{4c^4}\sqrt{\frac{3M}{2}\,|c^2-1|}>0\,. \tag{6.66}$$

The potential $\psi\,(\rho,z)$ depends only on one variable, $\rho+z$. The symmetry $\rho\leftrightarrow z$ implies the equality of the two components,

$$B_\rho=B_z=\begin{cases}2\omega\zeta\,\cot\Big(\omega\,(\rho+z)\Big)\,, & c^2-1>0\,,\\ 2\omega\zeta\,\coth\Big(\omega\,(\rho+z)\Big)\,, & c^2-1<0\,.\end{cases} \tag{6.67}$$

These two solutions are physically different because they have different periodicity, for instance.

Still, it is necessary to verify Eqs. (6.48) and (6.50). Given that the diagonal torsion depends only on $z+\rho$, these can be rewritten as

$$\begin{aligned}2\partial_\rho B_\rho+\frac{1}{\rho^2}\,B_\rho &= \frac{m+2bB_\rho^2}{2c^2}\,,\\ 4\,(\partial_\rho B_\rho)^2+\frac{1}{\rho^4}\,B_\rho^2 &= 4\alpha B_\rho^4+2\beta B_\rho^2+\gamma\,.\end{aligned} \tag{6.68}$$

A more simplified form of these equations, where the square of the derivative has been eliminated, is

$$\begin{aligned} 2\partial_\rho B_\rho &= -\frac{1}{\rho^2}\,B_\rho + \frac{m+2bB_\rho^2}{2c^2}\,, \\ 0 &= \left(4\alpha - \frac{b^2}{c^4}\right) B_\rho^4 + \frac{2bB_\rho^3}{\rho^2 c^2} + \left(2\beta - \frac{2}{\rho^4} - \frac{2mb}{c^2}\right) B_\rho^2 + \frac{mB_\rho}{\rho^2 c^2} + \gamma - \frac{m^2}{4c^4}\,. \end{aligned} \tag{6.69}$$

In the above equations, the terms $\frac{1}{\rho^2}$ break the symmetry between ρ and z, meaning that these equations cannot be satisfied for all (ρ, z). Therefore, it is assumed that a solution exists only on the ring $\mathcal{R}$, with radius $\bar{\rho}$, located in the horizontal plane centered at $\bar{z} = 0$, where the radial component $B_\rho(\bar{\rho}, \bar{z}) = \Omega$ is a constant parameter. It can then be shown that $\Omega \neq 0$; otherwise, the equations become inconsistent. Moreover, by taking the radial derivative of (6.67) and evaluating it at the ring $\mathcal{R}$, $\partial\rho B\rho$ can be expressed in terms of Ω, yielding

$$\text{At } \mathcal{R}: \quad \rho = \bar{\rho}\,, \quad z = 0\,, \quad B_\rho = \Omega\,, \quad \partial_\rho B_\rho = -2\zeta\omega^2 \mathrm{sgn}(c^2-1) - \frac{\Omega^2}{2\zeta}\,. \tag{6.70}$$

With this at hand, the equations become algebraic,

$$\begin{aligned} 0 &= \frac{3(c^2-1)}{c^2}\,\Omega^2 + \frac{\Omega}{\bar{\rho}^2} + m\,, \\ 0 &= \frac{3\,(3c^2-1)\,(4c^2+3)}{c^4}\,\Omega^4 + \frac{3\,(c^2-1)}{\bar{\rho}^2 c^4}\,\Omega^3 + \frac{m\Omega}{\bar{\rho}^2 c^2} - \frac{m^2}{1-c^2} \\ &\quad + \left(\frac{3\,(c^2-1)\,(1-2c^2)\,m}{2c^6} - \frac{(1-3c^2)\,(3+4c^2)\,m}{c^2\,(c^2-1)} + \frac{3m}{c^2} - 8c^2 m - \frac{2}{\bar{\rho}^4}\right)\Omega^2\,, \end{aligned} \tag{6.71}$$

where all the quantities are expressed in terms of the four free parameters $(c, m, \Omega, \bar{\rho})$, with c being the dislocation parameter, Ω the strength of the torsion field, $\bar{\rho}$ the radius of the ring, and m the mass parameter that determines the temperature of the holographic QFT as

$$m = \frac{2\pi^2}{c^2}\,T^2 > 0\,. \tag{6.72}$$

These parameters must be solved in such a way that (6.71) is satisfied. The first equation leads to the following solution for the radius of the ring:

$$\frac{1}{\bar{\rho}^2} = \frac{3(1-c^2)}{c^2}\,\Omega - \frac{m}{\Omega}\,. \tag{6.73}$$

When $c^2 > 1$, the r.h.s. of the above equation is always positive when Ω is negative while, when $c^2 < 1$, there are two cases when the r.h.s. becomes positive. This can be summarized by

$$\begin{array}{rcll} & \Omega < 0\,, & m > 0\,, & c^2 - 1 > 0\,, \\ \bar{\rho}^2 > 0 \quad \Rightarrow & \Omega > 0\,, & 0 < m < \frac{3(1-c^2)}{c^2}\,\Omega^2 \quad , & c^2 - 1 < 0\,, \\ & \Omega < 0\,, & m > \frac{3(1-c^2)}{c^2}\,\Omega^2\,, & c^2 - 1 < 0\,, \end{array} \tag{6.74}$$

such that a positive solution $\bar{\rho} = \bar{\rho}(m, c, \Omega)$ always exists, according to the above inequalities. Replacing obtained $\frac{1}{\bar{\rho}^2}$ in the second equation (6.71), it is possible to determine Ω from the polynomial

$$P(\Omega) = P_4\,\Omega^4 + mP_2\,\Omega^2 + m^2 P_0 = 0\,, \tag{6.75}$$

with the coefficients that depend only on c,

$$\begin{aligned} P_4 &= \frac{3(6c^6 + 14c^4 - 3c^2 - 3)}{c^6}\,, \\ P_2 &= -\frac{16c^{10} - 16c^8 - 46c^6 - 3c^4 + 24c^2 - 3}{2c^6(c^2 - 1)}\,, \\ P_0 &= -\frac{2c^4 - 2c^2 - 1}{c^2(c^2 - 1)}\,. \end{aligned} \tag{6.76}$$

The existence of real solutions to the above quadratic polynomial in Ω^2 depends on its discriminant, $m^2\Delta = (mP_2)^2 - 4m^2 P_4 P_0$. Consequently, the normalized discriminant, Δ, is solely a function of the dislocation parameter,

$$\begin{aligned} \Delta &= \frac{1}{c^{12}(c^2 - 1)^2}\Big(64c^{20} - 128c^{18} - 160c^{16} + 392c^{14} + 73c^{12} \\ &\quad + 165c^{10} - \frac{999}{4}\,c^8 - 39c^6 + \frac{225}{2}\,c^4 - 36c^2 + \frac{9}{4}\Big)\,. \end{aligned} \tag{6.77}$$

By solving the quadratic equation (6.75) for Ω^2, two solutions linear in m are obtained,

$$\Omega^2 = m\,\frac{-P_2 \pm \sqrt{\Delta}}{2P_4} \equiv m\,\Omega^2_{0,\pm}(c)\,, \tag{6.78}$$

where $\Omega_{0,\pm}$ is m-independent part. Its explicit form is

$$\Omega^2_{0,\pm} = \frac{16c^{10} - 16c^8 - 46c^6 - 3c^4 + 24c^2 - 3 \pm 2c^6|c^2 - 1|\sqrt{\Delta}}{12\,(c^2 - 1)\,(6c^6 + 14c^4 - 3c^2 - 3)}\,. \tag{6.79}$$

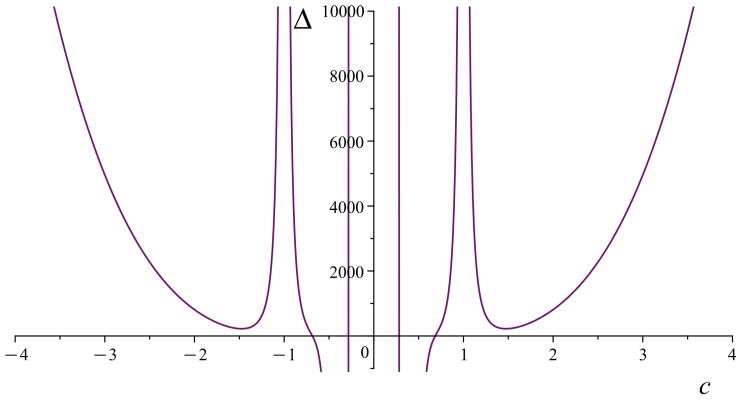

Figure 6.1: The discriminant Δ given by Eq. (6.77) as a function of the dislocation parameter c.

Then, the radius (6.73) can be solved as

$$\frac{1}{\bar{\rho}^2} = \frac{\sqrt{m}}{R^2(c)} \quad \Rightarrow \quad \bar{\rho} = m^{-\frac{1}{4}} R(c)\,, \tag{6.80}$$

with the c-dependent radial function given by

$$R(c) = \left(\frac{3\,(1-c^2)}{c^2}\,\Omega_{0,\pm} - \frac{1}{\Omega_{0,\pm}} \right)^{-\frac{1}{2}}. \tag{6.81}$$

The above expressions fully determine the dependence of the torsion strength Ω on m, as the parameter ω can also be factorized as

$$\omega = \sqrt{m}\,\omega_0(c)\,, \qquad \omega_0(c) = \frac{1+2c^2}{4c^4}\sqrt{3c^2|c^2-1|}\,. \tag{6.82}$$

To guarantee the existence of physical solutions, the following conditions must be satisfied:

1) Ω^2 *is real.* This condition is satisfied when the discriminant Δ, as given by (6.77), is non-negative, i.e., $\Delta \geq 0$. It holds for all dislocations in the intervals $0 < |c| \leq c_{01} \approx 0.288$ and $|c| \geq c_{02} \approx 0.685$, except at the points $|c| = 1$, where it becomes divergent. This can be see in the Fig. 6.1.

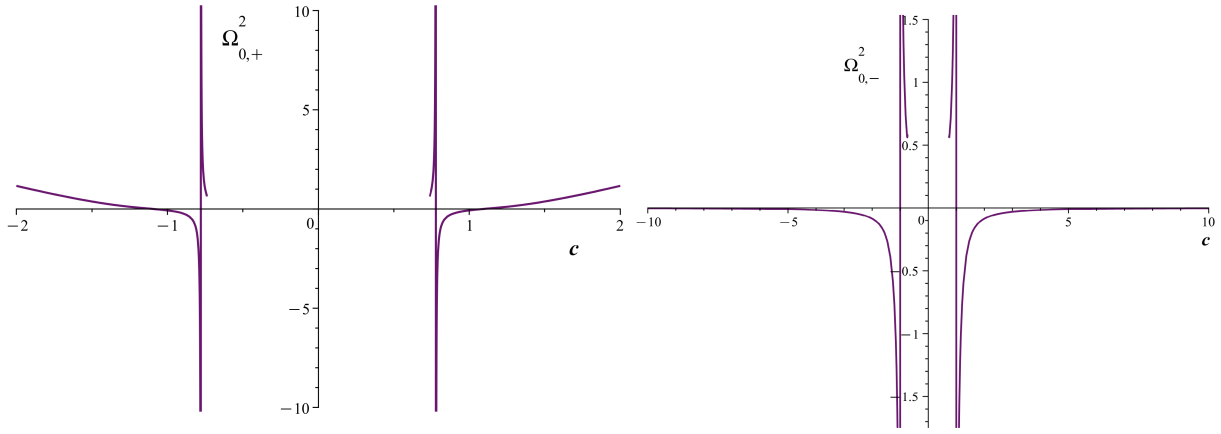

Figure 6.2: The square of the function $\Omega_{0,\pm}$, as defined in Eq. (6.79), depends on the dislocation parameter c. On the left, the positive solution $\Omega^2_{0,+}$ is shown, while on the right, the negative solution $\Omega^2_{0,-}$ is displayed.

2) Ω *is real.* This is analyzed based on the positivity of $\Omega^2_{0,\pm}$, as given by (6.79). This condition is satisfied for $\Omega^2_{0,+}$ when the dislocations lie within the intervals $c_{02} \leq |c| < c_\infty$ and $|c| > c_*$, where $c_\infty \approx 0.719$ is a divergence point due to the zero of the polynomial in the denominator, while $c_* \approx 1.169$ is the point where the polynomial vanishes. On the other hand, $\Omega^2_{0,-}$ is positive for the dislocations within the interval $c_{02} \leq |c| < 1$, avoiding the divergent point at $|c| = 1$. In Fig. 6.2, the behaviour of the functions can be observed.

3) $\bar{\rho}$ *is real.* This condition has already been discussed based on the positivity of $\bar{\rho}^2$, as given by Eqs. (6.73). This requirement is satisfied under the conditions specified in (6.74).

4) *Dependence on* m *is consistent.* The m-dependence of all previously discussed quantities has been determined. Its consistency is confirmed by comparing the m-dependence on both sides of equation (6.70). In general, these dependencies differ, unless the mass is a function of the dislocation parameter. This leads to a specific relation between the temperature $T = \sqrt{\frac{m}{2}}\frac{|c|}{\pi}$ and the dislocation parameter c. Finally, it should be verified whether the obtained $m(c)$ (or $T(c)$) satisfies the inequalities provided in

(6.74)

The critical points c of the solutions are summarized in the following table:

c	$= 0$			$\rightarrow$	excluded point;
$\lvert c\rvert$	$= c_{01}$	$\approx$	0.288	$\rightarrow$	vanishing discriminant, $\Delta = 0$;
$\lvert c\rvert$	$= c_{02}$	$\approx$	0.685	$\rightarrow$	vanishing discriminant, $\Delta = 0$;
$\lvert c\rvert$	$= c_{\infty}$	$\approx$	0.719	$\rightarrow$	divergence of $\Omega^2_{0,+}$;
$\lvert c\rvert$	$= 1$			$\rightarrow$	excluded point;
$\lvert c\rvert$	$= c_{*}$	$\approx$	1.169	$\rightarrow$	zero of $\Omega^2_{0,+}$.

(6.83)

To ensure the fulfillment of the four conditions, the analysis is first carried out for the periodic solutions, which correspond to large dislocation values, $c^2 - 1 > 0$, followed by the non-periodic solutions, associated with small dislocation values, $c^2 - 1 < 0$.

Periodic solution Examining the case of a large dislocation parameter, it has been demonstrated that the first three conditions are met exclusively in the positive branch of the torsion field when $\Omega_{0,+} < 0$, for dislocation parameters satisfying $|c| > c_*$. The radial dependence of the torsion field is determined by (6.66) and (6.67), expressed as

$$\Omega_{0,+}(c) = -\sqrt{\frac{c^2}{3(c^2-1)}}\,\cot\left(m^{\frac{1}{4}}\,\omega_0(c)R(c)\right) < 0\,, \tag{6.84}$$

here, the known expression for $\bar{\rho}$ from (6.81) has been substituted. The diagonal component of the torsion field becomes negative when the argument of the cotangent is within the interval $\left(0, \frac{\pi}{2}\right)$. To ensure the expression is invertible, the analysis is limited to the first period.

The fourth condition still needs to be enforced. Since the function $\Omega_{0,+}(c)$ can only depend explicitly on the dislocation parameter and not on the temperature, which scales as $\sqrt{m}$, the consistency of the identity above requires that m must be a function of c. This implies that the mass is not an independent parameter. By inverting the relations in (6.84),

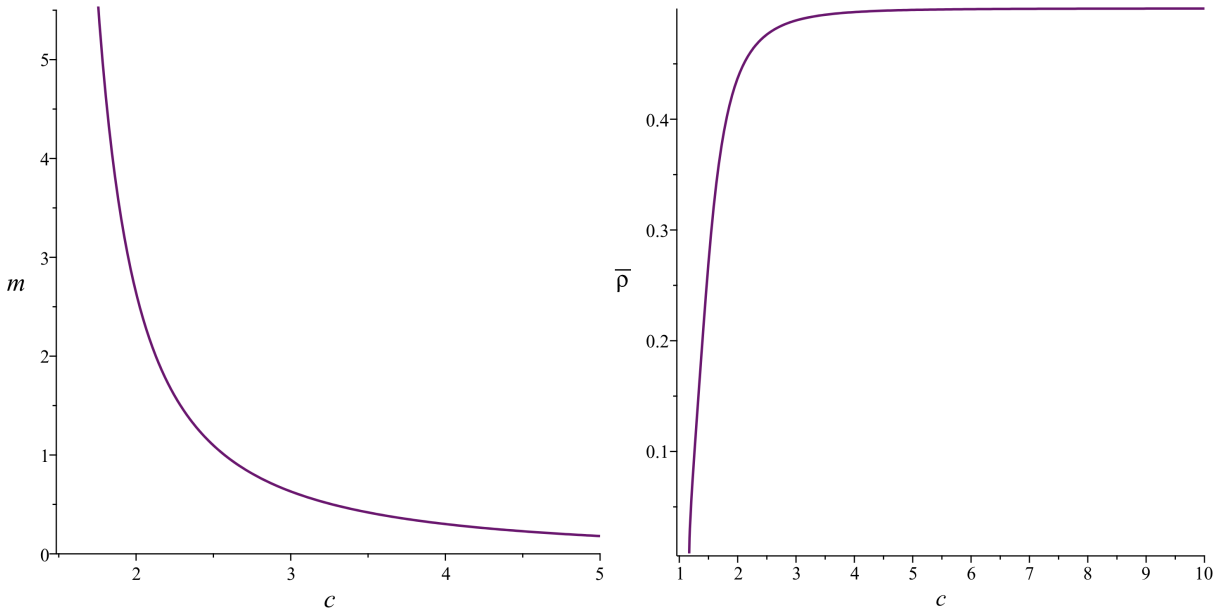

Figure 6.3: Periodic solution with the strength of the torsion field given by Eq. (6.84): (Right) The mass parameter m, as given by Eq. (6.85). (Left) And the radius of the ring, $\bar{\rho}$, as given by Eqs. (6.80) and (6.81), as a function of the dislocation parameter, c.

it is found that the mass of the black hole, or equivalently the temperature $T = \sqrt{\frac{m}{2}}\frac{|c|}{\pi}$ of the holographic field theory, is not arbitrary but depends on the dislocation parameter $|c| > c_* \approx 1.169$.

$$m = \frac{\operatorname{arccot}^4\left(-\sqrt{\frac{3(c^2-1)}{c^2}}\,\Omega_{0,+}\right)}{\omega_0^4 R^4}\,. \tag{6.85}$$

It can be directly verified that the argument of the cotangent falls within the required interval for any $c > c_*$. Additionally, the behavior of the function is illustrated in Fig. 6.3 (left).

To analyze the physical behavior of the system, Fig.6.3 (right) and Fig.6.4 display the temperature T, the nodal line radius $\bar{\rho} = m^{-\frac{1}{4}}R$ of the holographic field theory as functions of the dislocation parameter, and $\bar{\rho}(T)$, within the interval[1] $c > c_*$. Both T

[1]The interval $c < -c_*$ is derived from the parity of $T(c)$ and $\bar{\rho}(c)$.

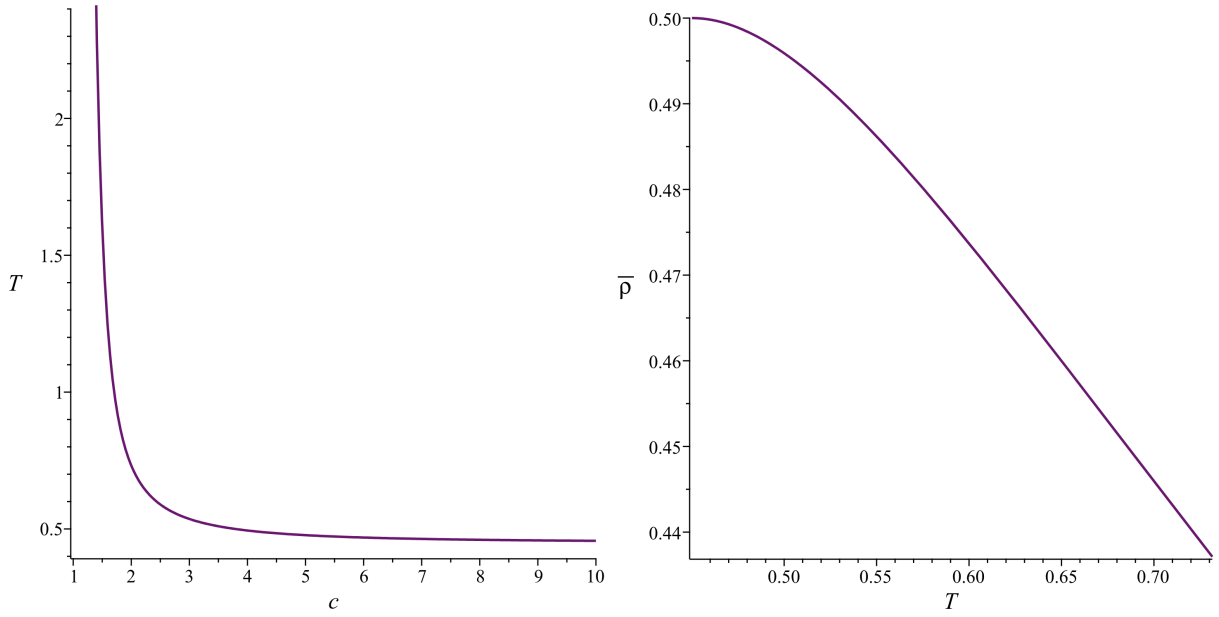

Figure 6.4: Periodic solution with the strength of the torsion field given by Eq. (6.84): (Left) Temperature, $T = \frac{|c|}{\pi}\sqrt{\frac{m}{2}}$, with the mass of the black hole in Eq. (6.85), as a function of the dislocation parameter, c. (Right) Dependence of the radius from the temperature, obtained from integrating out the dislocation parameter numerically.

and $\bar{\rho}$ exhibit monotonic behavior with respect to c. As shown in Fig.6.3 (right), the ring radius increases with c, while the temperature, illustrated in Fig.6.4 (left), decreases as the torsion (dislocation parameter) grows. For weak torsion, near c_*, the temperature becomes extremely high, resulting in a very small ring. This relationship is further supported by Fig. 6.4 (right), which demonstrates that larger rings correspond to lower temperatures. In the strong-torsion limit, as $c \to \infty$, both the temperature and the ring radius converge to finite values, specifically $\frac{\sqrt{2}}{\pi}$ and $\frac{1}{2}$, respectively, indicating the stability of the holographic WSM in this regime.

Non-periodic solution Now consider the case of small dislocation parameters. The first three conditions required for the existence of physical solutions are satisfied in the positive branch of the torsion field when the dislocation parameter lies within the narrow

interval $c_{02} \leq |c| < c_\infty$, as shown in Table (6.83). For the negative branch, these conditions hold when the dislocation parameter is within the range $c_{02} \leq |c| < 1$. In both scenarios, the sign of the torsion must align with the requirement specified in Eq. (6.74).

Using the obtained solutions, the torsion strength becomes

$$\Omega_{0,\pm}(c) = \sqrt{\frac{c^2}{3(1-c^2)}} \coth\left(m^{\frac{1}{4}}\,\omega_0(c)R(c)\right) . \tag{6.86}$$

It remains positive at all times since the argument of the hyperbolic cotangent is always positive. Consequently, as required by Eq. (6.74), the condition $1 < \frac{3(1-c^2)}{c^2}\,\Omega_{0,\pm}^2$ must also be satisfied.

Given that the left-hand side of the equation is independent of the mass parameter while the right-hand side depends on it, consistency requires the mass parameter to depend on the dislocation parameter c, specifically:

$$m_\pm = \frac{\operatorname{arccoth}^4\left(\sqrt{\frac{3(1-c^2)}{c^2}}\,\Omega_{0,\pm}\right)}{\omega_0^4 R^4} , \tag{6.87}$$

Within an appropriate range of the dislocation parameter c for each branch of the torsion field, the dependence of the mass $m_\pm(c)$ as a function of c can be seen in Fig. 6.5.

The dependence of the temperature and nodal radius on the dislocation parameter, as described by Eqs.(6.80) and (6.81), is presented in Figs.6.6 and 6.7. These figures also display the numerically obtained relationship between the nodal radius and temperature, $\bar{\rho}(T)$, for both positive and negative branches of the diagonal torsion.

For the positive branch, the solution exists within a very narrow range of the dislocation parameter, displaying significant changes in its properties. For example, the temperature decreases monotonically, as shown in Fig.6.6 (left), while Fig.6.6 (center) illustrates a notable reduction in the size of the nodal circle within this interval. Ultimately, as the temperature increases, the radius of the holographic field theory grows, as depicted in Fig. 6.6 (right).

In the negative branch, the temperature exhibits a maximum, as shown in Fig.6.7 (left). It starts at a small but finite value near c_{02}, increases until reaching $T_{\max} \approx 0.162$

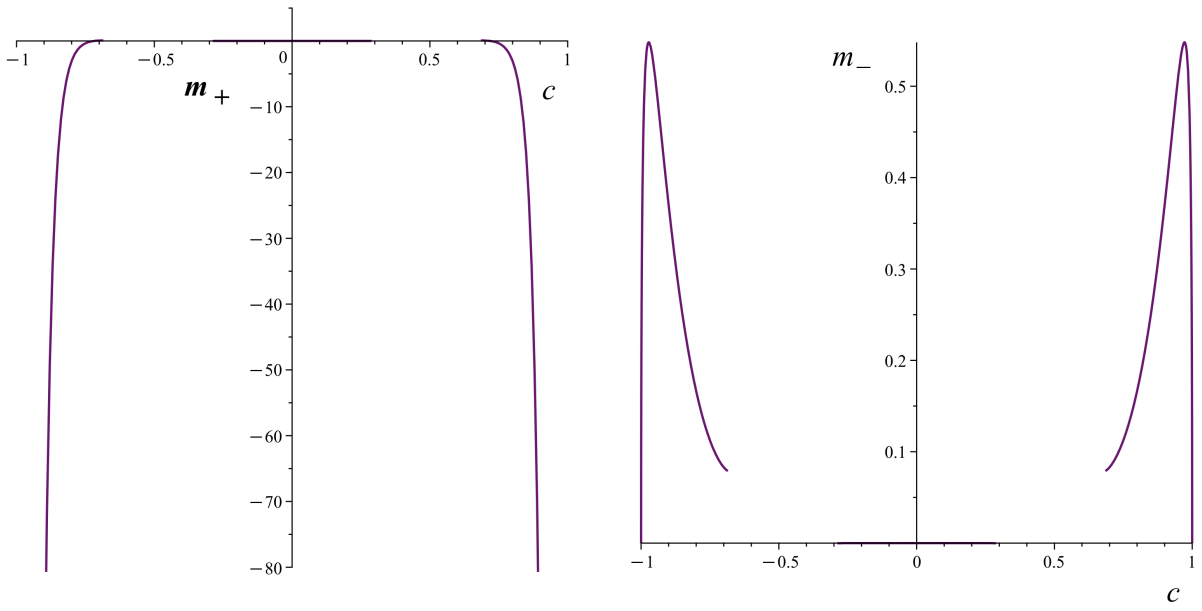

Figure 6.5: The mass in the positive branch (left) and the mass in the negative branch (right), in case of the non-periodic solution, as a functions of the c parameter.

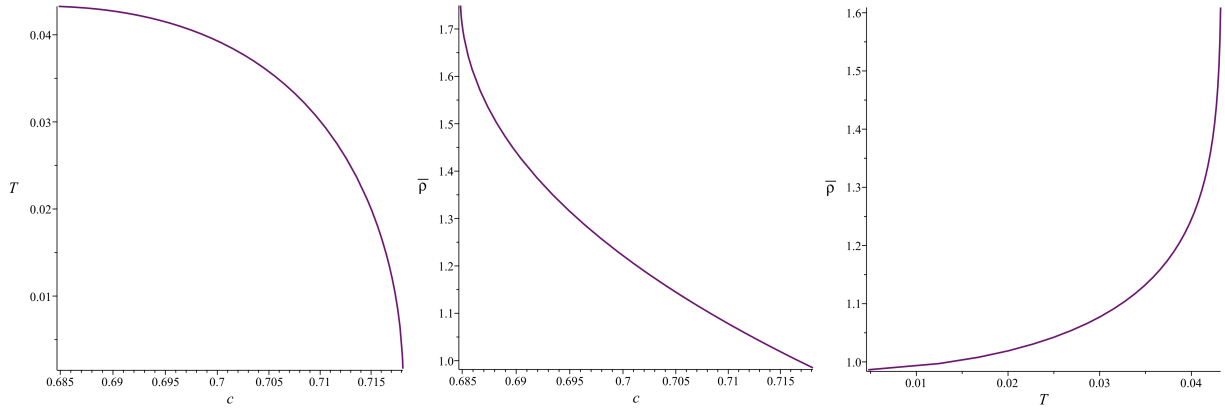

Figure 6.6: **Non-periodic solution, positive branch.** Temperature (left) and the nodal ring radius (center) as functions of the dislocation parameter c, as well as the dependence $\bar{\rho}(T)$ (right). The solution exists in the narrow interval $c_{02} \leq |c| < c_{\infty}$, as shown in Table (6.83).

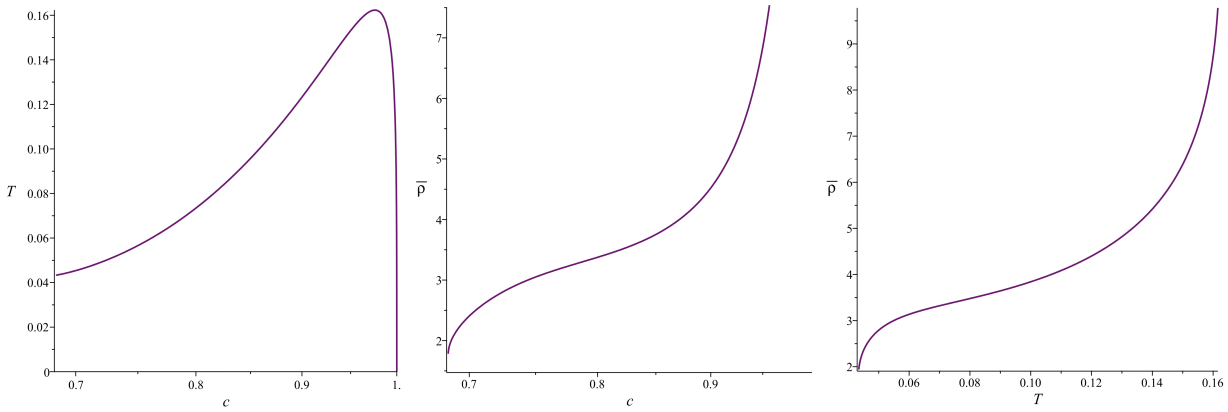

Figure 6.7: **Non-periodic solution, negative branch.** Temperature (left) and the nodal ring radius (center) as functions of the dislocation parameter. The direct dependence $\bar{\rho}(T)$ (right). The solution exists in the interval $c_{02} \leq |c| < 1$, as shown in Table (6.83).

at $|c| \approx 0.976$, and then rapidly decreases to small values as $|c|$ approaches 1. The nodal radius increases monotonically, as seen in Fig.6.7 (center), starting at small values for small $|c|$ and growing larger as $|c|$ nears 1. In contrast, as a function of temperature, the nodal radius increases from very small values to large ones, as shown in Fig. 6.7 (right)

The behavior of the solutions varies significantly among the three described cases. For example, in the periodic case, the nodal radius decreases as the temperature rises, whereas in the non-periodic case, it increases with temperature. This lack of universality is a consequence of the non-linearity inherent in the holographically dual theory, specifically CS AdS gravity. Physically relevant scenarios involve dislocations with torsion far from the critical points, where either the temperature or the nodal radius diverges. Notable examples include the regions near $\pm c_*$ for the periodic solution and $\pm c_{02}$ or ± 1 for the non-periodic solutions.

6.3.5 Abelian anomaly in the solutions

Up to this point, a well-defined holographic field theory at a fixed temperature, including dislocations, can be identified. Inspired by nodal Weyl semimetals, in which Weyl fermions

appear as quasiparticles only along a ring, the previously solutions can be interpreted as describing a system with an emergent type of quasiparticle that exists exclusively on the ring $\mathcal{R}$ of radius $\bar{\rho}$, located in the plane $\bar{z} = 0$. Since this emergent state exists only in the presence of the torsion fields $A_i(\bar{\rho}, z = 0)$ and $B_i(\bar{\rho}, z = 0)$, it follows that these fields act as sources for the holographic field theory. However, to confirm that these emergent states are indeed Weyl quasiparticles, it is necessary to demonstrate that the Abelian odd-parity anomaly corresponds to a genuine chiral anomaly.

The observable quantities—the temperature and the nodal radius—depend on the dislocation parameter c, which characterizes the internal twisting of the torsion field (or equivalently, the size of the torsional vortex), as well as on the intensity $\Omega(c)$ of the torsion field. This configuration exists only within three distinct intervals of c, each corresponding to a specific class of holographic field theories. Outside the ring, the torsion field vanishes; nevertheless, the temperature remains nonzero, as the entire system is in thermal equilibrium. Thus, T is a continuous and constant parameter throughout the space. In contrast, the torsion field is discontinuous due to the presence of an $\mathbb{S}^1$ topological defect representing the localized torsional vortex.

To determine the form of the Abelian anomaly, the torsion field in the holographic QFT -— or, more practically, the contorsion field (5.40) -— is first reconstructed along the nodal circle. As discussed previously, it takes the form

$$K^{ab} = \begin{cases} \bar{K}^{ab}\,, & \rho = \bar{\rho}\,, \quad z = \bar{z} = 0\,, \\ 0\,, & \rho \neq \bar{\rho}\,, \quad z \neq 0\,. \end{cases} \tag{6.88}$$

By utilizing the metric (5.23), (5.29), and the relation $A_i = 8c, B_i$ from (6.41), it is found that the contorsion at the points of the nodal circle is given by

$$\bar{K}_{\mu\nu} = \left(-\frac{1}{32}\,\bar{\rho}\,\epsilon_{\mu\nu\alpha\beta}\,A^{\beta} - B_{\mu}g_{\nu\alpha} + B_{\nu}g_{\mu\alpha} \right) \mathrm{d}x^{\alpha}\,. \tag{6.89}$$

It contains six independent components. Considering that $A_t, A_\varphi = 0$ and $B_t, B_\varphi = 0$, and using the notation (5.3), where $\epsilon_{t\rho\varphi z} = 1$, the following expression is obtained:

$$\begin{aligned} \bar{K}^{01} &= \Omega\,(\mathrm{d}t + 4c\bar{\rho}\,\mathrm{d}\varphi)\,, & \bar{K}^{12} &= -\Omega\,(4c\,\mathrm{d}t + \bar{\rho}\mathrm{d}\varphi)\,, \\ \bar{K}^{02} &= 4c\Omega\,(-\mathrm{d}\rho + \mathrm{d}z)\,, & \bar{K}^{13} &= \Omega\,(\mathrm{d}\rho - \mathrm{d}z)\,, \\ \bar{K}^{03} &= \Omega\,(\mathrm{d}t - 4c\bar{\rho}\,\mathrm{d}\varphi)\,, & \bar{K}^{23} &= \Omega\,(-4c\,\mathrm{d}t + \bar{\rho}\mathrm{d}\varphi)\,. \end{aligned} \tag{6.90}$$

In this calculation, the metric components were substituted, using $B_\rho = B_z = \Omega$ and $A^\rho = A^z = 32c, \Omega$. Additionally, the four-dimensional spacetime indices were projected onto the tangent space via the vielbein (5.22), specifically $\bar{K}^{ab} = e^{a\mu} e^{b\nu} \bar{K}_{\mu\nu}$.

Using the previous results, the Abelian anomaly (5.62) can be evaluated. The derivatives $\partial_\rho A^\rho = \partial_z A^z$ are determined directly from the first equation in (6.69)

$$\partial_\rho A^\rho = 32c\, \partial_\rho B_\rho = 32c \left(\frac{mc^2 + 3(c^2-1)\Omega^2}{4c^4} - \frac{\Omega}{2\bar{\rho}^2} \right) . \tag{6.91}$$

Using the identity (6.73), the dependence of the anomaly on the dislocation parameter is determined, expressed in a form that differentiates between the two branches:

$$A_{\text{odd}}(c) = 32^2 \kappa m c^3 \left[\frac{m^{\frac{3}{4}} \Omega_{0,\pm}}{R} + \frac{1+2c^2}{2c^2}\, m \left(1 + \frac{3(c^2-1)}{c^2}\, \Omega_{0,\pm}^2 \right) \right] . \tag{6.92}$$

All the quantities m, $\Omega_{0,\pm}$, and R are known functions of c, and the anomaly is present only in the range of c where these quantities are well-defined.

Fig. 6.8 shows the Abelian anomaly as a function of the dislocation parameter when the gravitational parameter is $\kappa = 1$. The graphs correspond only to the region $c > 0$, while the anomaly in the region $c < 0$ can be reconstructed using the property $\mathcal{A}_{\text{odd}}(-c) = -\mathcal{A}_{\text{odd}}(c)$. In general, the anomaly is not a monotonous function of the dislocation, but it exhibits one extremum for $c > 0$.

For large $|c|$, the Abelian anomaly becomes non-trivial when $|c| > c_*$. As shown in Fig. 6.8 (left), the anomaly is very large near c_*, then decreases until it reaches a minimum at $c \approx 3.386$, before increasing again linearly for large values of c. On the positive branch, shown in Fig.6.8 (center), the anomaly has a minimum when $c > 0$, but it remains negative. In contrast, in the negative branch, as seen in Fig.6.8 (right), the anomaly reaches a maximum when $c > 0$. Importantly, outside the ring, the anomaly is zero.

The previous analysis applies to an ideal holographic field theory with dislocations that does not account for dissipation, which may arise, for instance, from additional matter fields in the theory. Including dissipation could smooth out some of the divergences occurring near the critical torsion, i.e., dislocation configurations.

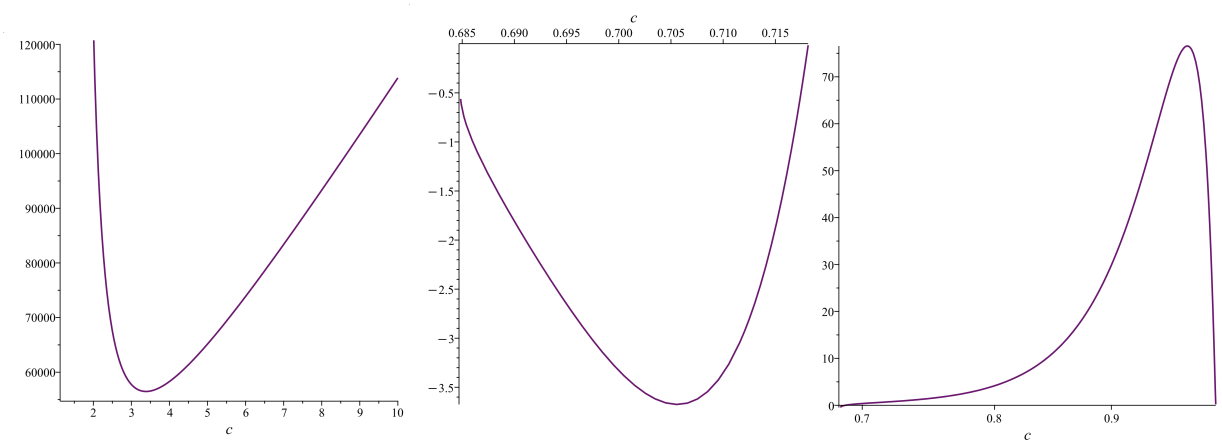

Figure 6.8: Abelian anomaly, $\mathcal{A}_{odd}$, given by Eq. (6.92), as a function of the dislocation parameter $c > 0$, for different classes of the solutions corresponding to distinct families of holographic field theories. (Left) $|c| > 1$, periodic solutions. (Center) $|c| < 1$, non-periodic solutions, positive branch. (Right) $|c| < 1$, non-periodic solutions, negative branch. The parameter κ is set to 1 in this analysis.

Abelian anomaly and topological invariant

The explicit expression for the Abelian anomaly was previously derived in Eq. (6.92). It is now demonstrated that this anomaly is proportional to the Nieh-Yan invariant $\mathcal{J}_{\rm NY}$, which represents the difference between the AdS Pontryagin invariant and the Lorentz invariant. This invariant is defined as:

$$T^a \wedge T_a - R^{ab} \wedge e_a \wedge e_b = \mathcal{J}_{\rm NY}\, \mathrm{d}^4x\,. \tag{6.93}$$

While the left-hand side can be locally expressed as $-\mathrm{D}(T^a \wedge e_a)$, it can yield a globally non-trivial contribution, leading to the Nieh-Yan topological invariant $\int \mathrm{d}^4x, \mathcal{J}_{\rm NY}$ [41]. The topological nature of the Abelian anomaly is closely related to this invariant, as shown below.

Using the torsion decomposition (5.40) and the metric (5.23), the following result is obtained:

$$T^a \wedge T_a = \frac{3\rho}{8}\, A^\mu B_\mu\, \mathrm{d}^4x\,. \tag{6.94}$$

In addition, since the curvature tensor decomposes as $R^{ab} = \mathring{R}^{ab} + \mathring{D}K^{ab} + K^{ac} \wedge K_c{}^b$ and $\mathring{R}^{ab} = 0$ for planar black holes, it follows that:

$$R^{ab} \wedge e_a \wedge e_b = \frac{3}{16} \left(\partial_\mu \left(\rho A^\mu \right) + 2\rho A^\mu B_\mu \right) \mathrm{d}^4 x \,. \tag{6.95}$$

When combining both terms, the $A^\mu B_\mu$ contribution cancels out, leaving the Nieh-Yan invariant in the form:

$$\mathcal{J}_{\mathrm{NY}} = -\frac{3}{16} \, \partial_\mu \left(\rho A^\mu \right) |_{\mathcal{R}} = -\frac{3}{16} \, \partial_i \left(\rho A^i \right) |_{\mathcal{R}} \,, \tag{6.96}$$

where $A^t = 0$ is used, and it is noted that the torsion field is non-trivial only along the ring $\mathcal{R}$. On the other hand, the Abelian anomaly, as given in Eq. (5.62), is directly proportional to the Nieh-Yan invariant:

$$\mathcal{A}_{\mathrm{odd}} = e_{\mathrm{odd}} \, \mathcal{J}_{\mathrm{NY}} \,. \tag{6.97}$$

The proportionality coefficient is written in terms of the gravitational constant G as

$$e_{\mathrm{odd}}(c) = \frac{8mc^2}{3\pi G \bar{\rho}} \,, \tag{6.98}$$

here, it is considered that $\ell = 1$, $\kappa = \frac{1}{64\pi G}$, and $M = 2mc^2$. Additionally, it is emphasized that the anomaly is non-zero only on the ring $\rho = \bar{\rho}$. The parameters m and $\bar{\rho}$ depend on the dislocation parameter c. The coefficient e_{odd} represents the central charge associated with the Abelian current. Central charges are significant physical observables, often encoding the number of degrees of freedom in a theory. In this context, e_{odd} depends on the black hole's mass, which is related to the temperature in the field theory.

Torsion-induced chiral anomalies are also known to be proportional to the Nieh-Yan invariant [97, 99], and renormalization conditions may affect their coefficients [101]. These result point that $\mathcal{A}_{odd}$ could be a chiral anomaly, in which case the obtained holographic theory could contain the quasiparticles analogous to those in Weyl semimetals. Nevertheless, for a clear answer, further investigation is needed.

To finish the section, it is essential to clarify why the anomaly, when evaluated on these solutions, takes the form of the Nieh-Yan tensor only on-shell. In the AdS/CFT correspondence, the on-shell bulk action $I_{\text{on-shell}}[e, \omega]$, is identified with the off-shell boundary

generating functional $W[e,\omega]$. To obtain physical solutions, we solve the bulk equations of motion (in the classical gravity regime, with a small gravitational constant G), ensuring that the torsion fields correspond to consistent configurations, such as topological defects like dislocations in our model. These on-shell solutions enable the computation of one-point correlation functions in the boundary QFT, such as the odd-parity Abelian current, by varying the generating functional with respect to the boundary sources. The on-shell condition in the bulk is necessary to ensure that these variations are performed only with respect to the boundary values of the fields, maintaining the consistency of the duality. However, the boundary QFT remains off-shell, as the generating functional encompasses all possible configurations, not just those satisfying the QFT's equations of motion. This reflects the weak/strong nature of the duality: classical gravity in the bulk computes strongly coupled quantum observables on the boundary. Thus, the equivalence of the anomaly to the Nieh-Yan tensor holds only on-shell, as it is only in these solutions that the torsion fields correctly encode the topological defects responsible for the anomaly's persistence in the holographic framework.

Another feature of this topological QFT configuration is the presence of a non-trivial Burgers vector, which is analyzed in the following section.

6.3.6 Burgers vector

In the geometric theory of defects, the Burgers vector is defined as the flux of the torsion tensor over a spatial surface, $b^i = \int T^i$ [39]. However, in a Lorentz-covariant system like this, it is more appropriate to define a 4-vector instead.

$$b^a = \int_{\mathcal{R}} T^a = \frac{1}{2} \int_{\mathcal{R}} T^a_{\mu\nu}\, \mathrm{d}x^\mu \wedge \mathrm{d}x^\nu \,. \tag{6.99}$$

Each component of the torsion tensor contains a (two-dimensional) Dirac delta function that restricts it to the value $\bar{T}^a_{\mu\nu}$, which is nontrivial along the nodal ring $\mathcal{R}$ located at $\rho = \bar{\rho}$ and $z = 0$. Given the static nature of the configuration, the integral is evaluated over a spacelike surface with constant time, setting $\mathrm{d}t = 0$. Using $\bar{T}^a = \bar{K}^{ab} \wedge e_b$, along with the four-dimensional contorsion (6.90) and the metric (5.22), the following expression

is obtained

$$\begin{aligned} \bar{T}^0 &= 4c\bar{\rho}\Omega\,(\mathrm{d}z-\mathrm{d}\rho)\wedge\mathrm{d}\varphi\,, \\ \bar{T}^1 &= -\bar{T}^3=\frac{\Omega}{2}\,\mathrm{d}\rho\wedge\mathrm{d}z\,, \\ \bar{T}^2 &= -\frac{\bar{\rho}\Omega}{2}\,(\mathrm{d}z+\mathrm{d}\rho)\wedge\mathrm{d}\varphi\,, \end{aligned} \tag{6.100}$$

This results in the Burgers 4-vector, projected from the tangent space onto the spacetime manifold, expressed as $b^\mu = e^\mu_a b^a = (b^t, \vec{b})$ with components given by:

$$b^t = -32\pi c\bar{\rho}\,\Omega\,, \qquad \vec{b} = (\Omega, 0, -\Omega)\ . \tag{6.101}$$

The non-vanishing nature of the Burgers 4-vector indicates the presence of a topological defect, or a torsional vortex, linked to the configuration of the torsion field. The torsion field strength Ω represents both the defect's strength and the magnitude of the Burgers vector. It characterizes an axially symmetric mixed screw-edge dislocation $b^\rho, b^z \neq 0$ within the spatial sector, excluding the time direction. Nevertheless, the b^t component introduces a connection to the time scale, implying the presence of a time crystal, where time-translational symmetry is spontaneously broken [102].

To further clarify the nature of the dislocation defects, the norm square of the Burgers vector (6.101) is calculated, yielding

$$b^2 = \left(\frac{1}{2} - 256\pi^2 c^2\bar{\rho}^2(c)\right)\Omega^2(c)\,. \tag{6.102}$$

It can be demonstrated that b^μ is a space-like vector (where b^2 is positive[2]) for the periodic solution within the very narrow range of dislocation parameters $c_* < c < 1.171$ (with $c_* \approx 1.169$). The upper limit of this interval corresponds to the space-time crystal, where the Burgers vector becomes null, $b^2 = 0$. In all other permitted dislocation ranges, the Burgers vector takes on a time-like nature ($b^2 < 0$), signifying a time-like dislocation defect in the time crystal, with continuous time-translation symmetry spontaneously broken. The associated time scale of this symmetry breaking is $\sim \sqrt{-b^2}$. Additionally, properties of space-time supersolids have been explored using holography in Ref. [103].

[2]The metric signature $(-,+,+,+)$ is used, meaning $b^2 > 0$ indicates a space-like vector.

Finally, the relationship between the torsional vortex (6.100) and the bulk geometry, specifically CS AdS gravity, is discussed. In the context of the four-dimensional holographic QFT, this defect is a codimension-2 surface, meaning it appears as a line in the 3D transversal plane. On the gravitational side, the components of torsion that contain defects affect both the AdS curvature and the bulk torsion, as seen from their radial expansions given in Eqs. (5.13). Thus, from the perspective of the gravitational theory, the topological defects manifest as codimension-3 surfaces within the torsional field.

Chapter 7

Application 2: Hyperbolic Case

This chapter is devoted to the analysis of the solutions corresponding to the hyperbolic horizon geometry. Non-compact horizons, planar or hyperbolic, correspond to QFTs on flat, infinite space, which align with low-energy description of condensed-matter systems [104, 105, 106] that, at least locally, can be modeled as spatially extended and unbounded. A Weyl semimetal described by low-energy field theory with Weyl excitations is a paradigmatic example in this sense. They allow well-defined densities (entropy, charge, energy), continuous momenta for transport and hydrodynamics, translational invariance and controlled breaking, and simpler numerical and analytic treatments. In particular, hyperbolic horizons probe holographic phases where negative curvature mimics an effective "frustration" scale [107]. In this case, the three-dimensional spatial sections of the bulk manifold possess negative constant curvature, $\varkappa = -1$, which considerably modifies the structure of the equations of motion compared to the planar case discussed previously. The presence of hyperbolic geometry introduces non-trivial dependencies on the radial coordinate and the dislocation parameter, making the analytical treatment more intricate.

The main objective of this chapter is to explore how the torsion fields interact in this background and to determine the conditions under which consistent solutions exist. We will show that [100], unlike the planar case—where two distinct families of solutions (periodic and aperiodic) appear—the hyperbolic configuration admits only a single family of aperiodic solutions, corresponding to the simplest branch that can be partially treated ana-

lytically. These solutions exhibit a well-defined dependence on the dislocation parameter c and on the black hole mass M, revealing a rich interplay between geometry and topological response.

As in the planar case, $k_{\mu\nu}$ is symmetric, implying that $k^a \wedge e_a = 0$. Consequently, equations (5.14) take the following form:

$$\begin{aligned} C &= \epsilon_{abcd}\, F^{ab} \wedge F^{cd}\,, & C_a &= \epsilon_{abcd}\, F^{bc} \wedge T^d\,, \\ C_{ab} &= 2\epsilon_{abcd}\, T^c \wedge \mathrm{D}k^d\,, & \bar{C}_a &= \epsilon_{abcd}\, F^{bc} \wedge \mathrm{D}k^d\,, \end{aligned} \tag{7.1}$$

where

$$\begin{aligned} \mathrm{D}k^a &= \mathring{\mathrm{D}}k^a + K^{ab} \wedge k_b\,, \\ F^{ab} &= \mathring{R}^{ab} + \mathring{\mathrm{D}}K^{ab} + K^{ac} \wedge K_c{}^b + 2\left(e^a \wedge k^b - e^b \wedge k^a\right)\,. \end{aligned} \tag{7.2}$$

where the boundary metric (5.23) is used, noting that the Riemannian part of the Riemann tensor is nonvanishing. From the Maurer–Cartan structural equation,

$$\mathring{\mathrm{D}}e^a = \mathrm{d}e^a + \mathring{\omega}^a{}_b \wedge e^b = 0\,, \tag{7.3}$$

the nonzero components of the torsion-free spin connection are found to be

$$\mathring{\omega}^{12} = -\cosh\chi\,\mathrm{d}\theta\,, \quad \mathring{\omega}^{13} = -\sinh\chi\,\mathrm{d}z\,. \tag{7.4}$$

In this way, the nonzero components of the torsion-free Riemann 2-form, $\mathring{R}^{ab}$, are

$$\mathring{R}^{12} = -\sinh\chi\,\mathrm{d}\chi\,\mathrm{d}\theta = -\tilde{e}^1 \wedge \tilde{e}^2\,, \tag{7.5}$$

$$\mathring{R}^{13} = -\cosh\chi\,\mathrm{d}\chi\,\mathrm{d}z = -\tilde{e}^1 \wedge \tilde{e}^3\,, \tag{7.6}$$

$$\mathring{R}^{23} = -\sinh\chi\cosh\chi\,\mathrm{d}\theta\,\mathrm{d}z = -\tilde{e}^2 \wedge \tilde{e}^3\,, \tag{7.7}$$

where dimensionless transverse vielbeins $\tilde{e}^m$ are defined as:

$$\begin{aligned} \tilde{e}^1 &= \mathrm{d}\chi\,, \\ \tilde{e}^2 &= \sinh\chi\,\mathrm{d}\theta\,, \\ \tilde{e}^3 &= \cosh\chi\,\mathrm{d}z\,. \end{aligned} \tag{7.8}$$

To proceed with the solution of equation (7.1), it is necessary to establish appropriate notation and carry out some preliminary calculations, including the derivation of relevant identities. This step is essential, as equation (7.1) is nonlinear in nature, arising from a nonlinear gravitational theory.

7.1 Notations and general identities: Hyperbolic case

First, some elements required for developing equations (7.1) are revisited. As an initial step, Eqs. (7.1) are expressed in tensorial form and simultaneously decomposed in terms of $x^\mu = (t, y^i)$, where $y^i = (\chi, \theta, z)$ denote the cylindrical coordinates of the hyperbolic horizon. The Lorentz indices are decomposed in the tangent space as $a = (0, m)$, with $m = 1, 2, 3$. Since both tangent and spacetime indices are represented by Latin characters, they are assigned as follows: curved indices are taken from the beginning of the alphabet $(i, j, k, l, \ldots)$, whereas flat indices are taken from the middle of the alphabet $(m, n, s, p, q, \ldots)$.

Notice that, by definition, in the three-dimensional hyperbolic space:

$$\mathring{\mathrm{D}} e^a = \mathrm{d}e^a + \mathring{\omega}^{ab} \wedge e_b = \mathring{\omega}^{ab} \wedge e_b = 0\,. \tag{7.9}$$

As a consequence, the following identity holds:

$$\mathring{\mathrm{D}} k^a \;=\; \frac{M}{2}\left(\mathrm{d}k^a + \mathring{\omega}^{ab} \wedge k_b\right) \propto M\, \mathring{\omega}^{ab} \wedge e_b = 0\,, \tag{7.10}$$

or in other words $\mathring{\mathrm{D}} k^a \propto \mathring{\mathrm{D}} e^a = 0$. To reduce the four-dimensional Levi-Civita symbol to three dimensions, the convention $\epsilon_{tijk} \equiv \epsilon_{ijk}$ is adopted, and the three-dimensional surface element is defined as $\mathrm{d}\sigma_i = \frac{\sinh\chi\cosh\chi}{2}\,\epsilon_{ijk}\,\mathrm{d}y^j \wedge \mathrm{d}y^k$.

Axial and diagonal torsion. The axial torsion field $A^\mu(x)$ and the diagonal torsion field $B_\mu(x)$ are both 4-vectors. However, under the axially symmetric ansatz introduced in Sec. 5.3, where the temporal components vanish identically and the fields are static, $A^i(y)$ and $B_i(y)$ reduce to 3-vectors defined on the transversal section $\partial\Sigma$. In this setting, the metric γ_{ij} and its inverse γ^{ij} are employed to lower and raise the spatial indices. Moreover,

a tilde is used to denote that the corresponding quantity is treated as three-dimensional, following the convention:

$$
\begin{array}{lll}
\mathrm{d}\sigma_i = \frac{\sinh\chi\cosh\chi}{2}\,\epsilon_{ijk}\,\mathrm{d}y^j\wedge\mathrm{d}y^k\,, & \mathrm{d}\tilde{\sigma}_m = \tilde{e}^i_m\,\mathrm{d}\sigma_i\,, & \\
A_{ij} = \sinh^2\chi\cosh\chi\,\epsilon_{ijk}\,A^k, & \tilde{A}^m_{\ j} = \tilde{e}^{mi}A_{ij}\,, & A_i = \gamma_{ij}A^j\,, \\
\tilde{A}^{mn} = \tilde{e}^{mi}\tilde{e}^{nj}A_{ij}, & \tilde{A} = \dfrac{1}{2}\,A_{ij}\,\mathrm{d}y^i\wedge\mathrm{d}y^j\,, & \\
\tilde{A}^m = \tilde{A}^m_{\ i}\mathrm{d}y^i, & A^m = \tilde{e}^m_i A^i\,, & A^2 = \gamma_{ij}A^iA^j\,, \\
\tilde{B}^m = \tilde{e}^{mi}B_i\,, & \tilde{B} = B_i\mathrm{d}y^i\,, & B^2 = \gamma^{ij}B_iB_j\,,
\end{array}
$$

which results in the identities:

$$
\tilde{A}^m\wedge\tilde{e}_m = -2\tilde{A}\,,\qquad \tilde{A}^{mn}\,\tilde{e}_n = \tilde{A}^m\,,\qquad \tilde{B}^n\tilde{e}_n = \tilde{B}\,,\qquad \mathrm{d}\tilde{\sigma}_m = \frac{1}{2}\,\epsilon_{mnk}\,\tilde{e}^n\wedge\tilde{e}^k\,. \quad (7.11)
$$

7.2 General equations at the boundary

The fundamental building blocks of the holographic equations are the following differential forms, expressed in terms of the quantities introduced in the preceding paragraph:

- 1-form $K^{ab} = e^{a\mu}e^{b\nu}K_{\mu\nu\lambda}\mathrm{d}x^\lambda$

$$
\begin{aligned}
K^{0m} &= \frac{1}{\ell}\,\tilde{B}^m\,\mathrm{d}t + \frac{\ell^2}{8}\,\tilde{A}^m + \ell B_t\,\tilde{e}^m\,, \\
K^{mn} &= \frac{\ell}{8}\,\Big(-\tilde{A}^{mn}\mathrm{d}t + A^t\,\epsilon^{mnk}\tilde{e}_k\Big) - \tilde{B}^m\tilde{e}^n + \tilde{B}^n\tilde{e}^m\,;
\end{aligned}
\quad (7.12)
$$

- 2-form $\mathrm{D}k^a$

$$
\begin{aligned}
\mathrm{D}k^0 &= \frac{M}{2}\,\mathrm{d}t\wedge\tilde{B} - \frac{\ell^3 M}{8}\,\tilde{A}\,, \\
\mathrm{D}k^m &= \frac{\ell M}{2}\,\left(B_t\,\mathrm{d}t\wedge\tilde{e}^m - \frac{\ell}{4}\,A^t\,\mathrm{d}\tilde{\sigma}^m + \tilde{e}^m\wedge\tilde{B}\right);
\end{aligned}
\quad (7.13)
$$

- 2-form $T^a = \frac{1}{2}\, e^{a\mu} T_{\mu\alpha\beta}\, \mathrm{d}x^\alpha \wedge \mathrm{d}x^\beta$

$$\begin{aligned} T^0 &= \frac{1}{2}\, \mathrm{d}t \wedge \tilde{B} - \frac{\ell^3}{8}\, \tilde{A}\,, \\ T^m &= -\mathrm{d}t \wedge \left(\frac{\ell^2}{8}\, \tilde{A}^m + \frac{\ell}{2}\, B_t\, \tilde{e}^m \right) - \frac{\ell^2}{8}\, A^t\, \mathrm{d}\tilde{\sigma}^m - \frac{\ell}{2}\, \tilde{B} \wedge \tilde{e}^m\,. \end{aligned} \tag{7.14}$$

Before calculating the 2-form components of F^{ab}, it is useful to analyze the third equation in (7.1), which has two distinct components, $C_{0m} = 0$ and $C_{mn} = 0$:

$$\begin{aligned} C_{0m} &= 2\epsilon_{mns} T^n \wedge \mathrm{D}k^s = -\frac{\ell^2 M}{2}\, \epsilon_{mns}\, \mathrm{d}t \wedge \left(\frac{\ell}{4}\, A^t\, \mathrm{d}\tilde{\sigma}^n - \tilde{e}^n \wedge \tilde{B} \right) \wedge \\ &\qquad \left(\frac{\ell}{4}\, \tilde{A}^s + 2B_t\, \tilde{e}^s \right)\,, \end{aligned} \tag{7.15}$$

$$C_{mn} = 2\epsilon_{mns} \left(T^0 \wedge \mathrm{D}k^s - T^s \wedge Dk^0 \right) = -\frac{\ell^4 M}{4}\, \epsilon_{mns}\, B_t\, \mathrm{d}t \wedge \tilde{A} \wedge \tilde{e}^s\,, \tag{7.16}$$

where $\tilde{B} \wedge \tilde{B} = 0$ and $\tilde{A} \wedge \tilde{A}^s = 0$ for symmetry reasons. The last equation can be solved when $A^i \neq 0$,

$$C_{mn} = 16\ell M \sinh\chi \cosh\chi\, \mathrm{d}^4x\, B_t\, \epsilon_{mns}\, A^s = 0 \quad \Rightarrow \quad B_t = 0\,. \tag{7.17}$$

The first equation, in this case, is developed term by term,

$$\begin{aligned} \epsilon_{mns}\, \mathrm{d}t \wedge \frac{\ell}{4}\, A^t\, \mathrm{d}\tilde{\sigma}^n \wedge \frac{\ell}{4}\, \tilde{A}^s &= \frac{\ell^2 \sinh\chi \cosh\chi}{8}\, \mathrm{d}^4x\, A^t A_m\,, \\ -\epsilon_{mns}\, \mathrm{d}t \wedge \tilde{e}^n \wedge \tilde{B} \wedge \frac{\ell}{4}\, \tilde{A}^s &= \frac{\ell \sinh\chi \cosh\chi}{4}\, \mathrm{d}^4x\, \tilde{B}^n \tilde{A}_{nm}\,, \end{aligned}$$

which implies

$$C_{0m} \;\propto\; \frac{\ell}{2}\, A^t A_m + \tilde{B}^n \tilde{A}_{nm} = 0\,. \tag{7.18}$$

A consistency equation is obtained by contracting with $A^m \neq 0$ (since $A^i \neq 0$), yielding

$$A^t A_i A^i = 0 \quad \Rightarrow \quad A^t = 0\,, \tag{7.19}$$

since $\tilde{\gamma}_{ij}$ is positive definite. This implies that

$$\tilde{B}^n \tilde{A}_{nm} = 0 \quad \Leftrightarrow \quad \epsilon_{ijk} \tilde{B}^j A^k = 0 \quad \Leftrightarrow \quad \epsilon^{ijk} B_j A_k = 0\,. \tag{7.20}$$

In general, the last equation is algebraic and admits nontrivial solutions, although it imposes a significant constraint on the vectors A^i and B_i, or, more importantly, on their functional dependence.

With $A_t = 0$ and $B_t = 0$, the remaining components for $R^{ab} + \frac{2}{\ell^2}\left(e^a \wedge k^b - e^b \wedge k^a\right)$ are

$$\begin{aligned} R^{0m} + \frac{2}{\ell^2}\left(e^0 \wedge k^m - e^0 \wedge k^m\right) &= \frac{1}{\ell}\,\mathrm{d}t \wedge \left(-\mathring{\mathrm{D}}\tilde{B}^m + \tilde{B}^m\tilde{B} - B^2\tilde{e}^m - \frac{\ell^4}{64}\,\tilde{A}^{mn}\tilde{A}_n\right) \\ &\quad + \frac{\ell^2}{8}\left(\mathring{\mathrm{D}}\tilde{A}^m - 2\tilde{A}\,\tilde{B}^m - \tilde{B}^n\tilde{A}_n \wedge \tilde{e}^m\right), \end{aligned} \tag{7.21}$$

and

$$\begin{aligned} R^{mn} + \frac{2}{\ell^2}\left(e^m \wedge k^n - e^n \wedge k^m\right) &= \frac{\ell}{8}\,\mathrm{d}t \wedge \Big[\mathring{\mathrm{D}}\tilde{A}^{mn} + 2\tilde{B}^m\tilde{A}^n - 2\tilde{B}^n\tilde{A}^m + \Big(\tilde{A}^{ms}\tilde{e}^n - \\ &\quad \tilde{A}^{ns}\tilde{e}^m\Big)\tilde{B}_s\Big] - \mathring{\mathrm{D}}\tilde{B}^m \wedge \tilde{e}^n + \mathring{\mathrm{D}}\tilde{B}^n \wedge \tilde{e}^m + \Big(-\tilde{B}^m\tilde{e}^n + \tilde{B}^n\tilde{e}^m\Big) \wedge \tilde{B} \\ &\quad + \frac{\ell^4}{64}\,\tilde{A}^m \wedge \tilde{A}^n + \left(M - B^2\right)\,\tilde{e}^m \wedge \tilde{e}^n\,. \end{aligned} \tag{7.22}$$

Before calculating the remaining equations, it is noted from equation (7.20) that the 3-dimensional vectors $A_i = \gamma_{ij}A^j$ and B_i satisfy $\vec{A} \times \vec{B} = 0$, which implies that they are parallel. Consequently, one can choose a particular solution in which the proportionality factor between the vectors is a function of the coordinates:

$$A_i = fB_i\,, \quad f = f(\chi, z) \neq 0\,. \tag{7.23}$$

Returning to the field equations (7.1), considering the identity by symmetry $\tilde{A}^m \wedge \tilde{A} = 0$, $\tilde{A}^{mn}\tilde{B}_n = 0$, $\tilde{B}^m\tilde{A}_m = 0$ and $\epsilon_{mns}\tilde{B}^m\tilde{B}^n = 0$ it is had

$$\begin{aligned} C &= \frac{4}{\ell}\,\epsilon_{mns}\,\mathrm{d}t \wedge \left(-\mathring{\mathrm{D}}\tilde{B}^m + \tilde{B}^m\tilde{B} - B^2\tilde{e}^m - \frac{\ell^4}{64}\,\tilde{A}^{mp}\tilde{A}_p\right) \wedge \Big[-2\mathring{\mathrm{D}}\tilde{B}^n \wedge \tilde{e}^s \\ &\quad -2\tilde{B}^n\tilde{e}^s \wedge \tilde{B} + \frac{\ell^4}{64}\,\tilde{A}^n \wedge \tilde{A}^s + \left(M - B^2 + \varkappa\right)\,\tilde{e}^n \wedge \tilde{e}^s\Big] \\ &\quad + \frac{\ell^3}{16}\,\epsilon_{mns}\,\mathrm{d}t \wedge \left(\mathring{\mathrm{D}}\tilde{A}^m - 2\tilde{A}\,\tilde{B}^m\right) \wedge \left(\mathring{\mathrm{D}}\tilde{A}^{ns} + 4\tilde{B}^n\tilde{A}^s\right), \end{aligned} \tag{7.24}$$

with $\varkappa = -1$,

$$\bar{C}_0 = \frac{\ell^2 M}{16}\,\epsilon_{mns}\,\mathrm{d}t \wedge \left(\mathring{\mathrm{D}}\tilde{A}^{mn} + 4\tilde{B}^m\tilde{A}^n\right) \wedge \tilde{e}^s \wedge \tilde{B}\,, \tag{7.25}$$

$$\begin{aligned}\bar{C}_m &= M\,\epsilon_{mns}\,\mathrm{d}t \wedge \left(2\mathring{\mathrm{D}}\tilde{B}^n + B^2\tilde{e}^n + \frac{\ell^4}{64}\,\tilde{A}^{nq}\tilde{A}_q\right) \wedge \tilde{e}^s \wedge \tilde{B} + \frac{M\ell^4}{64}\,\epsilon_{mns}\,\mathrm{d}t \wedge \mathring{\mathrm{D}}\tilde{A}^{ns} \wedge \tilde{A} \\ &\quad -\frac{M}{2}\,\epsilon_{mns}\,\mathrm{d}t \wedge \left(\frac{\ell^4}{64}\,\tilde{A}^n \wedge \tilde{A}^s + \left(M - B^2 + \varkappa\right)\,\tilde{e}^n \wedge \tilde{e}^s\right) \wedge \tilde{B}\,,\end{aligned} \tag{7.26}$$

and

$$\begin{aligned}C_0 &= -\frac{\ell^2}{16}\,\epsilon_{mns}\,\mathrm{d}t \wedge \left(\mathring{\mathrm{D}}\tilde{A}^{mn} + 4\tilde{B}^m\tilde{A}^n\right) \wedge \tilde{B} \wedge \tilde{e}^s + \frac{\ell^2}{4}\,\epsilon_{mns}\,\mathrm{d}t \wedge \left(\mathring{\mathrm{D}}\tilde{B}^m \wedge \tilde{e}^n\right. \\ &\quad \left. + \tilde{B}^m\tilde{e}^n \wedge \tilde{B} - \frac{\ell^4}{128}\,\tilde{A}^m \wedge \tilde{A}^n - \frac{M - B^2 + \varkappa}{2}\,\tilde{e}^m \wedge \tilde{e}^n\right) \wedge \tilde{A}^s\,,\end{aligned} \tag{7.27}$$

$$\begin{aligned}C_m &= -\,\epsilon_{mns}\,\mathrm{d}t \wedge \left(\mathring{\mathrm{D}}\tilde{B}^n + B^2\tilde{e}^n + \frac{\ell^4}{64}\,\tilde{A}^{nq}\tilde{A}_q\right) \wedge \tilde{B} \wedge \tilde{e}^s + \frac{\ell^4}{32}\,\epsilon_{mns}\,\mathrm{d}t \wedge \left(\mathring{\mathrm{D}}\tilde{A}^n - 2\tilde{A}\,\tilde{B}^n\right) \wedge \tilde{A}^s \\ &\quad + \epsilon_{mns}\,\mathrm{d}t \wedge \left(\mathring{\mathrm{D}}\tilde{B}^n \wedge \tilde{e}^s - \frac{\ell^4}{128}\,\tilde{A}^n \wedge \tilde{A}^s - \frac{M - B^2 + \varkappa}{2}\,\tilde{e}^n \wedge \tilde{e}^s\right) \wedge \tilde{B}\,.\end{aligned} \tag{7.28}$$

Let us consider the simplest equation, (7.25), while taking into account the particular solution 7.23:

$$\bar{C}_0 \propto \epsilon_{mns}\,\mathring{\mathrm{D}}_i\tilde{A}^{mn}\tilde{e}^s{}_j B_k\epsilon^{ijk} \propto \epsilon^{ijk}\partial_i A_j B_k \propto \epsilon^{ijk}\partial_i\left(f\,B_j\right)B_k = 0\,. \tag{7.29}$$

Equation (7.26) is considered, and term by term yields

$$\begin{aligned}2M\,\epsilon_{mns}\,\mathrm{d}t \wedge \mathring{\mathrm{D}}\tilde{B}^n \wedge \tilde{e}^s \wedge \tilde{B} &= \mathrm{d}^4x\,M\,\sinh\chi\cosh\chi\left(\frac{1}{2}\,\tilde{e}^i_m\,\partial_i B^2 - \tilde{B}_m\,\mathring{\mathrm{D}}_n\tilde{B}^n\right), \\ M\,\epsilon_{mns}\,\mathrm{d}t \wedge B^2\tilde{e}^n \wedge \tilde{e}^s \wedge \tilde{B} &= -\mathrm{d}^4x\,2\sinh\chi\cosh\chi M\,B^2\tilde{B}_m\,, \\ M\,\epsilon_{mns}\,\mathrm{d}t \wedge \frac{\ell^4}{64}\,\tilde{A}^{nq}\tilde{A}_q \wedge \tilde{e}^s \wedge \tilde{B} &= \mathrm{d}^4x\,\frac{\ell^4 M}{32}\,\sinh\chi\cosh\chi\,\tilde{B}_m A^2\,, \\ \frac{M\ell^4}{64}\,\epsilon_{mns}\,\mathrm{d}t \wedge \mathring{\mathrm{D}}\tilde{A}^{ns} \wedge \tilde{A} &= -\mathrm{d}^4x\,\frac{M\ell^4}{32}\,\sinh\chi\cosh\chi\,A^i\mathring{\mathrm{D}}_i A_m\,, \\ -\frac{M}{2}\,\mathrm{d}t \wedge \frac{\ell^4}{64}\,\epsilon_{mns}\,\tilde{A}^n \wedge \tilde{A}^s \wedge \tilde{B} &= \mathrm{d}^4x\,\frac{\ell^4 M}{64}\,\sinh\chi\cosh\chi\,A_m A^i B_i\,, \\ -\frac{M}{2}\,\mathrm{d}t \wedge \left(M - B^2 + \varkappa\right)\,\epsilon_{mns}\,\tilde{e}^n \wedge \tilde{e}^s \wedge \tilde{B} &= \mathrm{d}^4x\,M\left(M - B^2 + \varkappa\right)\sinh\chi\cosh\chi\,\tilde{B}_m\,.\end{aligned}$$

Summing all these terms yields:

$$0 = \bar{C}_m \propto \frac{1}{2}\,\tilde{e}^i_m\,\partial_i B^2 - \left(\mathring{\mathrm{D}}_n \tilde{B}^n + 3B^2 - M - \varkappa - \frac{\ell^4}{32}\,A^2\right)\tilde{B}_m \\ - \frac{\ell^4}{32}\,A^i\left(\mathring{\mathrm{D}}_i - \frac{1}{2}\,B_i\right)A_m\,. \tag{7.30}$$

Multiplying the above equation by $2\tilde{e}^m_j$ and using $A_i = f\,B_i$, the equation takes the form

$$0 = \bar{C}_m \propto \partial_i B^2 - 2\left[\mathring{\mathrm{D}}_n \tilde{B}^n - M - \varkappa + 3\left(1 - \frac{\ell^4}{64}\,f^2\right)B^2\right]B_i - \frac{\ell^4}{16}\,f\tilde{B}^j\tilde{e}^m_i\mathring{\mathrm{D}}_j\left(f\tilde{B}_m\right)\,. \tag{7.31}$$

The equation C_0 is analyzed term by term, revealing that all terms vanish due to symmetry, except for two, which vanish as a consequence of the equations of motion (7.20) and (7.29),

$$\begin{aligned} -\frac{\ell^2}{16}\,\epsilon_{mns}\,\mathrm{d}t\wedge\mathring{\mathrm{D}}\tilde{A}^{mn}\wedge\tilde{B}\wedge\tilde{e}^s &= \frac{\ell^2}{8}\,\mathrm{d}^4x\,\epsilon^{ijk}\partial_i A_k B_j = 0\,, \\ \frac{\ell^2}{4}\,\epsilon_{mns}\,\mathrm{d}t\wedge\mathring{\mathrm{D}}\tilde{B}^m\wedge\tilde{e}^n\wedge\tilde{A}^s &= \frac{\ell^2}{4}\,\mathrm{d}^4x\,\epsilon^{ijk}\,\partial_i B_j A_k = 0\,, \end{aligned}$$

showing that the equation is automatically satisfied, $C_0 \equiv 0$.

For equation (7.28), a term-by-term analysis yields

$$\begin{aligned} -\epsilon_{mns}\,\mathrm{d}t\wedge\mathring{\mathrm{D}}\tilde{B}^n\wedge\tilde{B}\wedge\tilde{e}^s &= \mathrm{d}^4x\,\sinh\chi\cosh\chi\left(\frac{1}{2}\,\tilde{e}^i_m\partial_i B^2 - \tilde{B}_m\mathring{\mathrm{D}}_n\tilde{B}^n\right)\,, \\ -\epsilon_{mns}\,\mathrm{d}t\wedge B^2\tilde{e}^n\wedge\tilde{B}\wedge\tilde{e}^s &= -2\sinh\chi\cosh\chi\,\mathrm{d}^4x\,B^2\tilde{B}_m\,, \\ -\epsilon_{mns}\,\mathrm{d}t\wedge\frac{\ell^4}{64}\,\tilde{A}^{nq}\tilde{A}_q\wedge\tilde{B}\wedge\tilde{e}^s &= \frac{\ell^4}{64}\,\mathrm{d}^4x\,\sinh\chi\cosh\chi\left(A_m A^i B_i + A^2\tilde{B}_m\right)\,, \\ \frac{\ell^4}{32}\,\epsilon_{mns}\,\mathrm{d}t\wedge\mathring{\mathrm{D}}\tilde{A}^n\wedge\tilde{A}^s &= -\frac{\ell^4}{32}\,\mathrm{d}^4x\,\sinh\chi\cosh\chi\mathring{\mathrm{D}}_n\left(A_m A^n\right)\,, \\ \epsilon_{mns}\,\mathrm{d}t\wedge\mathring{\mathrm{D}}\tilde{B}^n\wedge\tilde{e}^s\wedge\tilde{B} &= \mathrm{d}^4x\,\sinh\chi\cosh\chi\left(\frac{1}{2}\,\tilde{e}^i_m\partial_i B^2 - \mathring{\mathrm{D}}_n\tilde{B}^n\tilde{B}_m\right)\,, \\ \epsilon_{mns}\,\mathrm{d}t\wedge\left(-\frac{\ell^4}{128}\,\tilde{A}^n\wedge\tilde{A}^s\right)\wedge\tilde{B} &= \frac{\ell^4}{64}\,\mathrm{d}^4x\,\sinh\chi\cosh\chi A_m A^i B_i\,, \\ \epsilon_{mns}\,\mathrm{d}t\wedge\left(-\frac{M - B^2 + \varkappa}{2}\,\tilde{e}^n\wedge\tilde{e}^s\right)\wedge\tilde{B} &= \left(M - B^2 + \varkappa\right)\,\mathrm{d}^4x\,\sinh\chi\cosh\chi\,\tilde{B}_m\,, \end{aligned}$$

such that the sum is (after removing $\mathrm{d}^4x\,\sinh\chi\cosh\chi$ only):

$$\begin{aligned} 0=C_m \;\propto\; & \tilde{e}^i_m\partial_i B^2-2\tilde{B}_m\mathring{\mathrm{D}}_n\tilde{B}^n-2B^2\tilde{B}_m+\left(M-B^2+\varkappa\right)\tilde{B}_m \\ & +\frac{\ell^4}{64}\left(2A_mA^iB_i+A^2\tilde{B}_m\right)-\frac{\ell^4}{32}\mathring{\mathrm{D}}_n\left(A_mA^n\right)\,. \end{aligned} \tag{7.32}$$

Multiplying the above equation by $2\tilde{e}^m_j$ and using $A_i=f\,B_i$, this equation takes the form

$$0=C_m\propto\partial_iB^2-\left[2\mathring{\mathrm{D}}_n\tilde{B}^n-M+3\left(1-\frac{\ell^4}{64}\,f^2\right)\,B^2\right]B_i-\frac{\ell^4}{32}\,\tilde{e}^m_i\mathring{\mathrm{D}}_n\left(f^2\tilde{B}_m\tilde{B}^n\right)\,. \tag{7.33}$$

Finally, equation (7.24) is analyzed term by term, considering only the nonvanishing contributions, where the following identities are employed

$$\begin{aligned} \epsilon^{ijk}\epsilon_{mns}\tilde{e}^s_k &= \sinh\chi\cosh\chi\left(\tilde{e}^i_m\tilde{e}^j_n-\tilde{e}^j_m\tilde{e}^i_n\right), \\ \tilde{A}_{mn} &= \epsilon_{mns}A^s\,, \\ \epsilon_{mns}\,\epsilon^{ijk}\tilde{e}^n_j\tilde{e}^s_k &= 2\sinh\chi\cosh\chi\,\tilde{e}^i_m\,, \end{aligned}$$

getting

$$\begin{aligned} \frac{8}{\ell}\,\epsilon_{mns}\,\mathrm{d}t\wedge\mathring{\mathrm{D}}\tilde{B}^m\wedge\mathring{\mathrm{D}}\tilde{B}^n\wedge\tilde{e}^s &= -\frac{8}{\ell}\,\mathrm{d}^4x\,\sinh\chi\cosh\chi\left(\left(\mathring{\mathrm{D}}_m\tilde{B}^m\right)^2-\mathring{\mathrm{D}}_n\tilde{B}^m\mathring{\mathrm{D}}_m\tilde{B}^n\right), \\ \frac{8}{\ell}\,\epsilon_{mns}\,\mathrm{d}t\wedge\left(-\tilde{B}^m\tilde{B}\right)\wedge\mathring{\mathrm{D}}\tilde{B}^n\wedge\tilde{e}^s &= \frac{8}{\ell}\,\mathrm{d}^4x\,\sinh\chi\cosh\chi\left(B^2\mathring{\mathrm{D}}_m\tilde{B}^m-\frac{1}{2}\,\tilde{B}^i\partial_iB^2\right), \\ \frac{8}{\ell}\,\epsilon_{mns}\,\mathrm{d}t\wedge B^2\tilde{e}^m\wedge\mathring{\mathrm{D}}\tilde{B}^n\wedge\tilde{e}^s &= -\frac{16}{\ell}\,\mathrm{d}^4x\,\sinh\chi\cosh\chi B^2\mathring{\mathrm{D}}_m\tilde{B}^m\,, \\ \frac{8}{\ell}\,\epsilon_{mns}\,\mathrm{d}t\wedge\frac{\ell^4}{64}\,\tilde{A}^{mp}\tilde{A}_p\wedge\mathring{\mathrm{D}}\tilde{B}^n\wedge\tilde{e}^s &= \frac{\ell^3}{8}\,\mathrm{d}^4x\,\sinh\chi\cosh\chi\left(A^2\mathring{\mathrm{D}}_m\tilde{B}^m+A_mA^n\mathring{\mathrm{D}}_n\tilde{B}^m\right), \end{aligned}$$

and

$$\begin{aligned} \frac{8}{\ell}\,\epsilon_{mns}\,\mathrm{d}t\wedge\mathring{\mathrm{D}}\tilde{B}^m\wedge\tilde{B}^n\tilde{e}^s\wedge\tilde{B} &= \frac{8}{\ell}\,\mathrm{d}^4x\,\sinh\chi\cosh\chi\left(B^2\mathring{\mathrm{D}}_m\tilde{B}^m-\frac{1}{2}\,\tilde{B}^i\partial_iB^2\right), \\ \frac{8}{\ell}\,\epsilon_{mns}\,\mathrm{d}t\wedge B^2\tilde{e}^m\wedge\tilde{B}^n\tilde{e}^s\wedge\tilde{B} &= \frac{16}{\ell}\,\mathrm{d}^4x\,\sinh\chi\cosh\chi\,B^4\,, \\ \frac{8}{\ell}\,\epsilon_{mns}\,\mathrm{d}t\wedge\frac{\ell^4}{64}\,\tilde{A}^{mp}\tilde{A}_p\wedge\tilde{B}^n\tilde{e}^s\wedge\tilde{B} &= -\frac{\ell^3}{8}\,\mathrm{d}^4x\,\sinh\chi\cosh\chi\left(A^2B^2+(A^iB_i)^2\right), \end{aligned}$$

and also

$$\begin{aligned}
\frac{\ell^3}{16}\,\epsilon_{mns}\,\mathrm{d}t\wedge\left(-\mathring{\mathrm{D}}\tilde{B}^m\right)\wedge\tilde{A}^n\wedge\tilde{A}^s &= \frac{\ell^3}{8}\,\mathrm{d}^4x\,\sinh\chi\cosh\chi A^iA_m\mathring{\mathrm{D}}_i\tilde{B}^m\,,\\
\frac{\ell^3}{16}\,\epsilon_{mns}\,\mathrm{d}t\wedge\tilde{B}^m\tilde{B}\wedge\tilde{A}^n\wedge\tilde{A}^s &= -\frac{\ell^3}{8}\,\mathrm{d}^4x\,\sinh\chi\cosh\chi(A^iB_i)^2\\
\frac{\ell^3}{16}\,\epsilon_{mns}\,\mathrm{d}t\wedge\left(-B^2\tilde{e}^m\right)\wedge\tilde{A}^n\wedge\tilde{A}^s &= \frac{\ell^3}{8}\,\mathrm{d}^4x\,\sinh\chi\cosh\chi A^2B^2\,,
\end{aligned}$$

and

$$\begin{aligned}
\frac{4}{\ell}\,\epsilon_{mns}\,\mathrm{d}t\wedge\left(M-B^2+\varkappa\right)\left(-\mathring{\mathrm{D}}\tilde{B}^m\right)\wedge\tilde{e}^n\wedge\tilde{e}^s &= \frac{8}{\ell}\,\mathrm{d}^4x\,\sinh\chi\cosh\chi\left(M-B^2+\varkappa\right)\mathring{\mathrm{D}}_m\tilde{B}^m\,,\\
\frac{4}{\ell}\,\epsilon_{mns}\,\mathrm{d}t\wedge\left(M-B^2+\varkappa\right)\tilde{B}^m\tilde{B}\wedge\tilde{e}^n\wedge\tilde{e}^s &= -\frac{8}{\ell}\,\mathrm{d}^4x\,\sinh\chi\cosh\chi\left(M-B^2+\varkappa\right)B^2\,,\\
\frac{4}{\ell}\,\epsilon_{mns}\,\mathrm{d}t\wedge\left(M-B^2+\varkappa\right)\left(-B^2\tilde{e}^m\right)\wedge\tilde{e}^n\wedge\tilde{e}^s &= \frac{24}{\ell}\,\mathrm{d}^4x\,\sinh\chi\cosh\chi\,\left(M-B^2+\varkappa\right)B^2\,,\\
\frac{4}{\ell}\,\epsilon_{mns}\,\mathrm{d}t\wedge\left(M-B^2+\varkappa\right)\left(-\frac{\ell^4}{64}\,\tilde{A}^{mp}\tilde{A}_p\right)\wedge\tilde{e}^n\wedge\tilde{e}^s &= -\frac{\ell^3}{4}\,\mathrm{d}^4x\sinh\chi\cosh\chi\,\left(M-B^2+\varkappa\right)A^2\,,
\end{aligned}$$

and finally

$$\begin{aligned}
\frac{\ell^3}{16}\,\epsilon_{mns}\,\mathrm{d}t\wedge\mathring{\mathrm{D}}\tilde{A}^m\wedge\mathring{\mathrm{D}}\tilde{A}^{ns} &= -\frac{\ell^3}{8}\,\mathrm{d}^4x\,\sinh\chi\cosh\chi\left(\mathring{\mathrm{D}}_mA^n\mathring{\mathrm{D}}_nA^m-(\mathring{\mathrm{D}}_mA^m)^2\right)\,,\\
\frac{\ell^3}{16}\,\epsilon_{mns}\,\mathrm{d}t\wedge\left(-2\tilde{A}\,\tilde{B}^m\wedge\mathring{\mathrm{D}}\tilde{A}^{ns}\right) &= \frac{\ell^3}{4}\,\mathrm{d}^4x\,\sinh\chi\cosh\chi\,\tilde{B}^mA^i\mathring{\mathrm{D}}_iA_m\,,\\
\frac{\ell^3}{16}\,\epsilon_{mns}\,\mathrm{d}t\wedge4\mathring{\mathrm{D}}\tilde{A}^m\wedge\tilde{B}^n\tilde{A}^s &= \frac{\ell^3}{4}\,\mathrm{d}^4x\,\sinh\chi\cosh\chi\,A^i\left(B_i\mathring{\mathrm{D}}_mA^m+\tilde{B}_m\mathring{\mathrm{D}}_iA^m\right)\,.
\end{aligned}$$

Summing all contributions, the last equation takes the form:

$$\begin{aligned}
0=C\;\propto\;&-\left(\mathring{\mathrm{D}}_m\tilde{B}^m\right)^2+\mathring{\mathrm{D}}_n\tilde{B}^m\mathring{\mathrm{D}}_m\tilde{B}^n-\tilde{B}^i\partial_iB^2+\left(M-B^2+\varkappa\right)\mathring{\mathrm{D}}_m\tilde{B}^m+2\left(M+\varkappa\right)B^2\\
&+\frac{\ell^4}{64}\,\Big[(\mathring{\mathrm{D}}_mA^m)^2-\mathring{\mathrm{D}}_mA^n\mathring{\mathrm{D}}_nA^m+A^2\mathring{\mathrm{D}}_m\tilde{B}^m+2A_mA^i\mathring{\mathrm{D}}_i\tilde{B}^m\\
&+4\tilde{B}_mA^i\mathring{\mathrm{D}}_iA^m+2A^iB_i\mathring{\mathrm{D}}_mA^m-2(A^iB_i)^2-2\left(M-B^2+\varkappa\right)A^2\Big]\,.
\end{aligned}\tag{7.34}$$

In summary, the system of equations takes the following form:

$$
\begin{aligned}
A_i &= f(\chi,z)B_i\,, && (7.35)\\
\bar{C}_0 &\propto \epsilon^{ijk}\partial_i\left(f\,B_j\right)B_k=0\,, && (7.36)\\
\bar{C}_m &\propto \partial_i B^2-2\left[\mathring{\mathrm{D}}_n\tilde{B}^n-M-\varkappa+3\left(1-\frac{\ell^4}{64}\,f^2\right)B^2\right]B_i\\
&- \frac{\ell^4}{16}\,f\tilde{B}^j\tilde{e}_i^m\mathring{\mathrm{D}}_j\left(f\tilde{B}_m\right)=0\,, && (7.37)\\
C_m &\propto \partial_i B^2-\left[2\mathring{\mathrm{D}}_n\tilde{B}^n-M+3\left(1-\frac{\ell^4}{64}\,f^2\right)\,B^2\right]B_i\\
&- \frac{\ell^4}{32}\,\tilde{e}_i^m\mathring{\mathrm{D}}_n\left(f^2\tilde{B}_m\tilde{B}^n\right)=0\,, && (7.38)\\
C &\propto -\left(\mathring{\mathrm{D}}_m\tilde{B}^m\right)^2+\mathring{\mathrm{D}}_n\tilde{B}^m\mathring{\mathrm{D}}_m\tilde{B}^n-\tilde{B}^i\partial_i B^2+\left(M-B^2+\varkappa\right)\mathring{\mathrm{D}}_m\tilde{B}^m\\
&+ 2\left(M+\varkappa\right)B^2+\frac{\ell^4}{64}\,\Big[(\mathring{\mathrm{D}}_m A^m)^2-\mathring{\mathrm{D}}_m A^n\mathring{\mathrm{D}}_n A^m+A^2\mathring{\mathrm{D}}_m\tilde{B}^m+2A_mA^i\mathring{\mathrm{D}}_i\tilde{B}^m\\
&+ 4\tilde{B}_mA^i\mathring{\mathrm{D}}_iA^m+2A^iB_i\mathring{\mathrm{D}}_mA^m-2(A^iB_i)^2-2\left(M-B^2+\varkappa\right)A^2\Big]=0\,, && (7.39)
\end{aligned}
$$

which will be analyzed in the next section.

7.3 Resolution of the boundary equations: case with constant proportionality coefficient

For simplicity, the analysis focuses exclusively on cases where the components of both axial and diagonal torsion are related by a proportionality constant, that is, the function $f(\chi,z)$ in equation (7.35) is taken to be constant and normalized as follows:

$$
f=\frac{8}{\ell^2}\,c\,,\qquad c=const\,. \tag{7.40}
$$

The parameter c is identified with the dislocation. Without loss of generality, $\ell=1$ is fixed. In this way, equations (7.36), (7.37), (7.38), and (7.39) take the form:

$$
0=\epsilon^{ijk}B_i\partial_jB_k\,, \tag{7.41}
$$

$$0 = \partial_i B^2 - 2\left[\mathring{\mathrm{D}}_n \tilde{B}^n - M + 1 + 3\left(1-c^2\right)B^2\right] B_i - 4c^2 \tilde{B}^j \tilde{e}_i^m \mathring{\mathrm{D}}_j \tilde{B}_m \,, \tag{7.42}$$

$$0 = \partial_i B^2 - \left[2\mathring{\mathrm{D}}_n \tilde{B}^n - M + 1 + 3\left(1-c^2\right)B^2\right] B_i - 2c^2 \tilde{e}_i^m \mathring{\mathrm{D}}_n \left(\tilde{B}_m \tilde{B}^n\right) \,, \tag{7.43}$$

and

$$\begin{aligned} 0 = {} & \left(c^2-1\right)\left[\left(\mathring{\mathrm{D}}_m \tilde{B}^m\right)^2 + \mathring{\mathrm{D}}_n \tilde{B}^m \mathring{\mathrm{D}}_m \tilde{B}^n - 2(M-1)B^2\right] \\ & + \left(3c^2-1\right)\left(\tilde{B}^i \partial_i B^2 + B^2 \mathring{\mathrm{D}}_m \tilde{B}^m\right) + (M-1)\mathring{\mathrm{D}}_m \tilde{B}^m \,. \end{aligned} \tag{7.44}$$

In the following sections, different sub branches of possibles solutions, will be analyzed.

7.3.1 Case $c^2 = 1$: 'no-go' for dislocation solution

One of the simplest solution spaces corresponds to the case where the dislocation parameter is fixed at $c^2 = 1$. In this situation, the equations of motion take the following forms. The first equation, Eq. (7.41), is identically satisfied since the component $B_\theta = 0$ and the other components are independent of θ. The remaining equations take the form

$$0 = \partial_i B^2 - 2\left[\mathring{\mathrm{D}}_n \tilde{B}^n - M + 1\right] B_i - 4\tilde{B}^j \tilde{e}_i^m \mathring{\mathrm{D}}_j \tilde{B}_m \,, \tag{7.45}$$

$$0 = \partial_i B^2 - \left[2\mathring{\mathrm{D}}_n \tilde{B}^n - M + 1\right] B_i - 2\tilde{e}_i^m \mathring{\mathrm{D}}_n \left(\tilde{B}_m \tilde{B}^n\right) \,, \tag{7.46}$$

$$0 = 2\left[\tilde{B}^i \partial_i B^2 + B^2 \mathring{\mathrm{D}}_m \tilde{B}^m\right] + (M-1)\mathring{\mathrm{D}}_m \tilde{B}^m \,. \tag{7.47}$$

By contracting Eqs. (7.45) and (7.46) with $\tilde{B}^i$, it is obtained

$$\begin{aligned} 0 &= \tilde{B}^i \partial_i B^2 + 2\left(\mathring{D}_m \tilde{B}^m - M + 1\right) B^2 \,, \\ 0 &= \left(-4\mathring{D}_m \tilde{B}^m + (M-1)\right) B^2 \,, \end{aligned} \tag{7.48}$$

since $B^2 \neq 0$, the last equation implies $\mathring{D}_m \tilde{B}^m = \frac{M-1}{4}$, which, when substituted into the first equation, yields

$$\tilde{B}^i \partial_i B^2 = \frac{3}{2}(1-M)B^2 \,. \tag{7.49}$$

Substituting $\mathring{D}_m \tilde{B}^m = \frac{M-1}{4}$ and Eq. (7.49) into Eq. (7.47) yields

$$B^2 = -\frac{M-1}{14}\,. \tag{7.50}$$

which lacks physical meaning, because requiring $B^2 > 0$ (for a real field) demands the condition $M < 1$, which in turn implies a naked singularity, $\mu = M-1 < 0$. Consequently, a well-defined solution with dislocations cannot be obtained under the dislocation parameter condition $c^2 = 1$.

7.3.2 Case $c^2 \neq 1$: A generic dislocation

When the dislocation parameter satisfies $c^2 \neq 0$ and $c^2 \neq 1$, the first two equations (7.42) and (7.43), can be treated as algebraic equations in $B_i \mathring{\mathrm{D}}_n \tilde{B}^n$ and $\tilde{e}_i^m \tilde{B}^j \mathring{\mathrm{D}}_j \tilde{B}_m$, and solved as follows:

$$B_i \mathring{\mathrm{D}}_n \tilde{B}^n = a \partial_i B^2\,, \qquad \tilde{e}_i^m \tilde{B}^j \mathring{\mathrm{D}}_j \tilde{B}_m = a\,\partial_i B^2 + (m + bB^2)\,B_i\,, \tag{7.51}$$

where the constants are introduced

$$m = \frac{M-1}{2c^2}\,, \qquad a = \frac{1}{2\,(1+2c^2)} > 0\,, \qquad b = \frac{3\,(c^2-1)}{2c^2} \neq 0\,. \tag{7.52}$$

From the contractions of Eqs. (7.51) with $\tilde{B}^i$, the following useful identities are obtained, mapping the differential expressions to algebraic ones:

$$\mathring{\mathrm{D}}_n \tilde{B}^n = \frac{m + bB^2}{2c^2}\,, \qquad \tilde{B}^i \partial_i B^2 = \frac{(m+bB^2)B^2}{2ac^2}\,, \tag{7.53}$$

where the identity $1 - 2a = 4ac^2$ has been applied. Consequently,

$$\partial_i B^2 = \frac{m + bB^2}{2ac^2}\,B_i\,, \qquad \tilde{e}_i^m \tilde{B}^j \mathring{\mathrm{D}}_j \tilde{B}_m = \frac{m+bB^2}{4ac^2}\,B_i\,. \tag{7.54}$$

It should be noted that Eq. (7.54) is merely a consequence of the previous equations and is not equivalent to them. Thus, when Eq. (7.54) is satisfied, the first equation of (7.53) still needs to be checked, whereas the second equation is automatically satisfied. Equation (7.44) then yields

$$\mathring{\mathrm{D}}_m \tilde{B}^n \mathring{\mathrm{D}}_n \tilde{B}^m = \alpha B^4 + \beta B^2 + \gamma\,, \tag{7.55}$$

with the coefficients

$$\begin{aligned}
\alpha &= \frac{3}{4c^4}\left[\frac{3\left(c^2-1\right)^2}{4c^4}-\left(1-3c^2\right)\left(3+4c^2\right)\right], \\
\beta &= (M-1)\left[\frac{3\left(c^2-1\right)}{8c^8}-\frac{\left(1-3c^2\right)\left(3+4c^2\right)}{4c^4\left(c^2-1\right)}+\frac{3}{4c^4}-2\right], \\
\gamma &= \frac{(M-1)^2}{4c^4}\left(\frac{1}{4c^4}-\frac{1}{1-c^2}\right).
\end{aligned} \tag{7.56}$$

These equations must be solved for the diagonal torsion $B_i(\chi, z)$. In components, for the first equation (7.54), it is found

$$\partial_\chi B^2 = \frac{m+bB^2}{2ac^2}\,B_\chi\,, \qquad \partial_z B^2 = \frac{m+bB^2}{2ac^2}\,B_z\,, \qquad B_\theta = 0\,, \tag{7.57}$$

where $B^2 = B_\chi^2 + \frac{1}{\cosh^2\chi}B_z^2$, which expands the first two equation in (7.57) as follow:

$$\begin{aligned}
B_\chi\partial_\chi B_\chi + \frac{B_z}{\cosh^2\chi}\partial_\chi B_z - \frac{\tanh\chi}{\cosh^2\chi}B_z^2 &= \frac{m+bB^2}{2ac^2}\,B_\chi\,, \\
B_\chi\partial_z B_\chi + \frac{B_z}{\cosh^2\chi}\partial_z B_z &= \frac{m+bB^2}{2ac^2}\,B_z\,.
\end{aligned} \tag{7.58}$$

The following identities are useful for the subsequent calculations:

$$\mathring{D}_n\tilde{B}^n = \partial_\chi B^\chi + \frac{1}{\cosh^2(\chi)}\partial_z B_z + (\coth\chi+\tanh\chi)\,B_\chi\,, \tag{7.59}$$

$$\begin{aligned}
\mathring{D}_m\tilde{B}^n\mathring{D}_n\tilde{B}^m &= (\partial_\chi B_\chi)^2 + \frac{1}{\cosh^4\chi}(\partial_z B_z)^2 + \left(\coth^2\chi+\tanh^2\chi\right)B_\chi^2 + 2\frac{\tanh^2\chi}{\cosh^2\chi}B_z^2 \\
&+ 2\frac{\tanh\chi}{\cosh^2\chi}\left(B_\chi\partial_z B_z - B_z\partial_\chi B_z - B_z\partial_z B_\chi\right) + \frac{2}{\cosh^2\chi}\partial_\chi B_z\partial_z B_\chi\,.
\end{aligned} \tag{7.60}$$

Thanks to $B_\theta = 0$ and $\partial_\theta = 0$, the equation $\epsilon^{ijk}B_i\partial_j B_k = 0$ is identically satisfied, while the second equation (7.54) reads in components

$$\begin{aligned}
B_\chi\partial_\chi B_\chi + \frac{B_z}{\cosh^2\chi}\partial_z B_\chi - \frac{\tanh\chi}{\cosh^2\chi}(B_z)^2 &= \frac{m+bB^2}{4ac^2}\,B_\chi\,, \\
B_\chi\partial_\chi B_z + \frac{B_z}{\cosh^2\chi}\partial_z B_z &= \frac{m+bB^2}{4ac^2}\,B_z\,.
\end{aligned} \tag{7.61}$$

Taking the difference between the first equation in (7.58) and the first equation in (7.61), and the differences between the second equation in (7.58) with the second in (7.61), a simpler system is obtained

$$\begin{aligned} \frac{B_z}{\cosh^2\chi}\left(\partial_\chi B_z - \partial_z B_\chi\right) &= 0\,, \\ B_\chi\left(\partial_z B_\chi - \partial_\chi B_z\right) &= 0\,, \end{aligned} \tag{7.62}$$

in this form, each equation becomes factorized, so that the result depends on which factor vanishes.

Therefore, excluding the point $\chi = 0$ where $\sinh(\chi) = 0$, the only possible allowed corresponds to both components non-vanishing, B_χ, $B_z \neq 0$. Then, it must hold:

$$\partial_\chi B_z = \partial_z B_\chi \qquad \Leftrightarrow \qquad \nabla \times \vec{B} = 0\,, \tag{7.63}$$

meaning that the field $\vec{B}$ is irrotational and can therefore be expressed as the gradient of a torsion potential,

$$\vec{B} = \nabla\psi \qquad \Leftrightarrow \qquad B_i = \partial_i \psi\,. \tag{7.64}$$

This results in only two independent equations,

$$\begin{aligned} B_\chi \partial_\chi B_\chi + \frac{B_z}{\cosh^2\chi}\partial_z B_\chi - \frac{\tanh\chi}{\cosh^2\chi}(B_z)^2 &= \frac{m + b\left(B_\chi^2 + \frac{1}{\cosh^2\chi}B_z^2\right)}{4ac^2}\, B_\chi\,, \\ B_\chi \partial_\chi B_z + \frac{B_z}{\cosh^2\chi}\partial_z B_z &= \frac{m + b\left(B_\chi^2 + \frac{1}{\cosh^2\chi}B_z^2\right)}{4ac^2}\, B_z\,. \end{aligned} \tag{7.65}$$

Finally, from Eq. (7.57), it is clear that there are two branches of solutions, corresponding either to a constant norm of the diagonal torsion, $B^2 = -\frac{m}{b}$, or to an arbitrary norm, $B^2 \neq$ const. It is found that only one of these branches allows a solution with a non-trivial Abelian anomaly, describing a holographic field theory, as shown below.

7.3.3 'No–go' for the constant norm $B^2 = const$

Assuming that the vector B_i has a constant norm, this norm takes the value

$$|B| \equiv \sqrt{B_\chi^2 + \frac{1}{\cosh^2(\chi)}B_z^2} = \sqrt{-\frac{m}{b}}\,. \tag{7.66}$$

The only possibility is $c^2 < 1$ because $M - 1 > 0$. A constant norm then implies

$$B_\chi = \sqrt{\frac{-m}{b}} \sin \Psi(\chi, z)\,, \quad B_z = \sqrt{\frac{-m}{b}} \cosh \chi \cos \Psi(\chi, z)\,, \tag{7.67}$$

with $\Psi(\chi, z)$ some real function.

From Eq. (7.53), the identities $\mathring{\mathrm{D}}_n \tilde{B}^n = 0$ and $\tilde{B}^i \partial_i B^2 = 0$ can be deduced. The first of these then implies:

$$\mathring{\mathrm{D}}_n \tilde{B}^n = \partial_\chi B_\chi + \frac{1}{\cosh^2 \chi} \partial_z B_z + (\coth \chi + \tanh \chi)\, B_\chi = 0\,, \tag{7.68}$$

while the second identity $\tilde{B}^i \partial_i B^2 = 0$ is satisfied identically. On the other hand, the equation (7.41) is identically zero, while (7.42) and (7.43) are equivalent:

$$-4c^2 B^j \tilde{e}_i^m \mathring{D}_j \tilde{B}_m = 0\,,$$

which, in components, reads:

$$B_\chi \partial_\chi B_\chi + \frac{1}{\cosh^2 \chi} B_z \partial_z B_\chi - \frac{\tanh \chi}{\cosh^2 \chi} B_z^2 = 0\,, \tag{7.69}$$

$$B_\chi \partial_\chi B_z + \frac{1}{\cosh^2 \chi} B_z \partial_z B_z = 0\,. \tag{7.70}$$

And the last equation (7.44) takes the form:

$$\mathring{\mathrm{D}}_m \tilde{B}^n \mathring{\mathrm{D}}_n \tilde{B}^m = \frac{2(M-1)^2}{3(1-c^2)}\,. \tag{7.71}$$

However, from (7.64) it follows that:

$$\begin{aligned} B_\chi &= \partial_\chi \psi(\chi, z) = \sqrt{\frac{-m}{b}} \sin \Psi(\chi, z)\,, \\ B_z &= \partial_z \psi(\chi, z) = \sqrt{\frac{-m}{b}} \cosh \chi \cos \Psi(\chi, z)\,, \end{aligned} \tag{7.72}$$

which can be resolved as:

$$\Psi(\chi, z) = \arccos\left(\frac{F(z)}{\cosh \chi}\right)\,, \tag{7.73}$$

for some real function $F(z)$. Due to the complexity of the above equations, a particular solution can be considered where $F(z) = F_0 = const.$. Substituting this solution into Eqs. (7.69) and (7.70) yields the same expression:

$$\partial_\chi \left(\arccos\left(\frac{F_0}{\cosh\chi} \right) \right) = \frac{1}{\sqrt{1 - \frac{F_0}{\cosh^2\chi}}} \tanh\chi \frac{F_0}{\cosh\chi} \,, \tag{7.74}$$

substituting this into Eq. (7.70) yields:

$$0 = F_0^2 \tanh^2\chi - F_0 \left(\coth\chi + \tanh\chi\right) + \cosh^2\chi \left(\coth\chi + \tanh\chi\right) \,. \tag{7.75}$$

However, this equation has a solution only at $\chi = 0$ for any value of F_0, which is not physically relevant for the study of the Abelian anomaly. Therefore, it can be concluded that the branch $B^2 = -\frac{m}{b}$ does not admit a consistent solution. Future work should reconsider this branch, for a given $F(z) \neq F_0$.

7.3.4 Irrotational holographic dislocation

Finally, consider an irrotational vector $B_i = \partial_i \psi$ with a non-constant norm. Due to the difficulty of solving this non-linear system of equations, it is convenient to begin with a simpler case. The first case considered is $\mathbf{B_z} = \mathbf{0}$, which implies that ψ does not depend on z, and the solutions will be invariant under translations along the z-axis. This leads to $\mathbf{B}_\chi(\chi) = \partial_\chi\psi(\chi) \neq \mathbf{0}$, so that the first equations of (7.57) and (7.65) are equivalent:

$$\partial_\chi^2\psi = \frac{m + b(\partial_\chi\psi)^2}{4ac^2} \Rightarrow \partial_\chi B_\chi = \frac{m + bB_\chi^2}{4ac^2} \,, \tag{7.76}$$

the first equation of (7.53) is reduced to:

$$\begin{aligned} \partial_\chi^2\psi + \left(\coth\chi + \tanh\chi\right)\partial_\chi\psi &= \frac{m + b(\partial_\chi\psi)^2}{2c^2} \\ \Rightarrow \partial_\chi B_\chi + \left(\coth + \tanh\chi\right)\chi\, B_\chi &= \frac{m + bB_\chi^2}{2c^2} \,, \end{aligned} \tag{7.77}$$

and the equation (7.55) is reduced to:

$$\begin{aligned} \left(\partial_\chi^2\psi\right)^2 &= \alpha(\partial_\chi\psi)^4 + \left(\beta - \tanh^2\chi - \coth^2\chi\right)(\partial_\chi\psi)^2 + \gamma \\ \Rightarrow \left(\partial_\chi B_\chi\right)^2 &= \alpha(B_\chi)^4 + \left(\beta - \tanh^2\chi - \coth^2\chi\right)(B_\chi)^2 + \gamma \,. \end{aligned} \tag{7.78}$$

Periodic case: $c^2 > 1$

Solving (7.76) yields

$$\Psi(\chi) = \Psi_0 - \frac{4ac^2}{b} \ln\cos\left(\frac{\sqrt{mb}}{4ac^2}\left(\pm\chi - \chi_0\right)\right), \tag{7.79}$$

the argument of the logarithm must be positive so that the cosine lies within the interval $\left[-\frac{\pi}{2} + n\pi\,, \frac{\pi}{2} + n\pi\right]$, where n is integer. Moreover, since the cosine is an even function, the $\pm$ signs correspond to equivalent solutions, allowing the selection of the positive $(+)$ sign. Accordingly, the B_χ component takes the form:

$$B_\chi = \sqrt{\frac{m}{b}}\,\tan\left(\frac{\sqrt{mb}}{4ac^2}\,\left(\chi - \chi_0\right)\right), \tag{7.80}$$

with the **important condition $\mathbf{c^2 - 1 > 0}$**, noting that c^2 can be smaller than one, which will be analyzed subsequently. From the solutions (7.79) and (7.80), the following limits are obtained:

$$\begin{aligned} -\frac{\pi}{2} + n\pi < \frac{\sqrt{mb}}{4ac^2}(\chi - \chi_0) < \frac{\pi}{2} + n\pi\,, \quad n = 0, 1, 2, \ldots \\ \chi_0 - \left(\frac{\pi}{2} - n\pi\right)\frac{4ac^2}{\sqrt{mb}} < \chi < \chi_0 + \left(\frac{\pi}{2} + n\pi\right)\frac{4ac^2}{\sqrt{mb}}\,, \end{aligned} \tag{7.81}$$

recall that χ is the radial coordinate, so $\chi > 0$ at all times.

Substituting Eq. (7.76) into Eq. (7.77) yields the equation

$$B_\chi^2 + \frac{\coth\chi + \tanh\chi}{b}\,B_\chi + \frac{m}{b} = 0\,, \tag{7.82}$$

with the algebraic solution

$$B_\chi = \frac{-\left(\coth\chi + \tanh\chi\right) \pm \sqrt{\left(\coth\chi + \tanh\chi\right)^2 - 4mb}}{2b}\,, \tag{7.83}$$

where the reality of B from (7.83) gives the condition

$$\begin{aligned} \left(\coth\chi + \tanh\chi\right)^2 &\geq 4mb \\ \coth\chi + \tanh\chi &\geq 2\sqrt{mb}\,. \end{aligned} \tag{7.84}$$

Up to this point, the two expressions (7.80) and (7.83) for B_χ indicate that only a particular value (one, several, or possibly none) $\chi = \bar{\chi}$ will satisfy both equations. Consequently, $B_\chi = \bar{B}_\chi$, which can be expressed as $\chi = \bar{\chi}(c, M) > 0$ and $B_\chi = \bar{B}_\chi(c, M) \in \mathbb{R}$. Moreover, using the solution obtained from Eq. (7.78), a function $f(c, M) = 0 \Rightarrow M = M(c)$ can be defined, such that this system of three equations with three unknowns $\{\psi(\chi),\, c,\, M\}$ is solved consistently. The following section examines whether this reasoning is indeed valid.

To solve the last equation, substituting Eqs. (7.76) and (7.82) into Eq. (7.78) yields the following equation

$$\left(\alpha - db^2\right)\, B_\chi^4 + \left(\beta + 2 - 2mdb\right)\, B_\chi^2 + \gamma - dm^2 = 0\,, \tag{7.85}$$

with $d = 1 + \frac{1}{16a^2c^4} = \frac{8c^4+4c^2+1}{4c^4}$, and with the algebraic solution

$$B_\chi^2 = \frac{-\left(\beta + 2 - 2mdb\right) \pm \sqrt{\left(\beta + 2 - 2mdb\right)^2 - 4\left(\alpha - db^2\right)\left(\gamma - dm^2\right)}}{2\left(\alpha - db^2\right)}\,. \tag{7.86}$$

It is important to note that this solution for the B_χ field, redefined as

$$B_\chi^2 \equiv \Omega_\pm^2(c, M)\,,$$

does not depend on the χ coordinate. This implies that, for a consistent system of solutions, the other solutions (7.80) and (7.83) must also be constant; in other words, they must exist for a particular value $\chi = \bar{\chi}(c, M)$ which correspond to a hyperbolic cylinder, as indicated by the previous reasoning. The following task is to study the reality of Eq. (7.86), and to determine the relation between the black hole mass M and the dislocation parameter c, $M = M(c)$, as well as the corresponding radial coordinate $\bar{\chi}$.

Two conditions follow from this solution (7.86):

a) - The positivity of $B_\chi^2 > 0$.

b) - The reality of B_χ: $\left(\beta + 2 - 2mdb\right)^2 - 4\left(\alpha - db^2\right)\left(\gamma - dm^2\right) \geq 0\,.$

From condition b), it can numerically extracted that

$$\left(\beta + 2 - 2mdb\right)^2 - 4\left(\alpha - db^2\right)\left(\gamma - dm^2\right) \geq 0 \quad \forall\, c^2 > 1\,. \tag{7.87}$$

Condition a) is satisfied only for the Ω_+ branch when $c > c_{03} \simeq 1.1688$ for $M = 2$[1], which can also be determined numerically.

By equating solutions (7.80) and (7.86), we find for the radial coordinate:

$$\chi(c, M) = \frac{4ac^2}{\sqrt{mb}} \arctan\left(\sqrt{\frac{b}{m}}\Omega_+(c, M)\right) > 0 \quad \forall\, c > c_0\,. \tag{7.88}$$

However, by equating (7.83) with (7.86), it follows that:

$$\begin{aligned}
\Omega_+ &= \frac{-\left(\coth\chi + \tanh\chi\right) \pm \sqrt{\left(\coth\chi + \tanh\chi\right)^2 - 4mb}}{2b} \\
\pm\sqrt{\left(\coth\chi + \tanh\chi\right)^2 - 4mb} &= 2b\,\Omega_+ + \coth\chi + \tanh\chi \quad |()^2 \\
\left(\coth\chi + \tanh\chi\right)^2 - 4mb &= 4b^2\,\Omega_+^2 + 4b\left(\coth\chi + \tanh\chi\right)\Omega_+) + \left(\coth\chi + \tanh\chi\right)^2 \\
\coth\chi + \tanh\chi &= \frac{-4mb - 4b^2\Omega_+^2}{4b\Omega_+} \\
\coth\chi + \tanh\chi &= -\frac{m + b\Omega_+^2}{\Omega_+} < 0 \quad \forall\, c > c_0\,,
\end{aligned} \tag{7.89}$$

Finally, since $\coth\chi + \tanh\chi > 0$ for a radial coordinate ($\chi > 0$), this implies that **no consistent solution exists for** $c^2 > 1$.

Non periodic case: $c^2 < 1$

Now, the case $\mathbf{c^2 - 1 < 0}$ can be analyzed, in which the constant satisfies $b < 0$. Using the property $\cos(ix) = \cosh(x)$, the solution of (7.76) is

$$\Psi(\chi) = \Psi_0 - \frac{4ac^2}{b} \ln\cosh\left(\frac{\sqrt{m|b|}}{4ac^2}\left(\chi - \chi_0\right)\right), \tag{7.90}$$

so the B_χ components take the form

$$B_\chi = \sqrt{\frac{m}{|b|}} \tanh\left(\frac{\sqrt{m|b|}}{4ac^2}\left(\chi - \chi_0\right)\right). \tag{7.91}$$

[1]Depending on the value of the black hole mass M, the value of c_{03} will change, but the behavior of the function remains the same, since $M - 1 > 0$ always.

The other solutions for the two remaining equations, (7.77) and (7.78), are the same as (7.83) and (7.86). Thus, similarly to the previous periodic case, from (7.86) we here find

$$\begin{aligned} B_\chi^2 &\equiv \Omega_\pm^2(c,M) \\ &= \frac{-\left(\beta+2-2mdb\right) \pm \sqrt{\left(\beta+2-2mdb\right)^2 - 4\left(\alpha-db^2\right)\left(\gamma-dm^2\right)}}{2\left(\alpha-db^2\right)} \,. \end{aligned} \tag{7.92}$$

The positivity and reality of $\Omega_\pm$ must be examined; however, an analytical study is very challenging, making the use of a numerical tool necessary. It is found that the constant solution is always real for all $c^2 < 1$ and $M - 1 > 0$:

$$\Omega_\pm(c,M) > 0 \quad \forall \;\; 0 < |c| \, 1 \,. \tag{7.93}$$

By equating (7.86) and (7.91), a relation between the radial coordinate χ and the parameters c and M is obtained:

$$\chi_\pm(c,M) = \frac{4ac^2}{\sqrt{m|b|}} \operatorname{arctanh}\left(\sqrt{\frac{|b|}{m}}\,\Omega_\pm\right) > 0 \quad \forall \;\; 0 < |c| < 1 \,. \tag{7.94}$$

As shown in Fig. 7.1, where the coordinate is plotted for a particular black hole mass, $M = 2$, the positive branch $\chi_+ \;\forall\; 0 < |c| < 1$ is represented in blue, and the negative branch $\chi_- \;\forall\; 0 < |c| < c_{04}$ with $c_{04} \simeq 0.7182$, is shown in red. In the following, $M = 2$ is consistently chosen as an example to facilitate the mathematical analysis; nevertheless, a more detailed numerical study is required to gain a deeper understanding. It should be noted that, although some values of c vary with M, the overall behavior remains unchanged.

To ensure the consistency of the solution, it is still necessary to analyze the behavior of solution (7.83) at the point $\Omega_\pm$, similarly to what is done in equation (7.89):

$$\begin{aligned} \coth\chi + \tanh\chi &= -\frac{m}{\Omega_\pm} + |b|\Omega_\pm > 0 \quad \text{only for} \;\; \Omega_- \,, \\ \frac{1}{\tanh\chi} + \tanh\chi &= -\frac{m}{\Omega_\pm} + |b|\Omega_- \\ \tanh^2\chi - \left(|b|\,\Omega_- - \frac{m}{\Omega_-}\right)\tanh\chi + 1 &= 0 \,, \end{aligned} \tag{7.95}$$

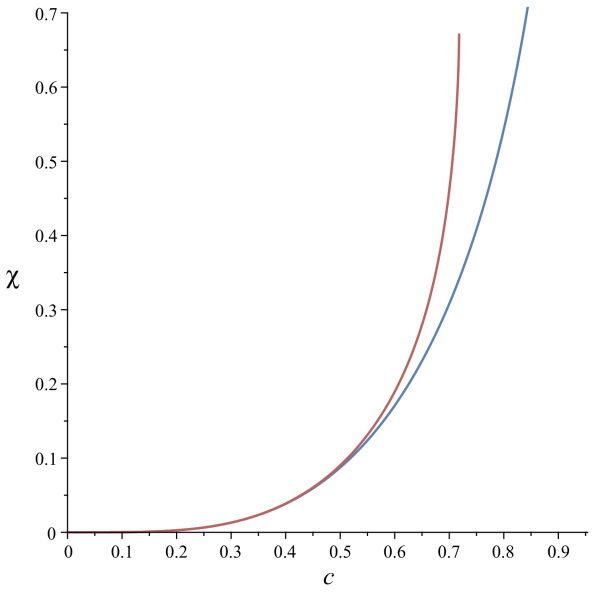

Figure 7.1: The plot of the $\chi_{\pm}(c, M)$ coordinate as a function of c and for selected values of $M > 1$, shows the two solutions, $\Omega_{+}(c, M)$ in blue and $\Omega_{-}(c, M)$ in red.

where only for Ω_{-} the first expression is positive ($\coth\chi + \tanh\chi > 0$). Since this is an algebraic equation for $\tanh\chi$, the solution is:

$$\tanh\chi = \frac{\left(|b|\,\Omega_{-} - \dfrac{m}{\Omega_{-}}\right) \pm \sqrt{\left(|b|\,\Omega_{-} - \dfrac{m}{\Omega_{-}}\right)^{2} - 4}}{2}\,. \tag{7.96}$$

This expression is real:

$$\Delta = \left(|b|\,\Omega_{-} - \frac{m}{\Omega_{-}}\right)^{2} - 4 > 0 \quad \forall \;\; c_{05} < |c| < c_{04}\,, \tag{7.97}$$

with $c_{05} \sim 0.6918$ for $M = 2$. Additionally, expression (7.96) is positive in both cases, $\pm$. The behavior of $\Omega_{-}(c)$ for $M = 2$ is shown in Fig. 7.2.

Finally, by substituting the first expression in (7.95) into solution (7.83), it follows:

$$B_{\chi}(c, M) = \Omega_{-}(c, M) = \frac{|b|\,\Omega_{-} - \dfrac{m}{\Omega_{-}} + \sqrt{\left(|b|\,\Omega_{-} - \dfrac{m}{\Omega_{-}}\right)^{2} - 4m|b|}}{2|b|} > 0\,. \tag{7.98}$$

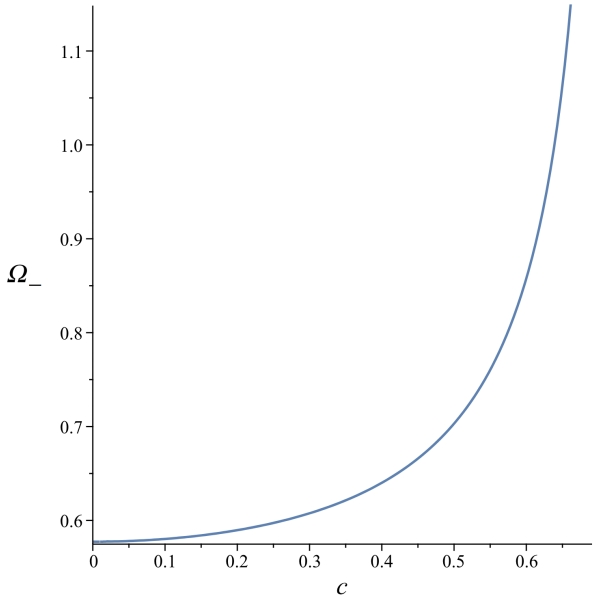

Figure 7.2: The plot of the $\Omega_{-}(c)$ solution as a function of c is shown for a particular case, $M = 2$. A maximum occurs at $c = c_{04} \sim 0.7182$.

From this, a numerical relation between c and M can be extracted: $M(c)$. However, the numerical techniques required are beyond the scope of this thesis. This analysis will be pursued in the near future. At present, it can be ensured that a finite set of points, $\bar{c}, \bar{M}$, satisfying equation (7.98) exists. This means that the solution exists only in the hyperbolic cylinder $\{\bar{\chi}(\bar{c}, \bar{M}),\, \theta,\, z\}$ for any $\theta \in [0,\, 2\pi]$ and $z \in]-\infty,\, \infty[$, in contrast to the planar case, where a particular value in the z coordinate could be chosen.

7.3.5 Abelian anomaly for the hyperbolic case

As a final result presented in this chapter, it is important to discuss the Abelian anomaly generated by the dislocation at the hyperbolic cylinder $\{\bar{\chi},\, \theta,\, z\}$, found for certain pairs of points $\bar{c}, \bar{M}$ for which the torsion fields are nonzero: $B_{\chi} = \Omega_{-}(\bar{c}, \bar{M})$, recalling that the axial torsion field is given by $A_{\chi} = 8c\, B_{\chi}$. From the definition of the Abelian anomaly

in (5.64), it is calculated:

$$
\begin{aligned}
\star \quad & (\coth\chi + \tanh\chi)\,|_{\chi=\bar{\chi}} = -\frac{m}{\Omega_-} + |b|\Omega_- \,, \\
\star \quad & (\partial_\chi A_\chi)\,|_{\chi=\bar{\chi}} = 8c\,\partial_\chi \left(\sqrt{\frac{m}{|b|}} \tanh\left(\frac{\sqrt{m|b|}}{4ac^2}\,\chi \right) \right) |_{\chi=\bar{\chi}} \\
& \qquad = \frac{2m}{ac}\left(1 - \tanh^2\left(\frac{\sqrt{m|b|}}{4ac^2}\,\chi \right) \right) = \frac{2m}{ac}\left(1 - \frac{|b|}{m}\,\Omega_-^2 \right) \,, \\
\therefore \quad & \mathcal{A}_{ch} = 16\kappa M \left((\coth\chi + \tanh\chi) A_\chi + \partial_\chi A_\chi \right) |_{\chi=\bar{\chi}} \\
& \qquad = \frac{64\kappa\, M(c)}{c} \left(m(c) - |b|\,\Omega_-^2(c) \right) \,,
\end{aligned}
\tag{7.99}
$$

being a function of the dislocation parameter, and noting that $\mathcal{A}_{ch} < 0$, $\forall\ 0 < |c| < c_{06}$, and $\mathcal{A}_{ch} > 0$, $\forall\ c_{06} < |c| < 1$. Fixing the black hole mass at $M = 2$, for example, one obtains $c_{06} \simeq 0.8164$, and the anomaly can be plotted to observe its behavior, as shown in Fig. 7.3. In this graph, it can be seen that the anomaly diverges negatively as $|c| \to 0$, then decreases until reaching zero at the point c_{06}, and continues increasing until diverging as $|c| \to 1$.

In conclusion, the analysis of the hyperbolic case has revealed a rich structure of solutions and highlighted the behavior of dislocations, represented by torsion fields in the holographic framework. While the simplest solutions have been characterized analytically and their main properties described, a more thorough understanding requires the use of numerical tools to explore the full solution space. A main feature of the solutions is that, in contrast with the planar case, the diagonal and axial torsion exist only in a hyperbolic cylinder of radius $\bar{\chi}$, which can be interpreted as a topological defect. Future work will involve a detailed numerical study of the relations between the parameters c and M, as well as the computation of the Burgers vector, which may provide a better understanding of the nature of this dislocation. Furthermore, it is expected that, similarly to the planar case, the odd-parity Abelian anomaly will be proportional to the Nieh-Yan topological invariant. These results provide a starting point for further investigation of holographic torsion and its manifestation as dislocations in materials, possibly in Weyl semimetals embedded in hyperbolic geometry.

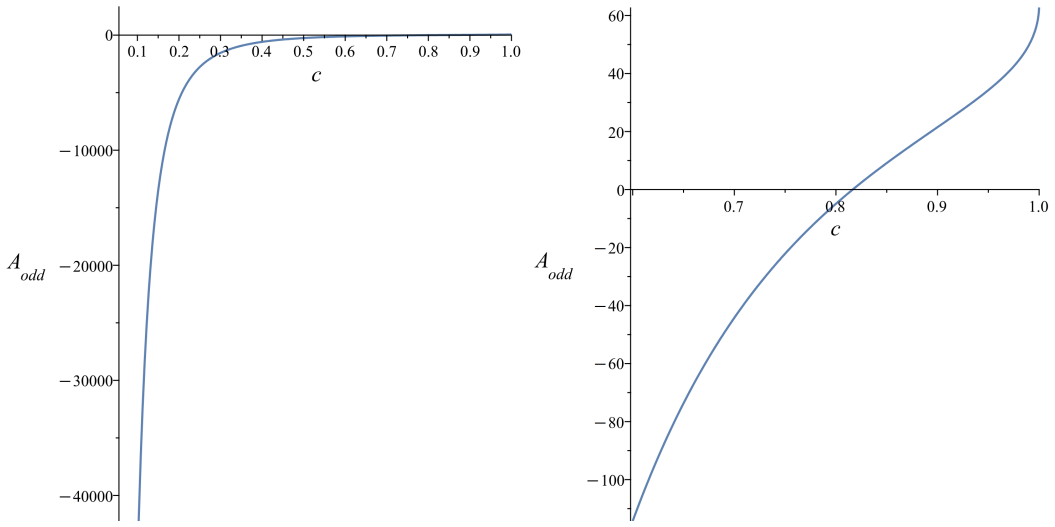

Figure 7.3: The graph of the Abelian anomaly, $\mathcal{A}_{odd}(c)$, as a function of c, is shown for the particular case $M = 2$. On the left, the anomaly is displayed for the entire range $|c| < 1$; on the right, a magnified view between $0.6 < |c| < 0.9$ is shown to highlight the change in sign.

Chapter 8

Conclusions

To conclude, using the AdS/CFT correspondence, the bulk solution can be understood from the perspective of the holographically dual theory. In this sense, this thesis has explored a holographic realization of a strongly coupled quantum field theory at finite temperature with dislocations—such as a superconductor [108, 109, 110] or an insulator [111]—within a $(4+1)$-dimensional bulk Chern-Simons AdS gravity framework incorporating a black hole and nontrivial torsion. In our case, since such dislocations can produce an unequal number of chiral quasiparticles, there arises the possibility that the Abelian anomaly $\mathcal{A}_{\text{odd}}$ realized on the ring corresponds to a chiral anomaly, with the system potentially describing holographic Weyl semimetals.

A detailed analysis reveals that, in the planar case, the theory admits two families of axially symmetric solutions: periodic solutions, as described by Eq. (6.84) and illustrated in Fig. 6.4, and aperiodic solutions, given by Eq. (6.86), which further exhibit positive and negative branches, as shown in Figs. 6.6 and 6.7, respectively. In the hyperbolic case, only one family of solutions was found: the aperiodic one, valid when the dislocation parameter satisfies $c^2 < 1$, as given by Eq. (7.92) and shown in Fig. 7.2. Despite the analytical complexity of the hyperbolic equations, partial information could be extracted for relatively simple solvable configurations. For both the radial coordinate χ and the diagonal torsion field B_χ, at fixed black hole mass, the behavior is monotonically increasing with the parameter c, reaching a maximum value as shown in Figs. 7.1 and 7.2. In contrast,

the anomaly behaves differently: it diverges negatively as $|c| \to 0$, vanishes at c_{06}, and then becomes positive and divergent as $|c| \to 1$.

The behavior of the planar solutions, however, differs significantly. For instance, the nodal radius evolves in opposite ways for the two families: in periodic solutions, it decreases with increasing temperature, whereas in aperiodic solutions, it increases. This nonuniversal behavior originates from the intrinsic nonlinearity of the underlying holographically dual theory, namely CS AdS gravity. Both classes of solutions exhibit an Abelian anomaly (Fig. 6.8). If such an Abelian anomaly indeed reduces to the chiral one, the holographically dual quantum field theory can be interpreted in terms of a WSM. Notably, the abelian anomaly is proportional to the Nieh–Yan torsional invariant, as explicitly shown in Eq. (6.97).

A key feature of this approach is that the torsion field (representing dislocation strength), the black hole mass (temperature), and the ring radius are determined self-consistently as functions of the dislocation parameter c in both the planar and hyperbolic cases. For the planar horizon, physically relevant configurations occur when the dislocation parameter departs from its critical values, where divergences in temperature or nodal radius emerge. Examples of such divergences appear near $\pm c_*$ for periodic solutions and near $\pm c_{02}$ or ± 1 for aperiodic ones (see Table (6.83)).

Holographic description of the dislocations motivates the study of its lattice version. In particular, it would be interesting to find the lattice realization of the torsion field in terms of the dislocation configuration and its coupling to the fermions. This would permit to directly test the predictions of our holographic theory in a lattice model, particularly the dependence of the Burgers vector and anomaly on the dislocation parameter encoding the strength of the torsion.

In light of our results, suggesting their possible relevance to holographic WSMs, it is worth emphasizing that previous holographic constructions of topological semimetals have been developed using alternative bulk gravitational theories [112, 113, 114, 115, 116, 117, 118, 119, 120, 121, 122]. Most notably, these approaches rely on torsion-free bulk theories, differing from the framework presented in this thesis.

An important avenue for future research involves investigating the instabilities of WSMs

in the holographic context, particularly by incorporating additional gauge and matter fields in the bulk to explore symmetry-breaking patterns and interaction-driven instabilities on the lattice, such as axion insulators [123, 124, 125, 126]. This is essential for a complete demonstration of the holographic WSM correspondence. Furthermore, supersymmetric extensions of AdS space in five dimensions [127] and in higher odd-dimensional spacetimes [128, 129, 130] offer intriguing prospects. These theories feature black hole solutions with nontrivial topological charges [84], potentially enabling the construction of holographic duals for strongly coupled states on the surfaces of topological insulators, with supersymmetric critical points in $(3 + 1)$ dimensions [131, 132, 133, 134]. However, it is crucial to emphasize that the present work avoids such instabilities by relying solely on a purely gravitational theory, without introducing additional matter or gauge fields.

Other promising directions for future exploration include employing alternative matter fields to induce dislocations in semimetals. Additionally, Einstein–Gauss–Bonnet AdS gravity, away from the CS point, offers another valuable route, as it introduces an additional free parameter—the Gauss–Bonnet coupling constant—that could further enrich the holographic modeling framework.

References

[1] Vladimir Juričić, Olivera Miskovic, and Francisca Ramírez Carrasco. Holography of dislocations and ring defects in Einstein–Gauss–Bonnet AdS gravity. *Eur. Phys. J. C*, 85(10):1134, 2025.

[2] H.B. Nielsen and M. Ninomiya. Absence of neutrinos on a lattice: (i). proof by homotopy theory. *Nuclear Physics B*, 185(1):20–40, 1981.

[3] H.B. Nielsen and M. Ninomiya. A no-go theorem for regularizing chiral fermions. *Physics Letters B*, 105(2):219–223, 1981.

[4] N. P. Armitage, E. J. Mele, and Ashvin Vishwanath. Weyl and Dirac semimetals in three-dimensional solids. *Rev. Mod. Phys.*, 90:015001, 2018.

[5] H.B. Nielsen and Masao Ninomiya. The Adler-Bell-Jackiw anomaly and Weyl fermions in a crystal. *Physics Letters B*, 130(6):389–396, 1983.

[6] AA Zyuzin and AA Burkov. Topological response in Weyl semimetals and the chiral anomaly. *Phys. Rev. B*, 86(11):115133, 2012.

[7] D.T. Son and B.Z. Spivak. Chiral Anomaly and Classical Negative Magnetoresistance of Weyl Metals. *Phys. Rev. B*, 88:104412, 2013.

[8] Xiaochun Huang, Lingxiao Zhao, Yujia Long, Peipei Wang, Dong Chen, Zhanhai Yang, Hui Liang, Mianqi Xue, Hongming Weng, Zhong Fang, et al. Observation of the chiral-anomaly-induced negative magnetoresistance in 3D Weyl semimetal TaAs. *Phys. Rev. X*, 5(3):031023, 2015.

[9] N. P. Ong and Sihang Liang. Experimental signatures of the chiral anomaly in Dirac–Weyl semimetals. *Nature Reviews Physics*, 3(6):394–404, 2021.

[10] R. Arouca, Andrea Cappelli, and T. H. Hansson. Quantum field theory anomalies in condensed matter physics. *SciPost Phys. Lect. Notes*, page 62, 2022.

[11] Edward Witten and Kazuya Yonekura. Anomaly inflow and the η-invariant. In *Memorial Volume for Shoucheng Zhang*, pages 283–352. World Scientific, 2022.

[12] M. Banados, A. Schwimmer, and S. Theisen. Chern-Simons gravity and holographic anomalies. *JHEP*, 05:039, 2004.

[13] Maximo Banados, Rodrigo Olea, and Stefan Theisen. Counterterms and dual holographic anomalies in CS gravity. *JHEP*, 10:067, 2005.

[14] Per Kraus and Finn Larsen. Holographic gravitational anomalies. *JHEP*, 01:022, 2006.

[15] Sergey N. Solodukhin. Holography with gravitational Chern-Simons. *Phys. Rev. D*, 74:024015, 2006.

[16] Sergey N. Solodukhin. Holographic description of gravitational anomalies. *JHEP*, 07:003, 2006.

[17] James Babington. Towards a holographic dual of SQCD: Holographic anomalies and higher derivative gravity. *Class. Quant. Grav.*, 24:277–290, 2007.

[18] Ali H. Chamseddine. Topological Gauge Theory of Gravity in Five-dimensions and All Odd Dimensions. *Phys. Lett. B*, 233:291–294, 1989.

[19] Ricardo Troncoso and Jorge Zanelli. Higher dimensional gravity, propagating torsion and AdS gauge invariance. *Class. Quant. Grav.*, 17:4451–4466, 2000.

[20] Maximo Banados, Olivera Miskovic, and Stefan Theisen. Holographic currents in first order gravity and finite Fefferman-Graham expansions. *JHEP*, 06:025, 2006.

[21] AA Burkov, MD Hook, and Leon Balents. Topological nodal semimetals. *Physical Review B—Condensed Matter and Materials Physics*, 84(23):235126, 2011.

[22] Chen Fang, Yige Chen, Hae-Young Kee, and Liang Fu. Topological nodal line semimetals with and without spin-orbital coupling. *Physical Review B*, 92(8):081201, 2015.

[23] Chen Fang, Hongming Weng, Xi Dai, and Zhong Fang. Topological nodal line semimetals. *Chinese Physics B*, 25(11):117106, 2016.

[24] Bitan Roy. Interacting nodal-line semimetal: Proximity effect and spontaneous symmetry breaking. *Physical Review B*, 96(4):041113, 2017.

[25] Qi-Feng Liang, Jian Zhou, Rui Yu, Zhi Wang, and Hongming Weng. Node-surface and node-line fermions from nonsymmorphic lattice symmetries. *Physical Review B*, 93(8):085427, 2016.

[26] Weikang Wu, Ying Liu, Si Li, Chengyong Zhong, Zhi-Ming Yu, Xian-Lei Sheng, YX Zhao, and Shengyuan A Yang. Nodal surface semimetals: Theory and material realization. *Physical Review B*, 97(11):115125, 2018.

[27] B-B Fu, C-J Yi, T-T Zhang, M Caputo, J-Z Ma, X Gao, BQ Lv, L-Y Kong, Y-B Huang, P Richard, et al. Dirac nodal surfaces and nodal lines in ZrSiS. *Science advances*, 5(5):eaau6459, 2019.

[28] AA Burkov. Quantum anomalies in nodal line semimetals. *Physical Review B*, 97(16):165104, 2018.

[29] Alberto Martín-Ruiz and Alberto Cortijo. Parity anomaly in the nonlinear response of nodal-line semimetals. *Physical Review B*, 98(15):155125, 2018.

[30] WB Rui, YX Zhao, and Andreas P Schnyder. Topological transport in Dirac nodal-line semimetals. *Physical Review B*, 97(16):161113, 2018.

[31] Daniel Bulmash, Pavan Hosur, Shou-Cheng Zhang, and Xiao-Liang Qi. Unified topological response theory for gapped and gapless free fermions. *Physical Review X*, 5(2):021018, 2015.

[32] MA Zubkov. Emergent gravity and chiral anomaly in Dirac semimetals in the presence of dislocations. *Annals of Physics*, 360:655–678, 2015.

[33] Hiroaki Sumiyoshi and Satoshi Fujimoto. Torsional chiral magnetic effect in a Weyl semimetal with a topological defect. *Physical review letters*, 116(16):166601, 2016.

[34] Maxim N Chernodub and MA Zubkov. Chiral anomaly in Dirac semimetals due to dislocations. *Physical Review B*, 95(11):115410, 2017.

[35] Ze-Min Huang, Jianhui Zhou, and Shun-Qing Shen. Topological responses from chiral anomaly in multi-Weyl semimetals. *Physical Review B*, 96(8):085201, 2017.

[36] Ze-Min Huang, Longyue Li, Jianhui Zhou, and Hong-Hao Zhang. Torsional response and Liouville anomaly in Weyl semimetals with dislocations. *Physical Review B*, 99(15):155152, 2019.

[37] Chong-Sun Chu and Rong-Xin Miao. Chiral current induced by torsional Weyl anomaly. *Physical Review B*, 107(20):205410, 2023.

[38] Rodrigo Soto-Garrido, Enrique Muñoz, and Vladimir Juričić. Dislocation defect as a bulk probe of monopole charge of multi-weyl semimetals. *Phys. Rev. Res.*, 2:012043, 2020.

[39] Hagen Kleinert. *Gauge Fields in Condensed Matter: Vol. 2: Stresses and Defects (Differential Geometry, Crystal Melting)*. World Scientific, 1989.

[40] C Fefferman and C R Graham. *Conformal invariants, The mathematical heritage of Elie Cartan, Numero Hors Serie, 95–116*. Asterisque, 1985.

[41] H. T. Nieh and M. L. Yan. An Identity in Riemann-cartan Geometry. *J. Math. Phys.*, 23:373, 1982.

[42] Igor Boettcher, Przemyslaw Bienias, Ron Belyansky, Alicia J. Kollár, and Alexey V. Gorshkov. Quantum simulation of hyperbolic space with circuit quantum electrodynamics: From graphs to geometry. *Phys. Rev. A*, 102:032208, Sep 2020.

[43] Igor Boettcher, Alexey V. Gorshkov, Alicia J. Kollár, Joseph Maciejko, Steven Rayan, and Ronny Thomale. Crystallography of hyperbolic lattices. *Phys. Rev. B*, 105(12):125118, 2022.

[44] Alicia J. Kollár, Mattias Fitzpatrick, and Andrew A. Houck. Hyperbolic lattices in circuit quantum electrodynamics. *Nature*, 571(7763):45–50, 2019.

[45] Zheng-Rong Liu, Chun-Bo Hua, Tan Peng, and Bin Zhou. Chern insulator in a hyperbolic lattice. *Phys. Rev. B*, 105(24):245301, 2022.

[46] Weixuan Zhang, Hao Yuan, Na Sun, Houjun Sun, and Xiangdong Zhang. Observation of novel topological states in hyperbolic lattices. *Nature Communications*, 13(1):2937, 2022.

[47] Lei Huang, Lu He, Weixuan Zhang, Huizhen Zhang, Dongning Liu, Xue Feng, Fang Liu, Kaiyu Cui, Yidong Huang, Wei Zhang, and Xiangdong Zhang. Hyperbolic photonic topological insulators. *Nature Communications*, 15(1):1647, 2024.

[48] Qiaolu Chen, Zhe Zhang, Haoye Qin, Aleksi Bossart, Yihao Yang, Hongsheng Chen, and Romain Fleury. Anomalous and chern topological waves in hyperbolic networks. *Nature Communications*, 15(1):2293, 2024.

[49] Canon Sun, Anffany Chen, Tomáš Bzdušek, and Joseph Maciejko. Topological linear response of hyperbolic Chern insulators. *SciPost Phys.*, 17(5):124, 2024.

[50] Yu-Liang Tao and Yong Xu. Higher-order topological hyperbolic lattices. *Phys. Rev. B*, 107:184201, May 2023.

[51] Junsong Sun, Chang-An Li, Shiping Feng, and Huaiming Guo. Hybrid higher-order skin-topological effect in hyperbolic lattices. *Phys. Rev. B*, 108:075122, Aug 2023.

[52] Conyers Herring. Accidental Degeneracy in the Energy Bands of Crystals. *Phys. Rev.*, 52:365–373, Aug 1937.

[53] Holger Bech Nielsen and M. Ninomiya. Absence of Neutrinos on a Lattice. 2. Intuitive Topological Proof. *Nucl. Phys. B*, 193:173–194, 1981.

[54] S. Y. Xu et al. Discovery of a Weyl Fermion semimetal and topological Fermi arcs. *Science*, 349:613–617, 2015.

[55] Leon Balents. Weyl electrons kiss. *Physics*, 4(36), 2011.

[56] Satoru NAKATSUJI. Large anomalous hall effect in an antiferromagnet. *Oyo Buturi*, 86(4):310–314, 2017.

[57] Robert-Jan Slager, Vladimir Juričić, and Bitan Roy. Dissolution of topological fermi arcs in a dirty weyl semimetal. *Phys. Rev. B*, 96:201401, Nov 2017.

[58] Hang Chi, Cheng Zhang, Genda Gu, Dmitri E Kharzeev, Xi Dai, and Qiang Li. Lifshitz transition mediated electronic transport anomaly in bulk zrte5. *New Journal of Physics*, 19(1):015005, jan 2017.

[59] Maxim N. Chernodub, Yago Ferreiros, Adolfo G. Grushin, Karl Landsteiner, and María A. H. Vozmediano. Thermal transport, geometry, and anomalies. *Phys. Rept.*, 977:1–58, 2022.

[60] C. Shekhar, A. Nayak, and Y. et al. Sun. Extremely large magnetoresistance and ultrahigh mobility in the topological Weyl semimetal candidate NbP. *Nature Phys*, 11(8):645–649, 2015.

[61] P. M. Chaikin and T. C. Lubensky. *Principles of Condensed Matter Physics*. Cambridge University Press, paperback ed. (with corrections) edition, 2000.

[62] Marcelo F. Ciappina, Alfredo Iorio, Pablo Pais, and Adamantia Zampeli. Torsion in quantum field theory through time-loops on Dirac materials. *Phys. Rev. D*, 101(3):036021, 2020.

[63] Jacob D. Bekenstein. Black Holes and Entropy. *Phys. Rev. D*, 7:2333–2346, Apr 1973.

[64] S. W. Hawking. Particle Creation by Black Holes. *Commun. Math. Phys.*, 43:199–220, 1975. [Erratum: Commun.Math.Phys. 46, 206 (1976)].

[65] Juan Martin Maldacena. The Large N limit of superconformal field theories and supergravity. *Adv. Theor. Math. Phys.*, 2:231–252, 1998.

[66] Sebastian De Haro, Jeroen van Dongen, Manus Visser, and Jeremy Butterfield. Conceptual analysis of black hole entropy in string theory. *Stud. Hist. Phil. Sci. B*, 69:82–111, 2020.

[67] Erdmenger Ammon. *Gauge/Gravity Duality Foundations and Applications*. Cambridge University Press, 2015.

[68] Sean A. Hartnoll. Lectures on holographic methods for condensed matter physics. *Class. Quant. Grav.*, 26:224002, 2009.

[69] Subir Sachdev. *Quantum Phase Transitions*. Cambridge University Press, 4 2011.

[70] Sean A. Hartnoll, Andrew Lucas, and Subir Sachdev. Holographic quantum matter. 12 2016.

[71] S. S. Gubser, I. R. Klebanov, and Alexander M. Polyakov. A Semiclassical limit of the gauge / string correspondence. *Nucl. Phys. B*, 636:99–114, 2002.

[72] Edward Witten. Anti-de Sitter space and holography. *Adv. Theor. Math. Phys.*, 2:253–291, 1998.

[73] Kostas Skenderis. Lecture notes on holographic renormalization. *Class. Quant. Grav.*, 19:5849–5876, 2002.

[74] Jan Zaanen, Ya-Wen Sun, Yan Liu, and Koenraad Schalm. *Holographic Duality in Condensed Matter Physics*. Cambridge Univ. Press, 2015.

[75] Sean A. Hartnoll, Christopher P. Herzog, and Gary T. Horowitz. Building a Holographic Superconductor. *Phys. Rev. Lett.*, 101:031601, Jul 2008.

[76] Subir Sachdev. What can gauge-gravity duality teach us about condensed matter physics? *Annual Review of Condensed Matter Physics*, 3, 08 2011.

[77] Steven S. Gubser. Breaking an abelian gauge symmetry near a black hole horizon. *Phys. Rev. D*, 78:065034, 2008.

[78] David G. Boulware and Stanley Deser. String Generated Gravity Models. *Phys. Rev. Lett.*, 55:2656, 1985.

[79] Olivera Miskovic and Rodrigo Olea. Quantum statistical relation for black holes in nonlinear electrodynamics coupled to einstein-gauss-bonnet ads gravity. *Phys. Rev. D*, 83:064017, Mar 2011.

[80] Jorge Zanelli. Lecture notes on Chern-Simons (super-)gravities. Second edition (February 2008). In *7th Mexican Workshop on Particles and Fields*, 2 2005.

[81] Olivera Miskovic, Ricardo Troncoso, and Jorge Zanelli. Dynamics and BPS states of AdS(5) supergravity with a Gauss-Bonnet term. *Phys. Lett. B*, 637:317–325, 2006.

[82] Rodrigo Aros and Mauricio Contreras. Torsion induces gravity. *Phys. Rev. D*, 73:087501, 2006.

[83] Fabrizio Canfora, Alex Giacomini, and Ricardo Troncoso. Black holes, parallelizable horizons and half-BPS states for the Einstein-Gauss-Bonnet theory in five dimensions. *Phys. Rev. D*, 77:024002, 2008.

[84] Laura Andrianopoli, Gaston Giribet, Darío López Díaz, and Olivera Miskovic. Black holes with topological charges in Chern-Simons AdS_5 supergravity. *JHEP*, 11:123, 2021.

[85] Gaston Giribet, Nelson Merino, Olivera Miskovic, and Jorge Zanelli. Black hole solutions in Chern-Simons AdS supergravity. *JHEP*, 08:083, 2014.

[86] Maximo Banados. Charged solutions in 5d Chern-Simons supergravity. *Phys. Rev. D*, 65:044014, 2002.

[87] Olivera Miskovic and Rodrigo Olea. Counterterms in Dimensionally Continued AdS Gravity. *JHEP*, 10:028, 2007.

[88] Maximo Banados, Claudio Teitelboim, and Jorge Zanelli. Dimensionally continued black holes. *Phys. Rev. D*, 49:975–986, 1994.

[89] Maximo Banados, Claudio Teitelboim, and Jorge Zanelli. The Black hole in three-dimensional space-time. *Phys. Rev. Lett.*, 69:1849–1851, 1992.

[90] M. Henningson and K. Skenderis. The Holographic Weyl anomaly. *JHEP*, 07:023, 1998.

[91] A. Schwimmer and S. Theisen. Universal features of holographic anomalies. *JHEP*, 10:001, 2003.

[92] A. Schwimmer and S. Theisen. Diffeomorphisms, anomalies and the Fefferman-Graham ambiguity. *JHEP*, 08:032, 2000.

[93] Stanley Deser and A. Schwimmer. Geometric classification of conformal anomalies in arbitrary dimensions. *Phys. Lett. B*, 309:279–284, 1993.

[94] Yu. N. Obukhov. SPECTRAL GEOMETRY OF THE RIEMANN-CARTAN SPACE-TIME AND THE AXIAL ANOMALY. *Phys. Lett. B*, 108:308–310, 1982.

[95] Yu. n. Obukhov. SPECTRAL GEOMETRY OF THE RIEMANN-CARTAN SPACE-TIME. *Nucl. Phys. B*, 212:237–254, 1983.

[96] L. F. Urrutia and J. D. Vergara. Consistent coupling of the gravitino field to a gravitational background with torsion. *Phys. Rev. D*, 44:3882, 1991.

[97] Osvaldo Chandia and Jorge Zanelli. Topological invariants, instantons and chiral anomaly on spaces with torsion. *Phys. Rev. D*, 55:7580, 1997.

[98] G. Aldazabal, D. Badagnani, Luis E. Ibanez, and A. M. Uranga. Tadpole versus anomaly cancellation in D = 4, D = 6 compact IIB orientifolds. *JHEP*, 06:031, 1999.

[99] Osvaldo Chandia and Jorge Zanelli. Reply to the comment by D. Kreimer and E. Mielke. *Phys. Rev. D*, 63:048502, 2001.

[100] Francisca Ramírez Carrasco. Holographic hyperbolic dislocations. *Manuscript in preparation*, 2025.

[101] Bitan Roy, Pallab Goswami, and Vladimir Juricic. Interacting Weyl fermions: Phases, phase transitions and global phase diagram. *Phys. Rev. B*, 95(20):201102, 2017.

[102] Michael P. Zaletel, Mikhail Lukin, Christopher Monroe, Chetan Nayak, Frank Wilczek, and Norman Y. Yao. Colloquium: Quantum and classical discrete time crystals. *Rev. Mod. Phys.*, 95:031001, 2023.

[103] Peng Yang, Matteo Baggioli, Zi Cai, Yu Tian, and Hongbao Zhang. Holographic Dissipative Spacetime Supersolids. *Phys. Rev. Lett.*, 131(22):221601, 2023.

[104] Jose L. F. Barbon and Javier Martin-Garcia. Holographic Complexity Of Cold Hyperbolic Black Holes. *JHEP*, 11:181, 2015.

[105] Roberto Emparan. AdS / CFT duals of topological black holes and the entropy of zero energy states. *JHEP*, 06:036, 1999.

[106] Jie Ren. Analytic solutions of neutral hyperbolic black holes with scalar hair. *Phys. Rev. D*, 106(8):086023, 2022.

[107] Seung Ki Baek, Hiroyuki Shima, and Beom Jun Kim. Curvature-induced frustration in the xy model on hyperbolic surfaces. *Phys. Rev. E*, 79:060106, Jun 2009.

[108] Jiliang Jing, Liangcheng Wang, Qiyuan Pan, and Songbai Chen. Holographic Superconductors in Gauss-Bonnet gravity with Born-Infeld electrodynamics. *Phys. Rev. D*, 83:066010, 2011.

[109] Sugumi Kanno. A Note on Gauss-Bonnet Holographic Superconductors. *Class. Quant. Grav.*, 28:127001, 2011.

[110] Xian-Hui Ge and Hong-Qiang Leng. Analytical calculation on critical magnetic field in holographic superconductors with backreaction. *Prog. Theor. Phys.*, 128:1211–1228, 2012.

[111] Qiyuan Pan, Jiliang Jing, and Bin Wang. Analytical investigation of the phase transition between holographic insulator and superconductor in Gauss-Bonnet gravity. *JHEP*, 11:088, 2011.

[112] Umut Gürsoy, Vivian Jacobs, Erik Plauschinn, Henk Stoof, and Stefan Vandoren. Holographic models for undoped Weyl semimetals. *Journal of High Energy Physics*, 2013:127, 2013.

[113] Karl Landsteiner, Yan Liu, and Ya-Wen Sun. Quantum phase transition between a topological and a trivial semimetal from holography. *Phys. Rev. Lett.*, 116:081602, 2016.

[114] Karl Landsteiner and Yan Liu. The holographic Weyl semi-metal. *Physics Letters B*, 753:453–457, 2016.

[115] Koji Hashimoto, Shunichiro Kinoshita, Keiju Murata, and Takashi Oka. Holographic Floquet states I: a strongly coupled Weyl semimetal. *Journal of High Energy Physics*, 2017:127, 2017.

[116] Yan Liu and Junkun Zhao. Weyl semimetal/insulator transition from holography. *Journal of High Energy Physics*, 2018:124, 2018.

[117] Yan Liu and Ya-Wen Sun. Topological nodal line semimetals in holography. *Journal of High Energy Physics*, 2018:72, 2018.

[118] Renato M. A. Dantas, Francisco Peña Benitez, Bitan Roy, and Piotr Surówka. Non-Abelian anomalies in multi-Weyl semimetals. *Phys. Rev. Res.*, 2:013007, 2020.

[119] Vladimir Juričić, Ignacio Salazar Landea, and Rodrigo Soto-Garrido. Phase transitions in a holographic multi-Weyl semimetal. *Journal of High Energy Physics*, 2020:52, 2020.

[120] Yan Liu and Xin-Meng Wu. An improved holographic nodal line semimetal. *Journal of High Energy Physics*, 2021(5):141, 2021.

[121] Xuanting Ji, Yan Liu, Ya-Wen Sun, and Yun-Long Zhang. A Weyl-Z_2 semimetal from holography. *Journal of High Energy Physics*, 2021:66, 2021.

[122] Sebastián Bahamondes, Ignacio Salazar Landea, and Rodrigo Soto-Garrido. Holographic description of an anisotropic Dirac semimetal. *Journal of High Energy Physics*, 2024:80, 2024.

[123] Zhong Wang and Shou-Cheng Zhang. Chiral anomaly, charge density waves, and axion strings from Weyl semimetals. *Phys. Rev. B*, 87:161107, 2013.

[124] Bitan Roy and Jay D. Sau. Magnetic catalysis and axionic charge density wave in Weyl semimetals. *Phys. Rev. B*, 92:125141, 2015.

[125] Bitan Roy, Pallab Goswami, and Vladimir Juričić. Interacting Weyl fermions: Phases, phase transitions, and global phase diagram. *Phys. Rev. B*, 95:201102, 2017.

[126] J. Gooth, B. Bradlyn, S. Honnali, C. Schindler, N. Kumar, J. Noky, Y. Qi, C. Shekhar, Y. Sun, Z. Wang, B. A. Bernevig, and C. Felser. Axionic charge-density wave in the Weyl semimetal $(TaSe_4)_2I$. *Nature*, 575:315, 2019.

[127] Ali H. Chamseddine. Topological gravity and supergravity in various dimensions. *Nucl. Phys. B*, 346:213–234, 1990.

[128] Maximo Banados, Ricardo Troncoso, and Jorge Zanelli. Higher dimensional Chern-Simons supergravity. *Phys. Rev. D*, 54:2605–2611, 1996.

[129] Ricardo Troncoso and Jorge Zanelli. New gauge supergravity in seven-dimensions and eleven-dimensions. *Phys. Rev. D*, 58:101703, 1998.

[130] Ricardo Troncoso and Jorge Zanelli. Gauge supergravities for all odd dimensions. *Int. J. Theor. Phys.*, 38:1181–1206, 1999.

[131] Sung-Sik Lee. Emergence of supersymmetry at a critical point of a lattice model. *Phys. Rev. B*, 76:075103, 2007.

[132] Bitan Roy, Vladimir Juričić, and Igor F. Herbut. Quantum superconducting criticality in graphene and topological insulators. *Phys. Rev. B*, 87:041401, 2013.

[133] Tarun Grover, D. N. Sheng, and Ashvin Vishwanath. Emergent space-time supersymmetry at the boundary of a topological phase. *Science*, 344:280, 2014.

[134] Pedro Ponte and Sung-Sik Lee. Emergence of supersymmetry on the surface of three-dimensional topological insulators. *New Journal of Physics*, 16:013044, 2014.

[135] Gary T. Horowitz. Introduction to Holographic Superconductors. *Lect. Notes Phys.*, 828:313–347, 2011.

[136] Sean A. Hartnoll, Christopher P. Herzog, and Gary T. Horowitz. Holographic superconductors. *JHEP*, 12:015, 2008.

[137] Alberto Martín-Ruiz and Alberto Cortijo. Parity anomaly in the nonlinear response of nodal-line semimetals. *Phys. Rev. B*, 98:155125, Oct 2018.

[138] Tero T Heikkilä, Nikolai Borisovich Kopnin, and Grigorii Efimovich Volovik. Flat bands in topological media. *JETP letters*, 94:233–239, 2011.

[139] Johanna Erdmenger, Ioannis Matthaiakakis, René Meyer, and Dmitri Vassilevich. The chiral torsional anomaly and the Nieh-Yan invariant with and without boundaries. 9 2024.

[140] Dam T. Son and Piotr Surowka. Hydrodynamics with Triangle Anomalies. *Phys. Rev. Lett.*, 103:191601, 2009.

[141] Nabamita Banerjee, Jyotirmoy Bhattacharya, Sayantani Bhattacharyya, Suvankar Dutta, R. Loganayagam, and P. Surowka. Hydrodynamics from charged black branes. *JHEP*, 01:094, 2011.

[142] Johanna Erdmenger, Michael Haack, Matthias Kaminski, and Amos Yarom. Fluid dynamics of R-charged black holes. *JHEP*, 01:055, 2009.

[143] Nabamita Banerjee, Jyotirmoy Bhattacharya, Sayantani Bhattacharyya, Sachin Jain, Shiraz Minwalla, and Tarun Sharma. Constraints on Fluid Dynamics from Equilibrium Partition Functions. *JHEP*, 09:046, 2012.

[144] Qiyuan Pan, Bin Wang, Eleftherios Papantonopoulos, J. Oliveira, and A. B. Pavan. Holographic Superconductors with various condensates in Einstein-Gauss-Bonnet gravity. *Phys. Rev. D*, 81:106007, 2010.

Appendices

Appendix A

Torsionless spin connection in five dimensions

The five-dimensional torsionless (Levi-Civita) spin connection $\hat{\mathring{\omega}}^{AB}$ depends only on the vielbein $\hat{e}^A$, and it is computed from Maurer-Cartan equation $\hat{\mathrm{D}}\hat{e}^A = \mathrm{d}\hat{e}^A + \hat{\mathring{\omega}}^{AB} \wedge \hat{e}_B = 0$. Then, the solution is given in terms of the Christoffel symbols:

$$\hat{\mathring{\omega}}^{AB} = \hat{e}^{BM} \left(-\partial_N \hat{e}^A_M + \hat{\Gamma}^K_{NM}\, \hat{e}^A_K \right) \mathrm{d}x^N \,, \tag{A.1}$$

with the Christoffel symbols defined in the usual way

$$\hat{\Gamma}^M_{KL} = \frac{1}{2}\, \hat{g}^{MN} \left(\partial_K \hat{g}_{NL} + \partial_L \hat{g}_{NK} - \partial_N \hat{g}_{KL} \right) . \tag{A.2}$$

For the dimensionally continued black hole metric (5.15), with the planar horizon, the non-zero components of the Christoffel symbols are

$$\begin{aligned}
\hat{\Gamma}^\sigma_{\sigma\sigma} &= -\frac{1}{\sigma} \,, & \hat{\Gamma}^\sigma_{zz} &= -\frac{M^2\sigma^2 - 1}{2} \,, & \hat{\Gamma}^z_{\sigma z} &= \frac{M\sigma - 1}{2\sigma\,(M\sigma + 1)} \,, \\
\hat{\Gamma}^\sigma_{\rho\rho} &= -\frac{M^2\sigma^2 - 1}{2} \,, & \hat{\Gamma}^t_{\sigma t} &= \frac{M\sigma + 1}{2\sigma\,(M\sigma - 1)} \,, & \hat{\Gamma}^\rho_{\varphi\varphi} &= -\rho \,, \\
\hat{\Gamma}^\sigma_{\varphi\varphi} &= -\rho^2\, \frac{M^2\sigma^2 - 1}{2} \,, & \hat{\Gamma}^\rho_{\sigma\rho} &= \frac{M\sigma - 1}{2\sigma\,(M\sigma + 1)} \,, & \hat{\Gamma}^\varphi_{\rho\varphi} &= \frac{1}{\rho} \,. \\
\hat{\Gamma}^\sigma_{tt} &= \frac{M^2\sigma^2 - 1}{2\ell^2} \,, & \hat{\Gamma}^\varphi_{\sigma\varphi} &= \frac{M\sigma - 1}{2\sigma\,(M\sigma + 1)} \,,
\end{aligned} \tag{A.3}$$

As a result, the five-dimensional Levi-Civita connection has non-zero components

$$\hat{\mathring{\omega}}^{04} = \frac{1+M\sigma}{2\ell\sqrt{\sigma}}\,\mathrm{d}t\,, \qquad \hat{\mathring{\omega}}^{m4} = \frac{1-M\sigma}{2\sqrt{\sigma}}\,\tilde{e}^m\,, \qquad \hat{\mathring{\omega}}^{12} = -\mathrm{d}\varphi\,. \tag{A.4}$$

Comparing with the general radial FG expansion (5.11) and the four-dimensional fields in the black hole solution (5.22), the components $\hat{\mathring{\omega}}^{a4}$ are in agreement.

The associated Riemann tensor, $\hat{\mathring{R}}^{AB} = \mathrm{d}\hat{\mathring{\omega}}^{AB} + \hat{\mathring{\omega}}^{AC} \wedge \hat{\mathring{\omega}}_C{}^B$, has the following components:

$$\begin{aligned} \hat{\mathring{R}}^{0m} &= \frac{M^2\sigma^2-1}{4\ell\sigma}\,\mathrm{d}t\wedge\tilde{e}^m\,, & \hat{\mathring{R}}^{04} &= \frac{M\sigma-1}{4\ell\sqrt{\sigma}\sigma}\,\mathrm{d}\sigma\wedge\mathrm{d}t\,, \\ \hat{\mathring{R}}^{m4} &= -\frac{M\sigma+1}{4\sqrt{\sigma}\sigma}\,\mathrm{d}\sigma\wedge\tilde{e}^m\,, & \hat{\mathring{R}}^{mn} &= -\frac{(M\sigma-1)^2}{4\sigma}\,\tilde{e}^m\wedge\tilde{e}^n\,. \end{aligned} \tag{A.5}$$